Università degli Studi di Pisa

FACOLTÀ DI INGEGNERIA
DIPARTIMENTO DI INGEGNERIA DELL'ENERGIA E DEI SISTEMI

Corso di Dottorato in
Automatica, Robotica e Bioingegneria
Settore Scientifico Disciplinare: ING-INF/04

Ph.D. Dissertation on

Isn't Appearance Enough?

Nonlinear Observability and Observers for Appearance Localization, Mapping, Motion Reconstruction and Servoing Problems and their application to Vehicle Navigation

Candidate Student: **Felipe Augusto Weilemann Belo**

Advisors: **Prof. Antonio Bicchi**
Dr. Ing. Daniele Fontanelli

Course Cycle XXII — Year of Enrolling 2007

To my mom

Abstract

In this thesis we investigate how monocular image measurements can be used as the single source of information for a vehicle to sense and navigate through its surroundings.

First we investigate what is the subset of vehicle location, environment mapping and vehicle motion that can be retrieved from images only. In particular, results apply to the case where no model of the vehicle, nor odometry or acceleration measurements are available. Then, we investigate the use of the information that can be extracted from images on visual servoing tasks and we define a servoing approach, named *Appearance Servoing*, that explicitly imposes the existing control constraints in the navigation of an *Appearance Map* ([1–4]). Finally, we present an experimental study case of the use of appearance where a sequence of images is used to construct a simple topological map of an office environment and then navigate a robot within it.

Acknowledgement

I dedicate this thesis to those who are fundamental to my life: my mom, my dad, my brother, my wife and my dog. And also to those who make life worth living: my family, my friends and my professors.

I am heartily thankful to my supervisor, Prof. Antonio Bicchi, who supported and constantly challenged me to do the best I could do.

I would also like to aknowledge that this thesis would not have been possible without the contribution of Dr. Ing. Daniele Fontanelli who strongly encouraged and motivated me throughout my academic program.

I made this thesis for my mom even though she would have preferred a poem.

March 2011
Pisa, Italy

Felipe Belo

Contents

List of Notations

Rigid Motion and Reference Frames

$\langle W \rangle$	Arbitrary fixed right-handed reference frame
$\langle C \rangle$	Moving camera or sensor reference frame
$\langle I \rangle$	Image plane
${}^{*}O$	Origin of frame $< * >$
${}^{*}X$	Axis X of frame $< * >$
${}^{*}Y$	Axis Y of frame $< * >$
${}^{*}Z$	Axis Z of frame $< * >$
${}^{*}x_{\#}$	Coordinate x of a point # w.r.t. frame $< * >$
${}^{*}y_{\#}$	Coordinate y of a point # w.r.t. frame $< * >$
${}^{*}z_{\#}$	Coordinate z of a point # w.r.t. frame $< * >$
θ	Orientation
(x, y, z)	Euclidean coordinates of a point
(ρ, β, ϕ)	Polar Coordinates of a point
$P \in \mathbb{R}^3$	Point position in an Euclidean space $\mathbb{R}^3$
$p \in \mathbb{R}^2$	Point position in an Euclidean space $\mathbb{R}^2$
$\bar{P} \in \mathbb{P}^3$	Homogeneous coordinates of a point P in a projective space $\mathbb{P}^3$
$\bar{p} \in \mathbb{P}^2$	Homogeneous coordinates of a point p in a projective space$\mathbb{P}^2$

System Modelling and Differential Geometry

Σ	System
$\xi \in \mathcal{X} := \mathbb{R}^n$	System state
Σ_e	Extended (or augmented) system
$\xi_{\mathbf{e}} \in \mathcal{X} := \mathbb{R}^n$	Extended (or augmented) system state
$\zeta \in \mathcal{X} := \mathbb{R}^n$	Coordinate mapping of system state
$\mathbf{y} \in \mathcal{Y} := \mathbb{R}^p$	System outputs
$\mathbf{u} \in \mathcal{U} := \mathbb{R}^m$	System inputs
$\mathbf{d} \in \mathcal{D} := \mathbb{R}^\eta$	System input disturbances
$\mathcal{O}$	Observation space
$\mathcal{O}^\perp$	Non observable space
$d\mathcal{O}$	Observability codistribution
O	Observability Matrix of linear systems
$\zeta_{\mathbf{o}}$	Observable subsystem state
$\zeta_{\bar{\mathbf{o}}}$	Unobservable subsystem state
Δ	Distribution
Ω	Codistribution

Auxiliar Notations

$*_r$	Refers to the vehicle
$*_d$	Refers to the input disturbances
$*_m$	Refers to a marker
$*_t$	Refers to a target
$*_e$	Refers to an extended or augmented variable

Chapter 1

Introduction

Vision systems are versatile, powerful, and cheap, providing a minimal sensing framework for dealing with fundamental robotic problems such as localization, environment mapping and robot motion. However, is appearance enough?

The term appearance is used in the *Computer Vision* community to describe sensory information coming from images. Appearance can be represented: using global descriptors , e.g., as a set of image histograms [5], as an ordered set of edge and color features [6], as Laplace or Mellin transformations [7], or as texture features [8]; or using local descriptors, e.g., as SIFT features [9, 10]. More recently, the term became extensively used in the context of *Appearance Mapping*, where the map is composed of a set of locations, each of which has an associated appearance model [1–4].

In this thesis, by appearance we mean the use of no other information but measurements of environment landmarks obtained from images only and we investigate when and how these measurements can be used as the single source of information for a vehicle to sense and navigate through its surroundings. The first question we pose regards sensing: we investigate what subset of internal states of a system composed of vehicle location (localization problem), environment landmarks positions (mapping problem) and vehicle motion (motion re-

construction problem) can be inferred from images, a problem known as system observability. Then, we investigate the use of the information extracted from images on navigation tasks, more specifically, visual servoing tasks, giving emphasis to the analysis of the real-time connection of our estimation algorithms and the feedback control laws developed. Finally, we present an experimental study case of the use of appearance where a sequence of images is used to construct a simple topological map of an office environment and then navigate a robot within it.

It is well known that the observability problem of statically retrieving camera localization and landmark positions is simple and straightforward when using stereo cameras. However, this is only true if previous knowledge of the system is available (e.g., well calibrated relative position of the cameras). Indeed, stereo cameras provide more than just appearance, the presence of two or more lenses allows the camera to capture three-dimensional images that carry much more information than simple images obtained from monocular cameras. However, isn't appearance enough? As is discussed in detail throughout this thesis, if monocular images only are being used, there is an one-dimensional subspace that can't be retrieved on most cases, and despite that, localization, mapping and navigation are still a possibility.

Indeed, a system-theoretic view of vision problems is not extensive in literature, e.g., the first observability analysis of the simultaneous localisation and mapping problem using vehicles and bearing measurements has only been presented and discussed in literature in [11]. Still, the results presented regard the possibility of retrieving information on the system state given that vehicle motion (e.g., linear and angular velocities) and measurement functions are completely known. However, what if inputs are not know or not completely available? What if only appearance is available? The observability problem under such conditions is known as unknown input observability and regards the possibility of retrieving information on both system state and system inputs if only the output function is completely known.

Such analysis asks for more refined use of nonlinear control theory tools than the straightforward application of the well known observability rank condition [12]. In fact, the observability rank condition can be applied to investigate the unknown input observability of linear and nonlinear affine systems, using proper methodology, and if some sufficient conditions hold as we discuss in chapter 2. In this, we not only present an appropriate methodology for doing so, but we also propose a novel nonlinear observer that can be adopted in order to reconstruct the observable subspace of input and state concurrently.

The procedure presented in chapter 2 allows us to present a rigorous unknown input observability analysis of the planar bearing localization, mapping and motion reconstruction problem in chapter 3. Our results use an unified observability framework to put the following different visual problems within the same perspective: Simultaneous Localization And Mapping (SLAM), used for landmark map construction and localization of the moving camera within the map; Structure From Motion (SFM), which applies when object structure reconstruction is to be recovered by a sequence of images; and Visual Odometry, adopted for robot position and orientation estimation from camera measurements.

Having investigated and fully characterized the sensing problem when using appearance, the motion problem is presented in 4, in order to close the loop between sensing and control. We pose the following question taking in consideration the control constraints that are raised by the task of navigating an *Appearance Map*: Is it possible to steer a vehicle to a desired pose in the plane, based only on comparing the visual appearance of the scene in view with a reference one? The vision–based control of robotic platforms, named *visual servoing*, is a well established theoretic framework in literature [13, 14]. Visual servoing techniques use visual information directly, by the computation of an image error signal, or indirectly, by the evaluation of the state of the system. These two approaches have been firstly classified in [15] as *Image Based Visual Servoing* (IBVS) and *Position Based Visual Servoing* (PBVS), respectively. While these classical definitions are broad

enough to cover most of the practical cases of servoing investigated in literature, they do not explicitly impose restrictions in the way a robotic system is controlled. More precisely, any restriction about parameters, known or available a priori, that may be included in the control law is not explicitly assumed. For these reasons, if only current and desired images (i.e., appearance), and no other information apart from system calibration parameters are available and involved in the control law, more strict definitions would better classify which control schemes are adequate. To this end, we derive a new strict definition of visual servoing, namely the *Appearance Servoing* approach (the choice of the term *Appearance* is motivated by its use in the *Appearance Mapping* [1–4]). Relying on the appearance servoing definition, we present visual servoing control schemes that, assuming only the a–priori knowledge of the intrinsic camera parameters, robustly steers an omnidirectional or unicycle vehicle to a goal position in the presence of unknown (or not modelled) inputs and by measuring only the image feature position of landmarks.

The minimum requirements of appearance servoing schemes allows us to explore alternative schemes of localization, mapping and navigation to the classical Visual SLAM approach. Conventionally, SLAM tracks the localization of a robot while building a map and fusing dead-reckoning information with landmark observations. A quite different approach relies on using acquired images only: mapping the path as a set of keyframes or organizing the acquired images in an appearance based graph (a topological map). Such approach is commonly associated to the terms *Visual Memory* [16] or *Image Memory* [17] when refering to the robot navigation using a sequence of images, and more recently to the concept of *Appearance Mapping* literature [1–4], when relating *Appearance* to the construction of a topological map. However, simplicity in the map results in a more difficult navigation phase (as discussed in [18]), since localization, planning and control algorithms must be image related only, and that's where appearance servoing schemes fit perfectly. Hence, we finish this thesis presenting an experimental study case of appearance topological

mapping and navigation (chapter 5) that illustrates the power of the use of appearance only.

While revisiting visual estimation techniques (e.g., SLAM, SFM, and Visual Odometry), the visual navigation problem (Visual Servoing), and, finally, abstract methods of representing and using visual maps (Appearance Mapping); we present a rigorous and formal analysis of the prior requirements, the many problem characterizations (e.g., regarding previous knowledge of scene landmarks or vehicle inputs) and the possibilities of using *Appearance* only.

Indeed, appearance is enough.

Part of the work described in this document is based on the following publications: [18, 33, 77, 80, 81].

1.1 Literature Review

In the following we will review and detail the state of art of localization, mapping and motion reconstruction in section 1.1.1 and the state of art of visual servoing in 1.1.2, giving emphasis to works that are relevant to the topics studied and developed in this thesis.

1.1.1 Localization, Mapping and Motion Reconstruction

Visual SLAM Simultaneous Localization and Mapping (SLAM) is a concept in which a mobile robot or an autonomous vehicle builds a map of an unknown environment while keeping track of its position and localizing itself. The concept was originally developed by Hugh Durrant-Whyte and John J. Leonard [19, 20]. Conventional SLAM tracks the localization of a robot while building a map fusing dead-reckoning information with landmark observations.

One possible approach to SLAM is Visual SLAM, in which the robot uses visual information as sensory information in order to do localization and mapping tasks. It was first introduced in [21], was further developed by Hugh Durrant-Whyte and John J. Leonard [19, 20] and has been an active research field ever since. Visual based SLAM methods have been receiving wide attention recently, with some interesting advances in the field [10, 22]. Until recently, vision systems were prohibitive because they were computationally intensive, the hardware required was costly and there was a lack of appropriate algorithms. Recently, however, high-performing computers are low-costly and cameras have become a commodity. Also, advances in computer vision [9] and probabilistic robotics [23] provide the required tools for such methods. VSLAM is particularly interesting given that environment landmarks can be easily retrieved from the rich sensory information obtained from vision systems. At the same time, the use of vision resembles how humans look at the world and is more intuitively appealing than sonars or lasers, for instance.

SLAM consists of the following parts: Landmark extraction, data association, state estimation, state update and landmark update. In VSLAM, many approaches extract Landmarks using features in the images. These can be line segments [24, 25], corners [26–28], image patches [22], or more reliable descriptors like SIFT [9, 29]. The initial estimation of landmark positions is usually obtained by odometry [29–31] or multiple view geometry [32]. Different approaches were proposed to update the visual landmarks, such as Extended Kalman Filters [22], Rao-Blackwellised Particle Filters [30] and Fast SLAM [29].

VSLAM methods also rely on different camera approaches like monocular cameras [22, 26–28, 33], omnidirectional cameras [34–36] and the use of multiple cameras [10, 37]. Here we are interested in the use of monocular cameras because, as was emphasized on section 1, by appearance we emphasize the use of measurements obtained from monocular images without the need of considering other *a-priori* information, e.g., the relative position of multiple cameras. The use of

single monocular cameras represents a particularly attractive solution for mobile agents navigation, mainly due to their low cost and their usage simplicity (e.g., no exogenous calibration is needed). However, the use of single monocular cameras is also a very challenging one because 3D positions from robot and landmarks aren't directly available from the measurements obtained from monocular cameras, which are composed of angular measurements related to each landmark, namely, bearings. In Bearing Only SLAM, the determination of the location of a landmark requires images from different points of view to be combined, then, landmark location is normally estimated using EKF with observations from these 2 or more robot poses. As the robot location and landmark positions cannot be determined from a single frame, an initial estimation is needed.

Practical implementations of monocular SLAM only appeared at [22] and were further developed in [38]. Finally, in [30], a framework for 3D vision based bearing only SLAM using a monocular camera is proposed. However, given that the SLAM problem was born within the probabilistic robotics community, a system-theoretic view of the Visual SLAM problem is not extensive in literature and it was only recently that the observability analysis of the planar bearing only problem has been completely presented and discussed in literature ([11], [39], [40], and [41]). Consequently, we are particularly interested in approaching the problem from a system-theoretic point of view.

Bearing Only Observability The feasibility of performing SLAM can be investigated rigorously through an observability analysis of the problem. The classic observability problem, called Unknown State Observability (USO), regards the possibility of retrieving information on the state of a system given that input and output functions are completely known [12]. When applied to the SLAM problem, it identifies the conditions of problem solvability using a unified framework with the control problem [11].

Different characterizations of the observability problem represent a field of active research, e.g. bearing only observability analysis in the

context of on-orbit space applications can be seen in [42]. A preliminary analysis that consider the motion of targets can be seen in [43], and the investigation of the multi–robot localization problem can be seen in [44]. Other recent studies focus on robust (or adaptive) control topics, like in [45], where the observability rank condition is applied in order to investigate on-line parameter identification problems concerning self calibration of the odometry.

However, bearing only SLAM methods usually require motion models, for which odometry and/or gyro sensors are used. As a matter of fact, the Unknown State Observability analysis, as presented in [11, 39–41], assume that system inputs are completely known and available. Hence, the observability results don't hold if only appearance is available. Indeed, they aren't valid not even on the case that external inputs (e.g., external forces) act on the robotic platform. The investigation of the problem under such conditions is called unknown input observability and regards the possibility of retrieving information on both system state and system inputs if only the output function is completely known. In fact, UIO is one of the main topics in control theory and was introduced by Basile and Marro in [46] and Guidorzi and Marro in [47]. While it is usually assumed the inputs are completely known, in practice, under many situations, some of the input variables may not be completely available and, for this reason, it is appropriate to distinguish inputs between control inputs and disturbances. UIO is known to be a difficult task and is commonly associated with the problems of robust model based fault detection, a problem that was introduced in [48] and further extended to the detection of both sensor and actuator faults in [49].

SFM and Visual Odometry An alternative and readily available procedure for reconstructing a camera trajectory through a sequence of images without requiring the knowledge of system inputs is using structure from motion [50] methods. In such a case, features are detected, matched between successive frames, used to estimate relative movements, and finally, associated with a 3d position. Consequently,

the movement of the camera can be robustly and automatically estimated without requiring additional measurements, like odometry. The two predominant procedures for SFM are off-line methods [28, 51–54] and methods without global optimization. In the first one a bundle adjustment optimization of the global geometry is carried out, then, the pose of the camera for the sequence of the image as well as features position are estimated in order to achieve the minimal error due to the positions detected in the image and the estimated re-projections. Building a map through these techniques is time-consuming and consequently, done off-line. A different approach is proposed by methods without global optimization. These are faster, whereas less accurate, given that errors accumulate in time. A promising method proposed by Nistér is referred to as visual odometry [55–60]. The robot motion estimation is done through the track of selected landmarks. The movement of stereo or simple cameras can be computed in real time from the only visual data only. Many algorithms have been proposed recently, differing mainly in the feature matching or estimation methods. From a practical point of view, the main difference of structure from motion is that it has been formulated as off-line algorithms. However, apart from the practical implementation differences, monocular visual odometry and monocular VSLAM can both be seen as a particular solution of SFM.

Appearance Mapping A quite different approach of mapping relies only on the raw sensor readings (images), i.e., maps can be modeled as a set of image keyframes [16,25,36], or in a topological manner where neighboring nodes correspond to images with similar appearance [7, 34, 35]. Similarly, when *Appearance* descriptions (or models) are associated to a set of locations, the approach is also commonly termed *Appearance Mapping* [1–4]. The key idea behind these approaches is that the higher is the similarity between two observations, the higher is the probability of them refering to the same place. During the mapping phase, images are organized in an appearance based graph, then during the navigation phase, the robot navigates through

the sequence of frames that describe the desired trajectory using some sort of visual servoing scheme.

The relevance of these approaches rely on the simplicity in which the map is constructed. However, in [18] it is discussed that the information thus stored in an appearance-based map is difficult to be effectively used in a control scheme. Indeed, only visual measurements taken from a camera, which possibly moves in the environment under the effect of corrupted inputs, are available to the servoing controller. Ultimately, the use of *Appearance Maps* forces localization, planning and control algorithms to be performed during the navigation phase must be only *Appearance* related. We will return to this discussion in section 1.1.2.

Our contributions Our contributions regarding localization, mapping and motion reconstruction are presented in chapters 2, 3 and 5. We believe that our main contribution is that of revisiting a range of estimation problems (e.g., SLAM, SFM and Visual Odometry) under a common system-theoretic view with the attention to the constraint of dealing with *Appearance* only.

First, we revisit the SLAM observability analysis shown in [11] investigating all possible configurations of previously known and unknown landmarks' positions. Moreover, since in [11] only the completely observable problems are discussed, we present a complete Kalman form decomposition of all partially observable problems investigated.

All observability analysis presented in this paper are derived or similar to the ones described in SFM [61]. However, as both SFM or visual odometry approaches rely on strong assumptions with regard to the environment and to the camera motion; both assume not only rigidity in the scene, but also constant velocity for the camera (or a given derivative of the velocity); in this thesis we extrapolate these assumptions, with results that are more general than the 2D version of known structure from motion observability results reported in [61]. The only assumption we made is that input disturbances are ana-

lytic, an assumption that is coherent with practical applications. In order to do so, we introduce a methodological analysis, based on a recursive application of the observability rank condition ([6]) using logical induction. Then, we apply this method to investigate state observability and left-invertibility concurrently considering a polynomial expansion of input disturbances. A complete observability analysis of the localization, mapping and motion problem is thus presented for all possible configurations of previously known and unknown landmarks' positions. Again, partially observable problems are further investigated and a complete Kalman form decomposition is derived.

Using a systems-theoretical approach, results can be viewed as an unified framework to VSLAM, SFM and Visual Odometry, extending and generalizing previous results, and with the minimum requirement of using appearance only. We also present an online solution to the reconstruction problem using an assymptotically stable nonlinear observer.

Finally, given that appearance maps illustrates the use of appearance in a compelling way, in chapter 5 we present an experimental study case of appearance topological mapping and navigation.

1.1.2 Visual Servoing

With the aim of discussing the use of appearance in robot control, we distinguish the measurements of a robotic platform in proprioceptive or exteroceptive sensor readings. Proprioceptive sensors are usually used to describe robot internal configuration, including positions (e.g., potentiometers, encoders, resolvers and linear displacement transducers), velocities (e.g., tachometers and piezoelectric velocity transducers), inertia (e.g., accelerometers and gyroscopes), and torques (e.g., optical and strain gauge torque transducers). On the other hand, typical exteroceptive measurements include force sensors (e.g. fiber optic, resistance and semiconductor strain gauge sensors), tactile sensors (e.g., resistive, magnetic or capacitive based sensors), proximity-range sensors (e.g., infrared, lasers or sonar), bearing sen-

sors (e.g., vision systems). Hence, a generic robotic system with its measurement functions can be described by

$$\begin{cases} \dot{\xi}_r = f\left(\xi_r, u, d, \lambda_{\text{int}}\right) \\ y_{\text{int}} = h_{int}\left(\xi_r, \lambda_{\text{int}}\right) \\ y_{\text{ext}} = h_{ext}\left(\xi_r, \lambda_{\text{int}}, \lambda_{\text{ext}}\right) \end{cases} \tag{1.1}$$

where $\xi_r \in \mathbb{R}^n$ is the robotic system state and describes the robot pose (e.g., vehicle position or joint configuration). $u \in \mathbb{R}^{m_u}$ are the available or known inputs of the system. $d \in \mathbb{R}^{m_d}$ are the unknown or not available inputs of the system and are also denominated input disturbances as introduced by Marro [62] (note that the concept is more general than the stochastic concept of disturbance, e.g., measurement noise). $y_{\text{int}} \in \mathbb{R}^{q_1}$ ($y_{\text{ext}} \in \mathbb{R}^{q_2}$) describes proprioceptive (exteroceptive) measurements, $\lambda_{\text{int}} \in \mathbb{R}^{l_1}$ are the internal parameters and $\lambda_{\text{ext}} \in \mathbb{R}^{l_2}$ the external parameters of the system, related to the proprioceptive and exteroceptive measurements respectively. Please note that internal measurements are not affected by extrinsic parameters, i.e., $\partial y_{\text{int}}/\partial \lambda_{\text{ext}} = 0$.

In this thesis we are interested in the use of exteroceptive measurements, more specifically, of vision measurements. And we pose the question: is appearance only enough for solving visual servoing tasks? By appearance only, we mean that proprioceptive measurements are not available and that input disturbances can't be assumed to be know and can't be neglected. Input disturbances are often neglected in the rather extensive visual servoing literature, although they usually have a negative impact on the servoing accuracy and performance.

From Classic Approaches to Appearance Servoing

The aim of vision-servoing schemes is to minimize an error $e(t)$ which is typically defined as [13]

$$e(t) = s(m(t), a) - s^*, \tag{1.2}$$

where: $m(t)$ is a set of image measurements, e.g., image coordinates of interest points or the parameters of a set of image segments; a a is a set of parameters that represent potential additional knowledge about the system, .e.g., coarse camera intrinsic parameters or three-dimensional model of objects; and $s(m(t), a)$ is a set of k visual features and s^* is the desired configuration. The concept of visual feature is rather general in literature as its embedded description can vary from the cartesian position on the image of a distinctive image point to the estimated state of the robot pose itself. Note that the same concept is also commonly associated to the term *Appearance* [5, 6, 8–10].

In order to put eq. (1.2) in conformity with the notation used in eq. (1.1), we can rewrite it as follows:

$$e(t) = \xi\left(y_{\text{ext}}(t), \lambda_{\text{int}}, \lambda_{\text{ext}}, y_{\text{int}}(t)\right) - \xi^*, \tag{1.3}$$

where ξ describes the state of the system. Here, $m(t)$ is substituted by $y_{\text{ext}}(t)$,i.e., the set of image measurements, and a is substituted by internal and external parameters λ_{int},λ_{ext}. From now on, we will use this notation instead of the original one. Moreover, we will use the notation $P_I = ({}^I p_1, {}^I p_2, {}^I p_3, \ldots, {}^I p_n)$ if we want to refer explicitly to the position of n image features on a camera's image plane, and we will use the notation ξ_c if we want to refer explicitly to the pose of the camera, i.e., its position and orientation w.r.t. to some adopted reference frame.

Classical visual servoing control laws consider holonomic systems, more specifically, serial manipulators. The most common and basic control scheme adopted is the one termed *velocity controller*, in which a *generic* control law is derived as follows [13]. Once ξ is chosen, it's dynamic is written as

$$\dot{\xi} = L_\xi u, \tag{1.4}$$

where L_ξ is named the interaction matrix related to ξ. Using eq. (1.3) and eq. (1.4) we can derive

$$\dot{e} = L_\xi u.$$

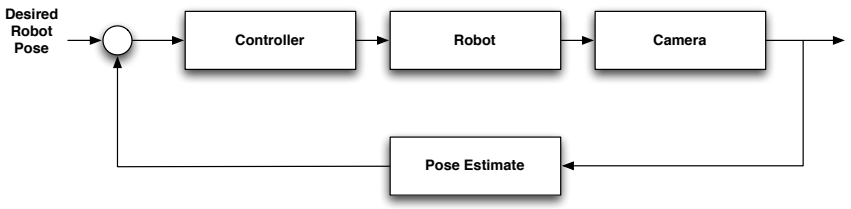

Figure 1.1: A traditional PBVS control scheme.

Hence, an exponential decoupled decrease of the error is obtained with a control law:

$$u = -\lambda L_{\xi}^{\dagger} e, \tag{1.5}$$

where $L_{\xi}^{\dagger}$ is chosen as the Moore-Penrose pseudo-inverse of L_{ξ}, a choice that allows $\left\| \dot{e} - \lambda L_{\xi} {L_{\xi}}^{\dagger} e \right\|$ to be minimal. Whenever L_{ξ} is squared, this control law coincides with the result of obtaining a controller based on a MIMO feedback linearization of the error dynamics.

Note that the presented control solution is not only simplistic but strongly limited as it only applies to driftless holonomic systems that can be described as eq. (1.4). Indeed, the classical visual-servoing definitions (IBVS and PBVS) mainly differ in the way that ξ is defined and not in the way the stabilizing control laws are constructed.

Formally, IBVS and PBVS (and their combination) is described as presented in the following sections. Note that we use the notation $g[0,T]$ to refer to a generic function $g(t)$ for all $t \in [0,T]$.

Position Based Visual Servoing

Definition 1.1 Position-based visual servoing - *System state consists of a set of 3-D parameters, which usually describe the robot pose ξ_r or camera pose ξ_c, and must be estimated from image measurements, i.e:*

$$\xi = \Upsilon\left(\xi_r\right),$$

or

$$\xi = \Upsilon\left(\xi_c\right),$$

and

$$\hat{\xi}_r = o\left(y_{ext}[0,t], u[0,t], \lambda_{int}, \lambda_{ext}, y_{int}[0,t]\right),$$

or

$$\hat{\xi}_c = o\left(y_{ext}[0,t], u[0,t], \lambda_{int}, \lambda_{ext}, y_{int}[0,t]\right),$$

where $\hat{\xi}_r$ or $\hat{\xi}_c$ is a pose estimate, given by the observer o.

We include $y_{\text{int}}(t)$ in $o(*)$ because it is not uncommon to have that proprioceptive measurements are assumed to be known, to be estimated or to be instantly available in order to retrieve $\hat{\xi}$ [13].

While there isn't an unique formal definition of a PBVS stabilizing control law in literature, a typical *static* stabilizing control law z for system state ξ (or a subsystem of) in *position based* schemes can be written in compliance with the following form:

$$u(t) = z\left(y_{\text{ext}}[t], \lambda_{\text{int}}, \lambda_{\text{ext}}, y_{\text{int}}[t]\right), \tag{1.6}$$

and a typical *dynamic* stabilizing control law z can be written in compliance with the following form:

$$\begin{cases} \hat{\xi}(t) = o\left(y_{\text{ext}}[0,t], u[0,t], \lambda_{\text{int}}, \lambda_{\text{ext}}, y_{\text{int}}[0,t]\right) \\ u(t) = z\left(\hat{\xi}_r(t), u(t), d(t)\right) \end{cases},$$

where $\hat{\xi}$ is a pose estimate, given by the observer o. Note that an estimate of the state is required given that it is not immediately available.

Traditional PBVS servoing schemes are usually similar to the one in fig. 1.1 (as seen in [63]). However, it is important to emphasize that PBVS refers only to the definition of the error $e(t)$ and there are no explicit rules on the construction of stabilizing control laws.

Image-based visual servoing

Definition 1.2 Image-based servoing - *System state ξ consists of a set of features that are immediately available in the image data,*

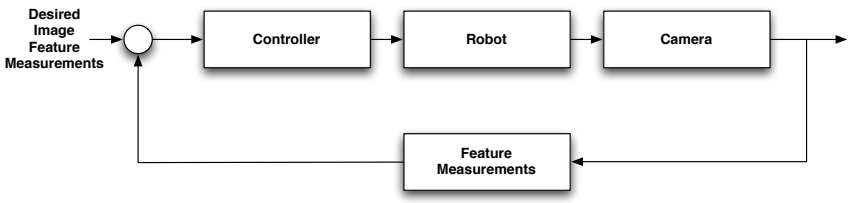

Figure 1.2: A traditional IBVS control scheme.

what is usually understood as a function of the position of the n image features $P_I = ({}^I p_1, {}^I p_2, {}^I p_3, \ldots, {}^I p_n)$*:*

$$\xi = \Xi(P_I).$$

While there is not an unique formal definition of an IBVS stabilizing control law in literature, a typical stabilizing control law z for system state ξ (or a subsystem of) can be written in compliance with the following form:

$$u(t) = z\left(\xi, y_{\text{ext}}[0,t], u[0,t], \lambda_{\text{int}}, \lambda_{\text{ext}}, y_{\text{int}}[0,t]\right) .$$

Note that an estimate of the state ξ is not required given that it is assumed to be immediately available and usually coincident to the camera measurements, i.e., $\xi = y_{ext}$. However, the controller may require an observer, being it static or dynamic, in order to derive other parameters that are not readily available. For example, *velocity controllers* (please refer to eq.(1.5)) use an approximation of the interaction matrix L_ξ that is usually written in terms of parameters related to the 3-d position of measured landmarks [64]. Therefore, the estimation of such parameters may be required at each iteration of the control scheme .

Traditional IBVS servoing schemes are usually similar to the one in fig. 1.2 (as seen in [63]). However, note that the presence of a possible observer between feature measurements and controller is omitted in such scheme.

Again it is important to emphasize that IBVS refers only to the definition of the error $e(t)$ and there are no explicit rules on the construction of stabilizing control laws.

On the PBVS and IBVS approaches Here we present the following limitations regarding the PBVS and IBVS classifications: whenever the approaches guarantee pose stabilization, they are equivalent from differential geometry perspective; these two classifications are hardly (or unclearly) applied, as originally defined, to nonholonomic systems; classical PBVS and IBVS schemes do no take input disturbances in consideration explicitly; PBVS and IBVS classifications refer only to the definition of the error $e(t)$ as there are no explicit rules on the construction of stabilizing control laws; These limitations are discussed in detail in the remaining of this section.

The first limitation to be discussed is the equivalence of IBVS and PBVS from a differential geometry point of view. The stabilization of the image based state description implies the stabilization of the robot in the desired position if there exists a diffeomorphism $\Phi : P_r \mapsto P_I$. In such a case, the systems are considered equivalent from a differential geometry perspective, i.e., properties such as accessibility, observability and stability remain independently of the coordinates chosen.

The second limitation regards the application of the original taxonomy (PBVS meaning $\xi = \Upsilon(\xi_c)$ and IBVS meaning $\xi = \Xi(P_I)$) to nonholonomic systems. Although the classical PBVS *velocity controller* (please refer to eq. (1.5)) can be classified as a input-state feedback control whilst the classical IBVS *velocity controller* is viewed as an input-output feedback control, this taxonomy cannot be directly applied to nonholonomic systems. Indeed, the feedback linearization techniques are hardly available in this case and, additionally, the well known Brockett's theorem [65] makes the stability of the point–to–point motion problem of a nonholonomic system via smooth, time invariant control laws very challenging. For example, [66] proposes a change of coordinates of the robot state in order to

solve the parking problem of a unicycle–like vehicle using visual feedback. As a consequence, it is common that the stability analysis cannot be carried out directly in the cartesian space or on the image space, but in a state space $\gamma = \Gamma(\xi)$, under the mapping function Γ. With reference to the definitions previously introduced, it follows that $\gamma = \Gamma(\Xi(P_I)) = \Gamma(\Xi(\Phi(\xi_c)))$ or $\gamma = \Gamma(\Upsilon(\xi_c)) = \Gamma(\Upsilon(\Phi^{-1}(P_I)))$, which leads to an unclear classification of the servoing approach as the error cannot be defined in the simplistic terms that were originally anticipated by the PBVS and IBVS classifications.

In addition, little is seen in the PBVS or IBVS literature regarding the presence of unknown or unavailable inputs. Whenever input disturbance is mentioned, it is usually assumed to be related to *measurement noise* and is treated with an stochastic approach, e.g., the use of EKF filters. Indeed, the analysis of the robustness to disturbances d of the IBVS, PBVS or the combination thereof is in any respect trivial.

Finally, given that the terms IBVS and PBVS refer only to the definition of the error $e(t)$, there are no explicit rules on the construction of stabilizing control laws, and consequently, there exists of a broad range of interpretations and definitions of IBVS and PBVS control laws in literature.

Prior work and contributions In this thesis we tackle the visual servoing task imposing all necessary constraints in order to meet the requirements of navigating Appearance Maps: our approach comprises a calibrated camera, i.e., for which the intrinsic camera parameters are known or correctly estimated, rigidly fixed on a robotic platform whose motion is constrained on a plane, e.g., a unicycle–like vehicle; without loss of generality for the analysis of the problem at hand, the camera is assumed to be *omnidirectional*; beyond the camera intrinsic parameters, only the current and desired images are assumed to be available, more precisely, a set of *point features* belonging to both the images are available from the measured visual entities and assumed to be continuously tracked along the servoed trajectories; finally, the

actuators available on the platform are assumed to be corrupted by an unknown disturbance; The objective of the control problem is to regulate the current position of the robot towards the pose described by the desired image.

Visual servoing schemes that respect one or some of these requirements are not new in literature. Homography or the epipolar geometry approaches gathers a lot of popularity in the servoing community for solving the described problem [67] and paved the way to efficient solutions in the field [68, 69]. Albeit these attempts of estimating the camera displacement from two views, given by the current and desired images, do not require strong a priori knowledge on the observed objects structure, constraints on the feature point configuration are implicitly assumed, i.e., point features should be coplanar and/or sufficiently numerous. In the particular case considered in this thesis, where the robotic platform moves on a plane, the visual model simplifies at the cost of a more complicated control law design. For example, the number of feature points needed for the control law in the scaled reconstruction is three [70, 71], which is lower than the number of features needed for a typical homography–based solution (where at least 7 correspondences must be available in order to compute the fundamental matrix). Usually, these solutions generalize already well known servoing schemes (e.g. clas) using a scaled representation of the camera displacement to the desired view. However, all these approaches are currently restricted to planar objects, i.e., the planar assumptions about scene model is made. More recently [72, 73], describe a solution for the servoing along both planar and non–planar objects assuming the availability of noisy control velocities. Finally [70] presents a static control that solves the *Appearance Servoing* task of parking a vehicle.

In the author opinion, a clear view of the servoing control problem as proposed in this thesis still lacks. The rather vast literature on the subject presents a lot of effective solutions to the problem, ranging from 3D–PBVS approaches to IBVS or hybrid solutions that make use of additional sensors or environmental knowledge, however we think that the very nature of an *Appearance-based* servoing task is in the

use of the *Appearance* only extracted from the images grabbed from a camera. Any other additional information on the measurement system or on the environment, if available, can be used to satisfy additional performance requirements, e.g., increasing the rate of convergence or robustifying the control law, but should not be essential to solve our servoing problem. As already discussed in this section, while the classical PBVS and IBVS definitions are broad enough to cover most of the practical cases of servoing, they do not explicitly consider the restrictions in the way a robotic system is controlled and how to deal with actuation disturbances. In particular, if only *Appearance* is available, an apropriate definition regarding the construction of stabilizing control laws is required. Hence, in chapter 4 we name the problem *appearance servoing*. The problem definition does not exclude the coexistence with a PBVS or IBVS classification as it does not depend on the way the error is defined.

Relying on the appearance servoing definition, we investigate the minimum requirements needed for doing pose regulation, and propose static and dynamic solutions and design different visual control schemes (PBVS and IBVS). We want to aknowledge that the presented solutions are strongly inspired by [67, 73], but in the context of vehicle navigation, and we also share results with [70] regarding the static servoing solutions presented. We believe that our main contribution is that of presenting a rigorous unknown input observability analysis of the problem (on the basis of the methodology developed and described in chapter 2) and to determine the minimal "knowledge" needed to effectively solve the servoing task (in terms of number of feature points. Our results point out that a scaled reconstruction of the surrounding environment and the vehicle pose can still be achieved under all the constraints imposed by the AS problem and, more importantly, that control laws can be easily defined on such quantities. In fact, it can be shown that if only the initial and desired images are available, the number of feature points that are necessary and sufficient to let the position of the robot being observable up to a scale factor, and hence solve the control problem, is three (a result that

complete the analysis found in [70, 71]). In this situation, the AS is said to be *static*. However, if an observer is available, the AS turns to be *dynamic*, a definition that is borrowed from the first definition of dynamic IBVS in [74]. In such case, the number of point features needed lowers down to two. Moreover, as the AS formalization takes into account unknown disturbances in the actuators explicitly, one can introduce classical disturbance rejection methodologies to AS schemes straightforwardly. Finally, theoretical results are validated by extensive simulation results.

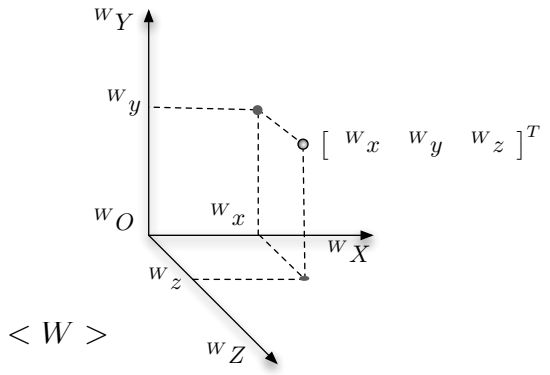

Figure 1.3: Reference frames.

1.2 Notation, definitions and preliminaries

1.2.1 Reference frames

We assume that coordinates are measured with respect to a dextrous reference frame $\langle W \rangle = \{^W O, ^W X, ^W Y, ^W Z\}$, fixed with the static environment (see fig. 1.2.1). Here we will refer to $\langle W \rangle$ as world frame.

A point position denoted in respect to $\langle W \rangle$ will be represented using the following notation:

$$^W P = \begin{bmatrix} ^W x \\ ^W y \\ ^W z \end{bmatrix}.$$

Similarly, points expressed in respect to a generic frame $\langle B \rangle$ will be denoted as $^B P$.

Many times it will be convenient to extend coordinate representations in $\mathbb{R}^n$ into the projective space $\mathbb{P}^n$. In particular, the homoge-

neous notation of a point P (in $\mathbb{R}^3$) will be denoted by $\bar{P}$ (in $\mathbb{P}^3$):

$$\bar{P} = \begin{bmatrix} P \\ 1 \end{bmatrix} = \begin{bmatrix} x \\ y \\ z \\ 1 \end{bmatrix}.$$

Such notation is usually convenient in order to represent rigid motions (rotations and translations), synthesised as follows:

$$^{A}\bar{P} = T_{A \leftarrow B}\, ^{B}\bar{P},$$

where $T_{A \leftarrow B}$ is the homogeneous transformation matrix that defines the transformation of a point represented in relation to the frame $\langle B \rangle$ to it's representation in relation to a frame $\langle A \rangle$. If this transformation is given by a rigid motion, we may write $T_{A \leftarrow B}$ as

$$T_{A \leftarrow B} = \begin{bmatrix} R_{A \leftarrow B} & P_{A \leftarrow B} \\ 0 & 1 \end{bmatrix},$$

where $R_{A \leftarrow B}$ is the rotation matrix that corresponds to the orientation displacement from $\langle B \rangle$ to $\langle A \rangle$, and $P_{A \leftarrow B}$ is the vector that denotes the position of the origin of coordinate frame $\langle B \rangle$ relative to coordinate frame $< A >$. We may also denote T, R and P as follows:

$$^{A}T_{B} = T_{A \leftarrow B},$$

$$^{A}R_{B} = R_{A \leftarrow B},$$

$$^{A}P_{B} = P_{A \leftarrow B}.$$

1.2.2 Vehicle Models

In this thesis, we mainly investigate problems related to vehicles moving on a plane. For this reason, given that robot coordinates are measured with respect to some arbitrary dextrous reference frame

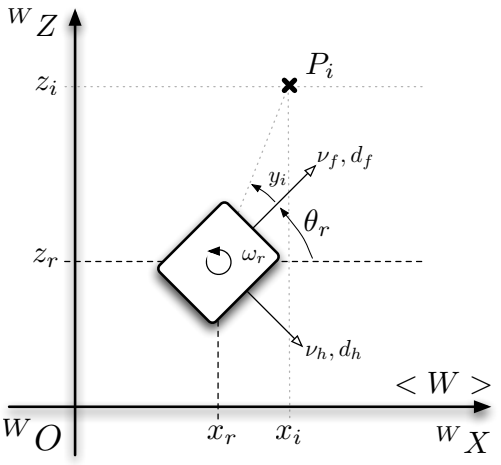

Figure 1.4: Vehicle kinematics.

$\langle W \rangle = \{^W O, ^W X, ^W Y, ^W Z\}$ we have that the $^W Y$ coordinate $y(t) = 0$, $\forall t$.

The configuration of a generic vehicle is described by $\xi_r = (x_r, z_r, \theta_r)$, where $p_r = (x_r, z_r)$ is the position w.r.t. $\langle W \rangle$ of a reference point in the vehicle and θ_r is the robot heading with respect to the $^W X$ axis (see figure 1.2.2). The subscript $*_r$ will be used along this thesis to refer to the vehicle.

Vehicle dynamics are considered to be slow enough to be neglected and kinematics can be represented by a generic driftless control–affine system Σ affected by the external disturbance vector d:

$$\Sigma = \begin{cases} \dot{\xi}_r = G(\xi_r)\, u_r + B(\xi_r)\, d_r \\ y = h(\xi_r)\,, \end{cases} \tag{1.7}$$

where u_r are control inputs, $G(\xi_r) \in \mathbb{R}^{3\times 3}$ represents the vector input fields that describe vehicle kinematics and $B(\xi_r) \in \mathbb{R}^{3\times 3}$ is a known disturbance input matrix associated with the disturbance vector d_r. In particular, we usually describe generic movements (and disturbances)

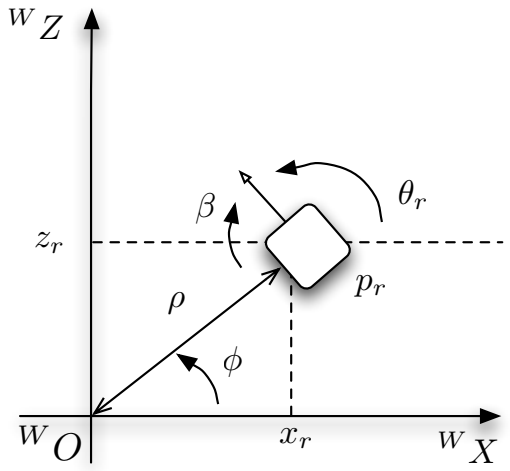

Figure 1.5: Cartesian and polar coordinates.

on a plane with the choice:

$$G = B = \left[\begin{array}{ccc} g_f & g_h & g_\omega \end{array} \right] = \left[\begin{array}{ccc} \cos(\theta_r) & -\sin(\theta_r) & 0 \\ \sin(\theta_r) & \cos(\theta_r) & 0 \\ 0 & 0 & 1 \end{array} \right], \qquad (1.8)$$

and $u_r = (v_f, v_h, \omega)$ and $d_r = (d_f, d_h, d_\omega)$. Note that eq. (1.8), with $d_r = \mathbf{0}$ is usually adopted to describe the motion of *omnidirectional–like* vehicles.

Specific vehicle kinematics can be described by choosing a $G(\xi_r)$ composed of subspaces of eq. (1.8) and the proper choice of u_r, e.g, *unycicle–like* vehicles are modelled just as above but choosing $v_h = 0$.

Polar Coordinates Depending on the problem studied, it may also be convenient to express vehicle configurations using polar coordinates (see figure 1.5). The pose displacement between ξ_r and $^W O$ represented on polar coordinates w.r.t. $\langle W \rangle$ is given by

$$\xi_{\text{rp}} = \Phi_p(\xi_r) = \begin{bmatrix} \rho \\ \beta \\ \phi \end{bmatrix} = \begin{bmatrix} \sqrt{{x_r}^2 + {z_r}^2} \\ \tan^{-1}\left(\frac{z_r}{x_r}\right) - \theta_r + \pi \\ \tan^{-1}\left(\frac{z_r}{x_r}\right) \end{bmatrix}, \tag{1.9}$$

where ρ represents the cartesian distance from the vehicle to the origin ${}^W O$, β represents the angle displacement between vehicle orientation and the line that passes through ${}^W O$ and vehicle position p_r and ϕ represents the angle formed by p_r with axis ${}^W X$. The notation $\Phi_p(*)$ is used to represent the transformation from cartesian to polar coordinates. Please note that the polar coordinates transformation is undefined for $\rho = 0$.

In order to verify if Φ_p is local diffeomorphism at ξ we compute its Jacobian:

$$J_p = \begin{bmatrix} \frac{x_r}{\sqrt{x_r^2+z_r^2}} & \frac{z_r}{\sqrt{x_r^2+z_r^2}} & 0 \\ -\frac{z_r}{x_r^2+z_r^2} & \frac{x_r}{x_r^2+z_r^2} & -1 \\ -\frac{z_r}{x_r^2+z_r^2} & \frac{x_r}{x_r^2+z_r^2} & 0 \end{bmatrix}. \tag{1.10}$$

Matrix rank of J_p is 3 apart from $|J_p| = 0$, i.e., when

$$|J_p| = \frac{1}{\rho} = \frac{1}{\sqrt{x_r^2 + z_r^2}} = 0.$$

Hence, we conclude that Φ is not a global diffeomorphism and is not defined for $\rho = 0$, as expected. For $\rho \neq 0$, its inverse is given by

$$\begin{bmatrix} x_r \\ z_r \\ \theta_r \end{bmatrix} = {\Phi_p}^{-1}(\xi_{\text{rp}}) = \begin{bmatrix} \rho\cos(\beta) \\ \rho\sin(\beta) \\ \alpha - \beta + \pi \end{bmatrix},$$

where the notation ${\Phi_p}^{-1}(\xi_{\text{rp}})$ is used to represent the mapping from polar to cartesian coordinates., i.e., inverse of the mapping defined in eq.(3.6).

Generic movements on the plane can be described on polar coordinates by the following kinematics:

$$G_p(\xi_p) = \begin{bmatrix} -\cos(\beta) & \sin(\beta) & 0 \\ \sin(\beta)/\rho & \cos(\beta)/\rho & -1 \\ \sin(\beta)/\rho & \cos(\beta)/\rho & 1 \end{bmatrix}.$$

1.2.3 Vision Models

Environmental scene landmarks are represented as points of the image plane, also denoted as features. Let $\langle W \rangle$ denote a global reference frame with respect to which all landmarks (or features) being observed by the camera are motionless.

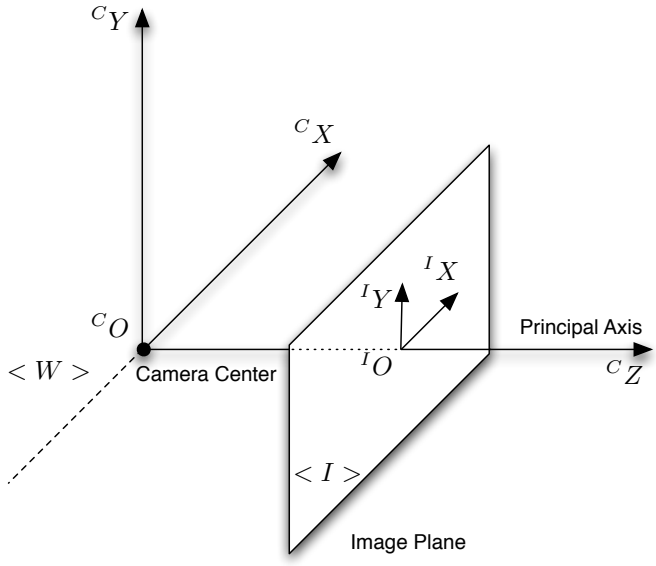

Figure 1.6: Camera Geometry.

In respect to $\langle W \rangle$, let's define the camera coordinate frame $\langle C \rangle = \{^C O, ^C X, ^C Y, ^C Z\}$, where $^C O$ is coincident to the camera centre, and

${}^{C}Z$ si coincident to the camera principal axis, i.e., the line from the camera centre perpendicular to the image plane. See Fig. 1.6. The point where the principal axis meets the image plane is called *principal point*.

Landmark positions are described w.r.t. the camera frame as ${}^{C}P_i = [{}^{C}x_i, {}^{C}y_i, {}^{C}z_i]^T$, where the index i corresponds to the ith feature.

We can introduce a reference frame $\langle I \rangle = \{{}^{I}O, {}^{I}X, {}^{I}Y\}$ on the image plane. The position ${}^{I}p = \left[{}^{I}x, {}^{I}y\right]^{T}$ of the features w.r.t. the image plane is described by a projective mapping $\Pi : \mathbb{R}^3 \to \mathbb{R}^2$.

We will consider cameras for which the measurement process is modelled by

$$\lambda \begin{bmatrix} {}^{I}x \\ {}^{I}y \\ 1 \end{bmatrix} = K_c \begin{bmatrix} 1 & 0 & 0 & 0 \\ 0 & 1 & 0 & 0 \\ 0 & 0 & 1 & 0 \end{bmatrix} \begin{bmatrix} {}^{C}x \\ {}^{C}y \\ {}^{C}z \\ 1 \end{bmatrix},$$

or simply by

$$\lambda {}^{I}\bar{p} = K_c \Pi \, {}^{C}\bar{P}, \tag{1.11}$$

where the matrix $K_c \in \mathbb{R}^{3\times3}$ is the intrinsic camera calibration matrix that describes the camera model and Π describes the projection from $\mathbb{R}^3$ to $\mathbb{R}^2$. Here, we will first present the basic pinhole camera model, and then, progressively generalize it till a general projective camera model.

Pinhole Camera The basic pinhole camera is shown in Fig. 1.7. Let the centre of projection be the origin of a Euclidean coordinate system [52], and consider the image plane (or focal plane) described by ${}^{I}Z = f$, where f is the camera focal length. Consider also that the principal point p_p is coincident with the origin of coordinates in the image plane and ${}^{C}X$ and ${}^{C}Y$ are parallel to image plane ${}^{I}X$ and ${}^{I}Y$, respectively. The central projection mapping from world to image

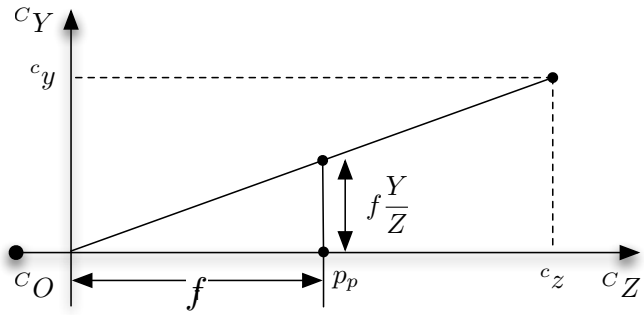

Figure 1.7: Pinhole Camera.

coordinates is given by

$$ {}^{I}p = \begin{bmatrix} {}^{I}x \\ {}^{I}y \end{bmatrix} = \begin{bmatrix} \frac{f\,{}^{C}x}{{}^{C}z} \\ \frac{f\,{}^{C}y}{{}^{C}z} \end{bmatrix}. \tag{1.12} $$

The presented transformation can be rewritten as a linear mapping using homogeneous coordinates by eq. (1.11) and

$$ K_c = \begin{bmatrix} f & 0 & 0 \\ 0 & f & 0 \\ 0 & 0 & 1 \end{bmatrix}. \tag{1.13} $$

Principal point offset Now, let's consider that the principal point is not coincident to the origin of coordinates in the image plane. Let's define $({}^{I}p_{p,x}, {}^{I}p_{p,y})^T$ as the coordinates of the principal point in the image plane. Equation (1.12) can be generalized for this case as follows:

$$ {}^{I}p = \begin{bmatrix} {}^{I}x \\ {}^{I}y \end{bmatrix} = \begin{bmatrix} \frac{f\,{}^{C}x}{{}^{C}z} + {}^{I}p_{p,x} \\ \frac{f\,{}^{C}y}{{}^{C}z} + {}^{I}p_{p,y} \end{bmatrix}, \tag{1.14} $$

which can be described using an homogeneous trasformation by eq. (1.11) and:

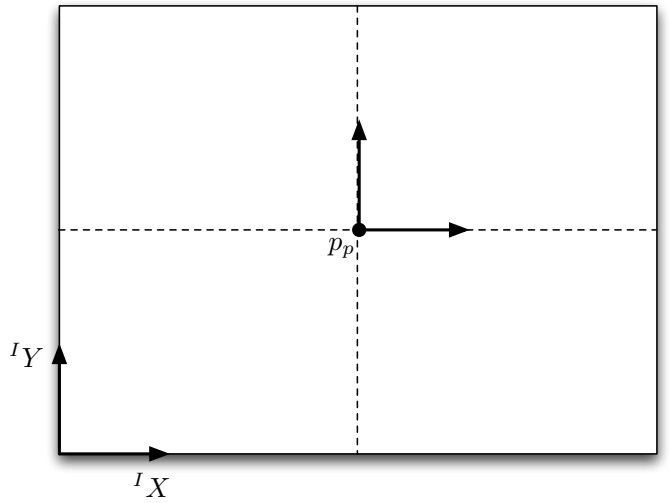

Figure 1.8: Principal Point Offset.

$$K_c = \begin{bmatrix} f & 0 & {}^I p_{p,x} \\ 0 & f & {}^I p_{p,y} \\ 0 & 0 & 1 \end{bmatrix}. \tag{1.15}$$

CCD Cameras The camera models presented till now assume projection mappings of identical pixel distortion (or scalar relationship) in both axial directions. In the case of CCD cameras, there is the possibility of having non-square pixels. Therefore, let's consider m_x and m_y as scale factors that relate metric coordinates to pixel coordinates of the point in directions ${}^I X$ and ${}^I Y$, respectively. Let's represent the focal length of the camera according to these scale factors as $\alpha_x = f m_x$ and $\alpha_x y = f m_y$. Now, equation (1.14) can be further generalized as follows:

$${}^I p = \begin{bmatrix} {}^I x \\ {}^I y \end{bmatrix} = \begin{bmatrix} \frac{\alpha_x {}^C x}{{}^C z} + {}^I p_{p,x} \\ \frac{\alpha_y {}^C y}{{}^C z} + {}^I p_{p,y} \end{bmatrix}, \tag{1.16}$$

which can be described using an homogeneous trasformation by eq. (1.11) and

$$K_c = \begin{bmatrix} \alpha_x & 0 & {}^I p_{p,x} \\ 0 & \alpha_y & {}^I p_{p,y} \\ 0 & 0 & 1 \end{bmatrix}. \tag{1.17}$$

Finite Projective Cameras Finally, for added generality, the intrinsic calibration matrix can be rewritten as

$$K_c = \begin{bmatrix} \alpha_x & s & {}^I p_x \\ 0 & \alpha_y & {}^I p_y \\ 0 & 0 & 1 \end{bmatrix}, \tag{1.18}$$

where s is the *skew* parameter. While $s = 0$ for normal cameras, it can assume non-zero values.

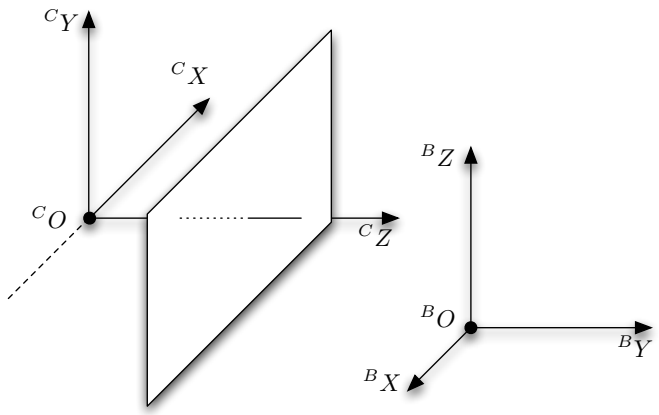

Figure 1.9: Camera Rotation and Translation.

Camera Rotation and Translation The projection matrixes presented were defined considering points represented w.r.t. the camera

frame $\langle C \rangle$. In general, points may be expressed w.r.t. a base frame $\langle B \rangle$. Therefore:

$$ {}^{C}P = \begin{bmatrix} {}^{C}x \\ {}^{C}y \\ {}^{C}z \\ 1 \end{bmatrix} = {}^{C}T_{B}\,{}^{B}P = \begin{bmatrix} {}^{C}R_{B} & {}^{C}P_{C \leftarrow B} \\ 0^{T} & 1 \end{bmatrix} \begin{bmatrix} {}^{B}x \\ {}^{B}y \\ {}^{B}z \\ 1 \end{bmatrix} . \tag{1.19} $$

Camera calibration matrix A camera that can be described by a general model that comprises intrinsic camera parameters and an extrinsic coordinate transformation to a base frame $< B >$:

$$ \lambda {}^{I}\bar{p} = K_{c} \Pi {}^{C}T_{B}\,{}^{B}\bar{P} \tag{1.20} $$

is called a *finite projective camera* and $\Xi = K_{c} \Pi {}^{C}T_{B}$ is called camera calibration matrix.

Normalized coordinates If a camera is calibrated and the intrinsic parameters of a camera are known, it may be convenient to refer to the normalized coordinates:

$$ \lambda {}^{I}\bar{p}^{*} = \Pi {}^{C}\bar{P}. $$

Note that image measurements on normalized coordinates are easily obtained by ${}^{I}\bar{p}^{*} = {K_{c}}^{-1}\,{}^{I}\bar{p}$. The measurement process described on normalized coordinates is simply

$$ {}^{I}p^{*} = \begin{bmatrix} {}^{I}x \\ {}^{I}y \end{bmatrix} = \begin{bmatrix} {}^{C}x / {}^{C}z \\ {}^{C}y / {}^{C}z \end{bmatrix} . $$

Omnidirectional sight and bearings The pinhole model is a particular version of the more general omnidirectional sight model, which is described by the horizontal and vertical bearings of a landmark with respect to the camera:

$$ (\phi_{1},\, \phi_{2}) = \left(\text{atan2}\left({}^{C}x, {}^{C}z \right), \text{atan2}\left({}^{C}y, {}^{C}z \right) \right) , \tag{1.21} $$

where atan2(a, b) gives the arc tangent of $\frac{a}{b}$ taking into account which quadrant the point a, b is in.

For ${}^{C}z > 0$ (as is defined for a pinhole camera), the relation between the models (1.2.3) and (1.21) is $(\phi_1,\, \phi_2) = \big(\text{atan}({}^{I}x),\, \text{atan}({}^{I}y)\big)$.

1.2.4 Observability Analysis

The observability analysis regards the possibility of retrieving information on the state of a system, given that input and output functions are completely or partially known [75]. The possibility of deriving the initial state $\xi(t_1)$ of a dynamic system Σ in the time interval $[t_1, t_2]$ is named observability of a system. Similarly, the possibility of deriving the final state $\xi(t_2)$ is denoted by reconstructability of a system. These problems may not admit a solution when the system presents states that are classified as *indistinguishable* in $[t_1, t_2]$. In this section we will introduce and briefly discuss these and other basic concepts of observability analysis theory.

Let's consider the state-space representation of a generic time-invariant dynamic system Σ:

$$\Sigma = \begin{cases} D\xi(t) = f(\xi(t), u(t)) \\ y(t) = h(\xi(t), u(t)) \end{cases},$$

where $\xi \in \mathcal{X} := \mathbb{R}^n$, $y \in \mathcal{Y} := \mathbb{R}^p$ and $u \in \mathcal{U} := \mathbb{R}^m$. Without loss of generality we can consider a time interval $[0, T]$. Let's represent $\xi(\bar{\xi}, u(\cdot), t)$ as the solution at time t correspondent to $\bar{\xi} = \xi(0)$ and control $u(\cdot) = u(\tau), \tau \in [0, t]$; Likewise, $y(\xi(0), u(\cdot), t) = h(\xi(\xi(0), u(\cdot), t), u(t))$.

Definition 1.3 (indistinguishable states) *Two initial states $\bar{\xi}_1$ and $\bar{\xi}_2$ are called indistinguishable in $[0, T]$ if*

$$\bar{\xi}_1 \, I_T \, \bar{\xi}_2 \Leftrightarrow y(\bar{\xi}_1, u(\cdot), t) = y(\bar{\xi}_2, u(\cdot), t), \forall t \in [0, T], \forall u(\cdot) \in \mathcal{U}.$$

It is denoted by $\bar{\xi}_1 \, I_T \, \bar{\xi}_2$.

Definition 1.3 states that a pair of points is indistinguishable if they realize the same input-output map in $[0, T]$ for every admissible input [12]. If there exists at least one input sequence for which the output is different for each point, these are said to be distinguishable.

Definition 1.4 (set of indistinguishable points) *The set of points that are indistinguishable from a given initial state $\bar{\xi}$ in $[0, T]$ is defined as*

$$I_T(\bar{\xi}) \stackrel{def}{=} \left\{ \bar{\xi}_1 \in \mathcal{X} | \, \bar{\xi} \, I_T \, \bar{\xi}_1 \right\}.$$

These previous definitions lead to the concept of the possibility of observing, or inferring knowledge on the state of a system.

Definition 1.5 (observable state) *A state $\bar{\xi}$ is said to be observable in $[0, T]$ if the set of states that are indistinguishable from $\bar{\xi}$ contains only $\bar{\xi}$:*

$$I_T(\bar{\xi}) = \{\bar{\xi}\}, \forall u(\cdot) \in \mathcal{U}, \forall y(.) \in \mathcal{Y}.$$

It can also be said that the system Σ is observable at $\bar{\xi}$.

A state is said to be observable if there exists at least one input function for which the output is distinguishable from any other state. However, it is important to notice that the observability of a state does not imply that for any given state, the input-output map is different for every admissible input. On the other hand, a state is said to be not observable if there exists a set of states for which the input-output map is the same for every admissible input.

Definition 1.6 (observable system) *A system Σ is said to be observable in $[0, T]$ if every state $\bar{\xi} \in \mathcal{X}$ is observable:*

$$\forall \bar{\xi} \in \mathcal{X} : I_t(\bar{\xi}) = \{\bar{\xi}\}.$$

The above definitions are considered in solving the following problems:

Problem 1.1 Unknown state observation: *Given corresponding known input and output functions $u(\cdot)$, $y(\cdot)$ and two instants of time $t_0 = 0$, $t_1 = T$, determine the unknown initial state $\bar{\xi}$ (or the set of initial states), such that $y(t) = y(\bar{\xi}, u(\cdot), t)$ for all $t \in [0, T]$;*

Problem 1.2 Unknown state reconstruction: *Given corresponding known input and output functions $u(\cdot)$, $y(\cdot)$ and two instants of time $t_0 = 0$, $t_1 = T$, reconstruct the state at a given moment $\bar{\xi}(\tau), \tau \in [0, T]$ (or the set of possible states), such that $y(t) = y(\bar{\xi}, u(\cdot), t)$ for all $t \in [0, T]$;*

For time-invariant continuous-time (TITC) systems, observability implies reconstructability. Therefore, as we will consider only TITC systems, here we will be interested in investigating Problem 1.1.

Linear time-invariant continuous-time systems

Let's consider the state-space representation of a linear system Σ:

$$\Sigma = \begin{cases} \dot{\xi}(t) = A\xi(t) + Bu \\ y(t) = C\xi(t) \end{cases}$$

In this case, the observability of Σ is reduced to the well-known criterion that if matrix

$$O = \begin{bmatrix} C \\ \mathrm{CA} \\ \vdots \\ \mathrm{CA}^{n-1} \end{bmatrix}$$

is of rank n, then the system is completely observable. O is called observability matrix and $\mathcal{O}^{\perp} = ker(O)$ is the non-observable subspace of Σ.

Non-linear time-invariant continuous-time systems

While the observability of the linear approximation of a non-linear system around a given $\bar{\xi}$ implies in the observability of the original

system on a neighborhood of $\bar{\xi}$ (weak observability), the opposite is not necessarily true. Observability is not a structural property of a non-linear system, i.e., the observability of a non-linear system does not imply in the observability of its linear approximation. Therefore, the definitions presented in section 1.2.4 and the criterion presented in section 1.2.4 aren't sufficient for studying the observability of non-linear systems.

Here we will discuss the concepts of local and weak observability, and present criterions for studying the observability of non-linear systems.

Local and weak observability

Observability as presented in 1.2.4 is a global concept, i.e., for a state to be distinguishable, long distances or time may be required. Therefore, a stronger local concept is introduced in [12].

Let $\mathcal{M}$ be a subset of $\mathcal{X}$ and $\bar{\xi}_1, \bar{\xi}_2 \in \mathcal{M}$.

Definition 1.7 (M-indistinguishability) *Two initial states $\bar{\xi}_1 \in \mathcal{M}$ and $\bar{\xi}_2 \in \mathcal{M}$ are called M-indistinguishable in $[0, T]$ if*

$$\bar{\xi}_1 \, I_{\mathcal{M},T} \, \bar{\xi}_2 \Leftrightarrow \bar{\xi}_1 \, I_T \, \bar{\xi}_2, \, \forall \xi(\bar{\xi}_1, u(\cdot), t) \in \mathcal{M}, \forall \xi(\bar{\xi}_2, u(\cdot), t) \in \mathcal{M}.$$

A state $\bar{\xi}_1$ is said to be indistinguishable from a state $\bar{\xi}_2$ if for every control $u(\cdot)$ whose trajectories $\xi(\bar{\xi}_1, u(\cdot), t)$ and $\xi(\bar{\xi}_1, u(\cdot), t)$ lie inside $\mathcal{M}$, the respective output functions $y_1(\cdot)$ and $y_1(\cdot)$ are indistinguishable.

Definition 1.8 (set of M-indistinguishable points) *The set of points that are M-indistinguishable from a given initial state $\bar{\xi} \in \mathcal{M}$ in $[0, T]$ is defined as*

$$I_{\mathcal{M},T}(\bar{\xi}) \stackrel{def}{=} \left\{ \bar{\xi}_1 \in \mathcal{X} | \, \bar{\xi} \, I_{\mathcal{M},T} \, \bar{\xi}_1 \right\}.$$

Definition 1.9 (local observability) *A state $\bar{\xi}$ is said to be locally observable if for every open neighborhood $\mathcal{M}$ of $\bar{\xi}$, the set of states that are M-indistinguishable from $\bar{\xi}$ contains only $\bar{\xi}$:*

$$I_{\mathcal{M},t}(\bar{\xi}) = \{\bar{\xi}\}, \forall \mathcal{M} \in \mathcal{X}.$$

A system Σ is said to be locally observable in $[0, T]$ if every given state $\bar{\xi}$ is locally observable.

A weaker concept of observability is also defined when the scope is that of distinguishing $\bar{\xi}$ within a local neighborhood.

Definition 1.10 (weak observability) *A state $\bar{\xi}$ is said to be weakly observable if there exists an open neighborhood $\mathcal{M}$ of $\bar{\xi}$, such that the set of states that are indistinguishable from $\bar{\xi}$ contains only $\bar{\xi}$:*

$$\exists \mathcal{M} : I_T(\bar{\xi}) \cap \mathcal{M} = \{\bar{\xi}\}, \forall u(\cdot) \in \mathcal{U}, \forall y(.) \in \mathcal{Y}.$$

A system Σ is said to be weakly observable in $[0, T]$ if it is so for every $\bar{\xi}$.

And one last definition:

Definition 1.11 (local weak observability)*A state $\bar{\xi}$ is said to be locally weakly observable if there exists an open neighborhood $\mathcal{M}$ of $\bar{\xi}$, such that for every open neighborhood $\mathcal{V}$ of $\bar{\xi}$ contained in $\mathcal{M}$, the set of states that are $\mathcal{V}$ indistinguishable from $\bar{\xi}$ contains only $\bar{\xi}$:*

$$\exists \mathcal{M} : I_{\mathcal{V},T}(\bar{\xi}) \cap \mathcal{M} = \{\bar{\xi}\}, \forall \mathcal{V}$$

Remark 1.1 *Local observability implies in observability and local weak observability. Observability implies in weak observability. Local weak observability implies in weak observability.*

Local Weak Observability of Nonlinear Systems

Let's consider the continuous time-invariant system Σ:

$$\Sigma = \begin{cases} \dot{\xi}(t) = f(\xi, u) \\ y(t) = h(\xi(t)) \end{cases} . \tag{1.22}$$

Let the the Lie derivative of a scalar function $\lambda(\xi)$ along the vector-field $f(\xi)$ be given by

$$L_f\lambda(\xi) = \frac{\partial \lambda}{\partial \xi} f(\xi).$$

And let the Lie derivative of order k be given by

$$L_f{}^{(k)}\lambda(\xi) = \overbrace{L_f\left(\ldots\left(L_f\lambda(\xi)\right)\right)}^{\text{k times}}.$$

Definition 1.12 (observation space) *The observation space $\mathcal{O}$ of Σ is the linear space (over $\mathbb{R}$) of functions on $\mathcal{X}$ that contain $h_1, h_2, \cdots, h_p$ and all repeated Lie-derivatives*

$$L_f{}^{(k)}h_j, j \in p\,,\ k = 1, 2, \cdots$$

Definition 1.13 (observability codistribution) *The observability codistribution $d\mathcal{O}$ associated with the observation space $\mathcal{O}$ is:*

$$d\mathcal{O}(q) = span\{dH(q) | H \in \mathcal{O}\}, q \in X.$$

The observability codistribution denotes the linear space of finite linear combinations of the gradients of the repeated Lie-derivatives of h_j along $f(\xi, u)$.

We can rewrite $d\mathcal{O}$ as follows:

$$d\mathcal{O}(\xi) = \text{span}\left(\partial_\xi h_1, \ldots, \partial_\xi h_p, \partial_\xi L_f h_1, \ldots, \partial_\xi L_f h_p, \partial_\xi L_f{}^{(1)} h_1, \ldots, \partial_\xi L_f{}^{(1)} h_p, \ldots\right). \tag{1.23}$$

The main theorem concerning weak observability of nonlinear systems (refer to definition 1.10) is the following:

Theorem 1.1 ([12])

A system Σ is locally weakly observable at $\xi = \bar{\xi}$ if the following is satisfied:

$$dim(d\mathcal{O}(\bar{\xi})) = dim(\bar{\xi}).$$

The above condition is called observability rank condition at $\bar{\xi}$.

The system Σ is locally weakly observable if the above is true for every $\xi \in \mathcal{X}$.

Local Weak Observability of Control Affine Systems

Let's consider the continuous time-invariant control affine system Σ:

$$\begin{array}{l} \dot{\xi} = f(\xi) + G(\xi)u \\ y = h(\xi) \end{array},$$

where the vector field f is the drift term and matrix G contains the m velocity fields (for $\dim(u) = m$):

$$G = \left[\begin{array}{ccc} g_1 & \dots & g_m \end{array} \right].$$

Let the Lie Derivative of a covector field $\omega(\xi)$ along a vector field $f(\xi)$ be given by:

$$L_f\omega = f^T \left[\frac{\partial \omega^T}{\partial \xi} \right]^T + \omega \frac{\partial f}{\partial \xi},$$

and let the lie derivative of a generic codistribution $\Omega = \left(\begin{array}{ccc} \omega_1 & \omega_2 & \dots \end{array} \right)^T$ along a distribution $\Delta = \left(\begin{array}{ccc} f_1 & f_2 & \dots \end{array} \right)$ be given by

$$L_\Delta \Omega = \left[\begin{array}{c} L_{f_1}\omega_1 \\ L_{f_2}\omega_1 \\ \vdots \\ L_{f_1}\omega_2 \\ L_{f_2}\omega_2 \\ \vdots \end{array} \right].$$

Now, let's define the codistribution Δ_Σ:

$$\Delta_\Sigma = \left[\begin{array}{cccc} f & g_1 & \dots & g_m \end{array} \right],$$

and the codistribution Ω_0:

$$\Omega_0 = \frac{\partial h(\xi)}{\partial \xi}.$$

If we apply the following observability codistribution algorithm:

$$\Omega_1 = \Omega_0 + L_{\Delta_\Sigma}\Omega_0 \tag{1.24}$$
$$\Omega_k = \Omega_k + L_{\Delta_\Sigma}\Omega_k \tag{1.25}$$

we will have that:

$$d\mathcal{O}(\xi) = \operatorname{span}\left[\Omega_\infty\right].$$

The result of the presented algorithm is equivalent to eq. 1.23.

We may refer to $\Omega^{(i)}$ to the ith submatrix of Ω that corresponds to the ith level of Lie Bracketing in the algorithm presented, i.e.:

$$\Omega_k = \left[\begin{array}{c} \Omega^{(0)} \\ \Omega^{(1)} \\ \Omega^{(k)} \end{array} \right].$$

Whenever necessary, we may also explicit the terms in $\Omega^{(i)}$ as follows:

$$\Omega^{(i)} = \left[\begin{array}{cccc} \partial_{\xi_1} L_{\Delta_\Sigma} h & \partial_{\xi_2} L_{\Delta_\Sigma} h & \dots \end{array} \right],$$

for a given $\xi = (\xi_1, \xi_2, \ldots)$.

Local Decomposition

If a control affine system is not observable in the sense of rank condition, there exists a coordinate mapping $\zeta = \Phi(\xi)$ for which it can be decomposed into observable and non observable subsystems as follows:

$$\begin{array}{l} \dot{\zeta}_{\bar{o}} = f_{\bar{o}}\left(\zeta_o, \zeta_{\bar{o}}\right) + g_{\bar{o}}\left(\zeta_o, \zeta_{\bar{o}}\right) u \\ \dot{\zeta}_o = f_o\left(\zeta_o\right) + g_o\left(\zeta_o\right) u \\ y = h_o\left(\zeta_o\right) \end{array}, \tag{1.26}$$

where the observable subsystem is given by ζ_o and the non-observable subsystem is given by $\zeta_{\bar{o}}$. The subsystem ζ_o satisfies the rank condition. The local decomposition for linear systems 1.26 was originally named Kalman observable canonical form.

Chapter 2

On the Unknown Input Observability Problem

2.1 Unknown State Left Invertibility as an Observability Problem

System invertibility (or left-invertibility) regards the possibility of reconstructing unknown inputs from the knowledge of the outputs. In this section we will show how the observability rank condition can be used to study the left invertibility of a system.

Definition 2.1 (unknown-state, unknown-input system invertibility) *A system is said to be unknown-state, unknown-input system reconstructable or invertible, if the map $x \to y$ is invertible, i.e., $ker(y) = 0$.*

However, one can pose the invertibility question as an observability problem. Questioning the possibility of reconstructing both state and input, given that only the measurements are available is a problem here defined as follows.

Problem 2.1 Unknown input and unknown state observation: *Given corresponding known output function $y(\cdot)$ and two instants of time*

$t_0 = 0$, $t_1 = T$, determine the initial state $\bar{x}$ (or the set of initial states), and input $\bar{u}(t)$ for all $t \in [0, T]$ (or the set of inputs), such that $y(t) = y(\bar{x}, \bar{u}(\cdot), t), \forall t \in [0, T]$;

In this section we will present a method for studying this problem using the observability rank condition (theorem 1.1). First we will show how to extend the use of rank condition in order to study the possibility of reconstructing both state and input when one can assume that inputs are constant over time, i.e., $\dot{u}(t) = 0$ (section 2.1.1). Then we will extend the concept to analytical inputs (section 2.1.1)).

2.1.1 UIUSO for unknown constant inputs

Let's consider the continuous time-invariant system Σ presented in eq. 1.22. Assuming constants inputs $\dot{u}(t) = 0$, we may define the extended (or augmented) system:

$$\xi_e = \begin{bmatrix} \xi_\Sigma \\ \xi_u \end{bmatrix} = \begin{bmatrix} \xi_1 \\ \xi_2 \end{bmatrix} = \begin{bmatrix} \xi \\ u \end{bmatrix},$$

where we will use the notation ξ_Σ to refer to the state of the original system Σ from now on. Hence, system dynamics becomes:

$$\dot{\xi_e} = f_e(\xi_e) = \begin{bmatrix} f(\xi_\Sigma) + g(\xi_\Sigma)\, u \\ 0 \end{bmatrix}.$$

To apply theorem 1.1 to the augmented system presented is to study the observability of both original state ξ_Σ and input u concurrently. Cases of such use of the rank condition can be found in literature, as for example in [61], where observability problems related to visual motion are investigated. If such a system is observable, one may foresee the design of observers that may construct not only the state ξ_Σ but also input u using only available measurements y.

However, one may question if ξ and u observable under the assumption that $\dot{u}(t) = 0$ implies that ξ and u are observable for any function $u = f(t)$. Let's investigate how to study that in the next section.

2.1.2 UIUSO for unknown analytical inputs

Here we will define an augmented system analogous to the one defined in the previous section. However we will relax the assumption made for the input function $u = f(t)$.

Taylor Expansion of Input

Assuming that the input is analytical, we may rewrite it as a Taylor expansion around $u(0)$:

$$u(0)=u_0,$$
$$u(t) = \sum_{i=0}^{\infty} {u_0}^{(i)} \frac{t^i}{i!}.$$

Now let's define ${}^n u(t)$ as the partial expansion:

$${}^n u(t) = u_0 + {u_0}^{(1)} t + \ldots + {u_0}^{(n)} \frac{t^n}{n!} + O(n+1),$$
$$u^{(n+1)} = 0.$$

One may verify that the infinite expansion ${}^\infty u(t)$ corresponds to the original input $u(t)$:

$${}^\infty u \approx u(t), {}^\infty u^{(\infty)} \approx 0.$$

System definition

Now, in a similar manner to what was done in section 2.1.1, let's define an augmented system for which the state ξ_e comprehends not only the original state ξ_Σ but also the input. If we rewrite $u(t)$ as presented in eq. 2.1.2, the augmented system ξ_e becomes

$$\xi_e = \begin{bmatrix} \xi_1 \\ \xi_2 \\ \xi_3 \\ \vdots \end{bmatrix} = \begin{bmatrix} \xi_\Sigma \\ u \\ \dot{u} \\ \vdots \end{bmatrix},$$

and corresponding system dynamics

$$\dot{\xi}_e = f_e(\xi_e) = \begin{bmatrix} f(\xi_\Sigma) + g(\xi_\Sigma)\, u \\ \xi_3 \\ \xi_4 \\ \vdots \end{bmatrix}.$$

Finally, system output is expressed as a function of ξ_1 only:

$$y = h(\xi_1)$$

Observability analysis

As one may note, the dimension of ξ_e is infinite, and the application of theorem 1.1 to such a system is not straightforward. Therefore, in order to show the observability of the system defined in eq. 2.1.2 we can proceed as follows.

Let's define the truncated state ${}^n\xi_e$ that corresponds to the partial input expansion ${}^n u(t)$:

$${}^n\xi_e = \begin{bmatrix} \xi_1 \\ \xi_2 \\ \xi_3 \\ \vdots \\ \xi_{n+2} \end{bmatrix} = \begin{bmatrix} \xi_\Sigma \\ u \\ u^{(1)} \\ \vdots \\ u^{(n)} \end{bmatrix}.$$

The dynamics of the truncated system on the natural assumption that $u^{(n+1)} = 0$ becomes

$${}^n\dot{\xi}_e = f_e({}^n\xi_e) = \begin{bmatrix} f(\xi_\Sigma) + g(\xi_\Sigma)\, u \\ \xi_3 \\ \xi_4 \\ \vdots \\ 0 \end{bmatrix},$$

and system output is expressed as shown before:

$$y = h(\xi_1).$$

Proposition 2.1 *The original system is observable if one is able to show :*

- ${}^{0}\xi_e$ *is observable*
- ${}^{k}\xi_e observable \rightarrow {}^{k+1}\xi_e observable$

Proof 2.1 *If* ${}^{0}\xi_e$ *is observable and* $({}^{k}\xi_e observable \rightarrow {}^{k+1}\xi_e observable)$*, then* ${}^{n}\xi_e$ *is observable* $\forall n$*, what implies that* ${}^{\infty}\xi_e$ *is observable.*

According to definition eq. 2.1.2:

$$ {}^{\infty}\xi_e = \xi_e = \begin{bmatrix} \xi_\Sigma \\ u \\ \dot{u} \\ \vdots \end{bmatrix}. $$

Hence, one may conclude that the original system is observable.

In the following sections we will apply the methodology proposed here to study the observability of both state and input for scalar SISO Linear Systems, for n-dimensional SISO Linear Systems and for Affine in Control SISO Nonlinear Systems.

2.2 UIUSO analysis of one-Dimensional SISO Linear Systems

Let's consider the scalar (one-dimensional) representation of the linear system presented in eq. 1.2.4:

$$ \Sigma = \begin{cases} \dot{\xi}_\Sigma = a\,\xi_\Sigma + b\,u \\ y = c\,x \end{cases}, $$

where $a, b, c, \xi \in \mathbb{R}^1$.

The observability matrix of the scalar system Σ is

$$ \mathrm{O}_\Sigma = (c). $$

And the condition for Σ to be observable is simply that $c \neq 0$.

2.2.1 Observability Matrix of ${}^n\xi_e$

Now, let's define the truncated augmented state ${}^n\xi_e$ (as seen in section 2.1.2) for the system Σ defined in eq. 2.2:

$$ {}^n\xi_e = \begin{bmatrix} \xi_\Sigma \\ u \\ \vdots \\ u^{(n+1)} \end{bmatrix}. $$

The associated system dynamics become:

$$ \begin{cases} {}^n\dot{\xi}_e = {}^nA_e \, {}^n\xi_e \\ {}^ny = {}^nC_e \, {}^n\xi_e \end{cases}, $$

where:

$$ {}^nA_e = \begin{bmatrix} a & b & 0 & \cdots & 0 \\ 0 & 0 & 1 & \cdots & 0 \\ \vdots & \vdots & \vdots & \ddots & \vdots \\ 0 & 0 & 0 & 0 & 1 \\ 0 & 0 & 0 & 0 & 0 \end{bmatrix} \in \mathbb{R}^{n+2,\,n+2}, $$

and

$$ {}^nC_e = \begin{bmatrix} c & 0 & \cdots & 0 \end{bmatrix} \in \mathbb{R}^{1,\,n+2}. $$

One may verify that the observability matrix associated to the truncated augmented system is

$$ {}^nO = \begin{bmatrix} c & 0 & 0 & \dots & 0 \\ \mathrm{ca} & \mathrm{cb} & 0 & \dots & 0 \\ \mathrm{ca}^2 & \mathrm{cab} & \mathrm{cb} & \dots & 0 \\ \mathrm{ca}^3 & \mathrm{ca}^2b & \mathrm{cab} & \ddots & \vdots \\ \mathrm{ca}^4 & \mathrm{ca}^3b & \mathrm{ca}^2b & \ddots & 0 \\ \vdots & \vdots & \vdots & \ddots & 0 \\ \mathrm{ca}^{n+1} & \mathrm{ca}^nb & \mathrm{ca}^{n-1}b & \dots & \mathrm{cb} \end{bmatrix} \in \mathbb{R}^{n+2,\,n+2}. $$

2.2.2 UIUSO Analisys

If we proceed with the observability analysis as presented in section 2.1.2 we obtain the following result:

Theorem 2.1 *Consider a system like in eq. 2.2. If ξ_Σ and u are observable for $\dot{u} = 0$, then ξ_Σ and u are observable for any $u(t) = f(t)$ if $f(t)$ is analytical.*

This theorem can be proved proceeding with the observability analysis as follows:

Proof 2.2 *The observability matrix for the augmented system ${}^0\xi_e = (\xi_\Sigma, u)$ when $\dot{u} = 0$, is given by*

$$ {}^0O_e = \begin{bmatrix} c & 0 \\ ca & cb \end{bmatrix}. $$

If system is observable that ${}^0\xi_e$ the following must be true:

- $c \neq 0$;
- $a \neq 0$;
- $b \neq 0$;

Now let's assume ${}^k\xi_e$ observable. We may simplify the observability matrix ${}^kO_e$ as

$$ \begin{bmatrix} * & \vec{0} \\ * & cb \end{bmatrix}. $$

If ${}^k\xi_e$ is observable then $rank({}^kO_e) = dim({}^k\xi_e) = k + 2$.
The observability matrix ${}^{k+1}O_e$ is

$$ {}^{k+1}O_e = \begin{bmatrix} {}^kO_e & 0 \\ * & cb \end{bmatrix}, $$

and it is straightforward to see that, as $cb \neq 0$, $rank\left({}^{k+1}O_e\right) = rank\left({}^{k}O_e\right) + 1$. *Consequently,*

$$rank\left({}^{k+1}O_e\right) = k + 3 = \dim\left({}^{k+1}\xi_e\right).$$

Therefore, ${}^{k}\xi_e$ *being observable implies in* ${}^{k+1}\xi_e$ *observable.*

Following proposition 2.1, one may conclude that both state and input are observable for any given analytical input.

2.3 UIUSO analysis of n-Dimensional SISO Linear Systems

Let's revisit the linear system presented already presented in eq. 1.2.4:

$$\Sigma = \begin{cases} \dot{\xi_\Sigma} = A\xi_\Sigma + Bu \\ y = C\xi_\Sigma \end{cases}$$

Here, we will consider the single input single output (SISO) case, i.e.,

$$n = dim(\xi_\Sigma)\ ,\ m = dim(u) = 1\ ,\ p = dim(y) = 1,$$

$$A \in \mathbb{R}^{\mathrm{nxn}}, B \in \mathbb{R}^{\mathrm{nx1}}, C \in \mathbb{R}^{\mathrm{pxn}}.$$

As already presented, the observability codistribution of this system is given by

$${}^{x}d\mathcal{O}_\Sigma = \mathrm{span}\left(\begin{bmatrix} C \\ \mathrm{CA} \\ \vdots \\ \mathrm{CA}^{n-1} \end{bmatrix}\right).$$

2.3.1 Observability Matrix of ${}^N\xi_e$

Now, let's define the truncated augmented state ${}^N\xi_e$ (as seen in section 2.1.2) for the system Σ defined in eq. 2.3:

$$ {}^N\xi_e = \begin{bmatrix} \xi_\Sigma \\ u \\ u^{(1)} \\ \vdots \\ u^{(N)} \end{bmatrix}, $$

which dimension is

$$ \dim\left({}^N\xi_e\right) = n + m * (N+1). $$

The corresponding system dynamics is

$$ {}^N\dot{\xi}_e = \begin{bmatrix} A & B & 0 & 0 & \dots & 0 \\ 0 & 0 & I & 0 & \dots & 0 \\ 0 & 0 & 0 & I & \dots & 0 \\ \vdots & \vdots & \vdots & \vdots & \ddots & \vdots \\ 0 & 0 & 0 & 0 & \dots & I \\ 0 & 0 & 0 & 0 & \dots & 0 \end{bmatrix} {}^N\xi_e, $$

$$ {}^Ny = \begin{bmatrix} C & 0 & 0 & \dots & 0 \end{bmatrix} {}^N\xi_e. $$

Finally, the observability codistribution that corresponds to ${}^N\xi_e$ is given by

$$ {}^Nd\mathcal{O}_e = \text{span}\left(\left[\begin{array}{cccc} C & 0 & \dots & 0 \\ \text{CA} & \text{CB} & \dots & 0 \\ \text{CA}^2 & \text{CAB} & \ddots & 0 \\ \vdots & \vdots & \vdots & \text{CB} \\ \text{CA}^{N+2} & \text{CA}^{N+1}B & \cdots & \text{CAB} \\ \vdots & \vdots & \dots & \vdots \\ \text{CA}^{N+n} & \text{CA}^{N+n-1}B & \dots & \text{CA}^{n-1}B \end{array}\right]\right). $$

2.3.2 UIUSO Analisys

Once again, proceeding with the observability analysis (section 2.1.2) leads us to the following theorem:

Theorem 2.2 *Consider the system defined in eq. 2.3. If ξ_Σ and u are observable for $\dot{u} = 0$ and:*

$$CA^iB = 0 \,\forall\, i \leq n-2,\ CA^{n-1}B \neq 0,$$

then ξ_Σ and u are observable for any $u(t) = f(t)$ if $f(t)$ is analytical.

Proof 2.3 *The observability matrix for the augmented system ${}^0\xi_e = (\xi_\Sigma, u)$ when $\dot{u} = 0$, is given by*

$${}^0O_e = \begin{bmatrix} C & 0 \\ CA & CB \\ CA^2 & CAB \\ \vdots & \vdots \\ CA^n & CA^{n-1}B \end{bmatrix}.$$

If system is observable for ${}^0\xi_e$, then rank $({}^0O_e) = n+1$,i.e., ${}^0O_e$ is full rank.

Note that

$$CA^i \in \mathbb{R}^{1\times n},\ CA^iB \in \mathbb{R}^{1\times 1}.$$

Now let's assume ${}^k\xi_e$ observable. We may simplify the observablity matrix ${}^kO_e$ as

$${}^kO_e = \begin{bmatrix} * & \dots & 0 \\ \vdots & \vdots & CB \\ CA^{k+2} & \cdots & CAB \\ \vdots & \dots & \vdots \\ CA^{k+n} & \dots & CA^{n-1}B \end{bmatrix}.$$

If ${}^kO_e$ is observable then rank $\left({}^kO_e\right) = k+n+1$.

The observability matrix of ${}^{k+1}\xi_e$ *is*

$$
{}^{k+1}O_e = \left[\begin{array}{ccccc|c}
C & 0 & \dots & 0 & | & 0 \\
CA & CB & \dots & 0 & | & 0 \\
CA^2 & CAB & \ddots & 0 & | & 0 \\
\vdots & \vdots & \vdots & CB & | & 0 \\
CA^{k+2} & CA^{k+1}B & \cdots & CAB & | & CB \\
\vdots & \vdots & \dots & \vdots & | & CAB \\
CA^{k+n} & CA^{k+n-1}B & \dots & CA^{n-1}B & | & \vdots \\
- - - & - - - & - - - & - - - & + & - - - \\
CA^{k+n+1} & CA^{k+n}B & \dots & CA^nB & | & CA^{n-1}B
\end{array}\right] =
$$

$$
=^{k+1} O_e = \left[\begin{array}{cc|c}
 & & 0 \\
 & & CB \\
{}^kO_e & | & CAB \\
 & & \vdots \\
- - - & + & - - - \\
* & | & CA^{n-1}B
\end{array}\right].
$$

If $CA^iB = 0 \,\forall\, i \leq n-2$ *and* $CA^{n-1}B \neq 0$ *then*

$$
{}^kO_e = \left[\begin{array}{cc|c}
* & | & 0 \\
- - - & + & - - - \\
* & | & CA^{n-1}B
\end{array}\right],
$$

and

$$
\textit{and } {}^{k+1}O_e = \left[\begin{array}{cc|c}
{}^kO_e & | & 0 \\
- - - & + & - - - \\
* & | & CA^{n-1}B
\end{array}\right],
$$

and, consequently

$$
rank\left({}^{k+1}O_e\right) = rank\left({}^kO_e\right) + 1.
$$

Therefore,

$$
CA^iB = 0 \forall i \leq n-2,
$$

and

$$CA^{n-1}B \neq 0 \| {}^{k}O_e \, observable \rightarrow {}^{k+1}O_e \, observable.$$

However, if $\exists i \leq n-2 \longrightarrow \mathrm{CA}^i B \neq 0$, ${}^{k}O_e$ observable does not imply that ${}^{k+1}O_e$ is observable and we can't say anything about the observability of an arbitrary analytical $u(t)$. One example of such a case is presented as follows:

Example 1

Consider a system defined in eq. 2.3 for which A, B, C are defined as follows:

$$A = \begin{bmatrix} 0 & 1 \\ -1 & 1 \end{bmatrix},$$

$$B = \begin{bmatrix} - & 1 \\ & 1 \end{bmatrix},$$

and

$$C = \begin{bmatrix} 0 & 1 \end{bmatrix}$$

The observability matrix of the augmented system, when assuming constant inputs, is

$${}^{0}O_e = \begin{bmatrix} 0 & 1 & 0 \\ 1 & -1 & 1 \\ -1 & 2 & -2 \end{bmatrix}.$$

The rank of the observability matrix is:

$$\mathrm{rank}\left({}^{0}O_e\right) = \dim({}^{0}\xi) = 3,$$

and consequently, ${}^{0}\xi$ is observable. However this is not true for any $u(t)$, as a matter of fact ${}^{73}\xi$ is not observable:

$$\mathrm{rank}\left({}^{73}O_e\right) = \dim({}^{73}\xi) - 1 = 75.$$

2.4 UIUSO analysis of Non-Linear Systems

Let's consider the state representation of a control-affine nonlinear system:

$$\Sigma = \begin{cases} \dot{\xi}_\Sigma = f(\xi_\Sigma) + g(\xi_\Sigma)\, u \\ y = h(\xi_\Sigma) \end{cases} . \tag{2.1}$$

Here, we will consider the single input single output (SISO) case, i.e.,

$$n = dim(\xi_\Sigma)\ ,\ m = dim(u) = 1\ ,\ p = dim(y) = 1.$$

In the following section we will study the observability codistribution form of the truncated augmented state ${}^N\xi_e$ that corresponds to Σ (as seen in section 2.1.2).

2.4.1 Codistribution Form

In order to apply the methodology proposed in section 2.1 to study the observability of both state and input (represented by the augmented state ξ_e), we have to investigate the observability codistribution form associated to the truncated augmented state ${}^N\xi_e$. While this analysis is particularly straightforward in the case of a linear system (as seen in section 2.3), it requires a more detailed investigation for the case of nonlinear systems.

In 2.4.1 we will study the codistribution form associated to the truncated state ${}^0\xi_e$. In 2.4.2 we will study some basic rules that show how the codistribution form evolves from basic configurations defined for ${}^k d\mathcal{O}_e$ to ${}^{k+1} d\mathcal{O}_e$. Finally we will apply this rules and use inductive reasoning to find a generic form of ${}^N\xi_e$ in 2.4.2.

Truncated system ${}^0\xi_e$

The augmented state ${}^0\xi_e$ of the system Σ from eq. 2.1 can be defined as:

$${}^0\xi_e = \begin{bmatrix} \xi_1 & \xi_2 \end{bmatrix}^T = \begin{bmatrix} \xi_\Sigma & u \end{bmatrix}^T ,$$

where

$$\dim(\xi_1) = n \ , \ \dim\left({}^0\xi_e\right) = n+1.$$

The corresponding system dynamics can be generalized as:

$$\begin{aligned} {}^0\dot{\xi}_e &= {}^0f_e(\xi_e), \\ y &= h(\xi_1), \end{aligned}$$

where

$${}^0f_e = \begin{bmatrix} \dot{\xi}_e & 0 \end{bmatrix} = \begin{bmatrix} z(\xi_1, \xi_2) & 0 \end{bmatrix}.$$

The observability codistribution can be written in a generic form as

$${}^0d\mathcal{O}_e = \text{span}\left(\begin{bmatrix} \eta(\xi_1) & 0 \\ * & a_0(\xi_1, \xi_2) \\ * & a_1(\xi_1, \xi_2) \\ * & * \end{bmatrix}\right), \text{where } \eta(\xi_1) = \frac{\partial h}{\partial \xi_1}.$$

We can further simplify it in order to represent a system where $a_i = 0$ for $i = 0 : m$, $m \geq 0$:

$${}^0d\mathcal{O}_e = \text{span}\left(\begin{bmatrix} \eta(\xi_1) & 0 \\ \boldsymbol{o}(\xi_1, \xi_2) & 0 \\ b(\xi_1, \xi_2) & \alpha(\xi_1, \xi_2) \\ * & * \end{bmatrix}\right). \tag{2.2}$$

Note that $\boldsymbol{o}(\xi_1, \xi_2)$ is $\{\}$ if $a_0 \neq 0$ and the codistribution would become

$${}^0d\mathcal{O}_e = \text{span}\left(\begin{bmatrix} \eta(\xi_1) & 0 \\ b(\xi_1, \xi_2) & \alpha(\xi_1, \xi_2) \\ * & * \end{bmatrix}\right).$$

2.4.2 Codistribution form evolution from ${}^kd\mathcal{O}_e$ to ${}^{k+1}d\mathcal{O}_e$

In this section we study three basic configurations for the codistribution matrix ${}^k\Omega_e$ associated to the observability codistribution ${}^kd\mathcal{O}_e$ and how they evolute in the codistribution ${}^{k+1}\Omega_e$.

Proposition 2.2 *If* ${}^{k}\Omega_e$ *has the following form:*

$$ {}^{k}\Omega_e \Rightarrow \begin{bmatrix} \vec{\eta} & 0 & \dots & 0 \\ * & * & * & * \end{bmatrix}, $$

then ${}^{k+1}\Omega_e$ *will have the following form:*

$$ {}^{k+1}\Omega_e \Rightarrow \begin{bmatrix} \vec{\eta} & 0 & \dots & 0 & 0 \\ * & * & * & * & * \end{bmatrix}. $$

Proof 2.4 *Let's detail the first row of* ${}^{k}\Omega_e$*:*

$$ {}^{k}\Omega_e \Rightarrow \begin{bmatrix} \vec{\eta} & 0 & \dots & 0 \\ * & * & * & * \end{bmatrix} = \begin{bmatrix} {}^{k}dh \\ * \end{bmatrix}, $$

where the derivative ${}^{k}dh$ *is*

$$ {}^{k}dh \Rightarrow \left[\frac{\partial h}{\partial \xi_1}, \frac{\partial h}{\partial \xi_2}, \dots, \frac{\partial h}{\partial \xi_{k+3}} \right] = [\vec{\eta}, 0, \dots, 0]. $$

For $k+1$ *we would have*

$$ {}^{k+1}dh \Rightarrow \left[\frac{\partial h}{\partial \xi_1}, \frac{\partial h}{\partial \xi_2}, \dots, \frac{\partial h}{\partial \xi_{k+3}}, \frac{\partial h}{\partial \xi_{k+4}} \right] = [\vec{\eta}, 0, \dots, 0, 0], $$

and ${}^{k+1}\Omega_e$ *becomes*

$$ {}^{k+1}\Omega_e \Rightarrow \begin{bmatrix} \vec{\eta} & 0 & \dots & 0 & 0 \\ * & * & * & * & * \end{bmatrix} = \begin{bmatrix} {}^{k}\Omega_e & 0 \\ & * \end{bmatrix}. $$

Hence, we can conclude that

$$ {}^{k}\Omega_e \Rightarrow \begin{bmatrix} \vec{\eta} & 0 & \dots & 0 \\ * & * & * & * \end{bmatrix} \rightarrow {}^{k+1}\Omega_e \Rightarrow \begin{bmatrix} \vec{\eta} & 0 & \dots & 0 & 0 \\ * & * & * & * & * \end{bmatrix} $$

Proposition 2.3 *If* ${}^{k}\Omega_e$ *has the following form:*

$$ {}^{k}\Omega_e \Rightarrow \begin{bmatrix} * & * \\ \vec{a} & 0 \\ \vec{b} & c \\ * & * \end{bmatrix}, $$

then ${}^{k+1}\Omega_e$ *will have the following form:*

$$ {}^{k+1}\Omega_e \Rightarrow \left[\begin{array}{ccc} * & * & * \\ \vec{a} & 0 & 0 \\ \vec{b} & c & 0 \\ * & * & * \end{array} \right]. $$

Proof 2.5 *Given* ${}^{k}\Omega_e$ *as defined in proposition 2.3, we can question the form of* ${}^{k+1}\Omega$ *in a symbolical way as follows:*

$$ {}^{k}\Omega_e \Rightarrow \left[\begin{array}{cc} * & * \\ \vec{a} & 0 \\ \vec{b} & c \\ * & * \end{array} \right] \rightarrow {}^{k+1}\Omega_e \Rightarrow \left[\begin{array}{ccc} * & * & * \\ \vec{a} & 0 & 0 \\ ? & ? & ? \\ * & * & * \end{array} \right]. $$

First, let's inspect ${}^{k}\Omega_e$ *in detail:*

$$ {}^{k}\Omega_e \Rightarrow \left[\begin{array}{cc} * & * \\ \vec{a} & 0 \\ \vec{b} & c \\ * & \end{array} \right] = \left[\begin{array}{c} * \\ {}^{k}dLf^{(i)}h \\ {}^{k}dLf^{(i+1)}h \\ * \end{array} \right], $$

where

$$ {}^{k}Lf^{(i+1)}h = {}^{k}f.\,{}^{k}dLf^{(i)}h = \ldots\ldots\,(z(*), \xi_3, \ldots, \xi_{k+2}, 0)\,.\,(\vec{a}, 0)\,, $$

and, consequently,

$$ \vec{b} = \frac{\partial\left({}^{k}Lf^{(i+1)}h\right)}{\partial\left(\xi_1, \ldots, \xi_{k+1}\right)} = \frac{\partial\left({}^{k}f.\vec{a}\right)}{\partial\left(\xi_1, \ldots, \xi_{k+1}\right)}, $$

and

$$ c = \frac{\partial\left({}^{k}Lf^{(i+1)}h\right)}{\partial\xi_{k+2}} = \frac{\partial\left({}^{k}f.\vec{a}\right)}{\partial\xi_{k+2}}. $$

Now let's further investigate ${}^{(k+1)}\Omega_e$*:*

$$ {}^{k+1}\Omega_e \Rightarrow \begin{bmatrix} * & * & * \\ \vec{a} & 0 & 0 \\ \vec{b}_* & c_* & d_* \\ * & * & * \end{bmatrix} = \begin{bmatrix} * \\ {}^{k+1}dLf^{(i)}h \\ {}^{k+1}dLf^{(i+1)}h \\ * \end{bmatrix}, $$

where

$$ {}^{k+1}Lf^{(i+1)}h = {}^{k+1}f.{}^{k}dLf^{(i)}h = $$
$$ = (z(*), \xi_3, \ldots, \xi_{k+2}, \xi_{k+3}, 0) \,.\, (\vec{a}, 0, 0) = $$
$$ = (z(*), \xi_3, \ldots, \xi_{k+2}, 0) \,.\vec{a} = {}^{k}Lf^{(i+1)}h. $$

Hence:

$$ \vec{b}_* = \vec{b},\ \vec{c}_* = \vec{c}, $$

and

$$ d_* = \frac{\partial \left({}^{k}f.\vec{a} \right)}{\partial \xi_{k+3}} = \frac{\partial (^*(\xi_1, \ldots, \xi_{k+2}))}{\partial \xi_{k+3}} = 0, $$

and we can conclude that

$$ {}^{k}\Omega_e \Rightarrow \begin{bmatrix} * & * \\ \vec{a} & 0 \\ \vec{b} & c \\ * & * \end{bmatrix} \rightarrow {}^{k+1}\Omega_e \Rightarrow \begin{bmatrix} * & * & * \\ \vec{a} & 0 & 0 \\ \vec{b} & c & 0 \\ * & * & * \end{bmatrix}. $$

Proposition 2.4 *If* ${}^{k}\Omega_e$ *has the following form:*

$$ {}^{k}\Omega_e \Rightarrow \begin{bmatrix} * & * \\ * & c \\ * & * \end{bmatrix}, $$

then ${}^{k+1}\Omega_e$ *will have the following form:*

$$ {}^{k+1}\Omega_e \Rightarrow \begin{bmatrix} * & * & * \\ * & c & 0 \\ * & * & c \end{bmatrix}. $$

Proof 2.6 *Once again, let's question the form of* ${}^{k+1}\Omega_e$ *in a symbolical way:*

$$ {}^{k}\Omega_e \Rightarrow \begin{bmatrix} * & * \\ * & c \\ * & * \end{bmatrix} \rightarrow {}^{k+1}\Omega_e \Rightarrow \begin{bmatrix} * & * & * \\ * & c & 0 \\ * & * & * \\ * & * & ? \end{bmatrix}. $$

Let's further inspect ${}^{k+1}\Omega_e$*:*

$$ {}^{k+1}\Omega_e \Rightarrow \begin{bmatrix} * \\ dLf^{ih} \\ dLf^{i+1}h \\ * \end{bmatrix} = \begin{bmatrix} * & * & * \\ * & c & 0 \\ * & * & \frac{\partial Lf^{i+1}h}{\partial \xi_{k+3}} \\ * & * & * \end{bmatrix}, $$

where

$$ Lf^{i+1}h = f.dLf^{ih} = (z, \xi_3, \ldots, \xi_{k+3}, 0) \,.\, (*, *, *, c, 0) = $$

$$ = * \left(\xi_1, \ldots, \xi_{k+2}\right) + c \left(\xi_1, \ldots, \xi_{k+2}\right) \xi_{k+3}, $$

and

$$ \frac{\partial Lf^{i+1}h}{\partial \xi_{k+3}} = \frac{\partial \left(* \left(\xi_1, \ldots, \xi_{k+2}\right) + c \left(\xi_1, \ldots, \xi_{k+2}\right) \xi_{k+3}\right)}{\partial \xi_{k+3}} = c. $$

Therefore, one may conclude that

$$ {}^{k}\Omega_e \Rightarrow \begin{bmatrix} * & * \\ * & c \\ * & * \end{bmatrix} \rightarrow {}^{k+1}\Omega_e \Rightarrow \begin{bmatrix} * & * & * \\ * & c & 0 \\ * & * & c \end{bmatrix}. $$

Codistribution ${}^{N}d\mathcal{O}_e$ through inductive reasoning

In this section we will finally conclude on the codistribution form of ${}^{N}d\mathcal{O}_e$ using inductive reasoning.

First, let's detail the augmented states ${}^{k}\xi_e$ and ${}^{k+1}\xi_e$:

$$ {}^{k}\xi_e = \begin{pmatrix} \xi_1 & \dots & \xi_{k+2} \end{pmatrix}, \dim\left({}^{k}\xi_e\right) = n+k+1, $$

$$ {}^{k+1}\xi_e = \begin{pmatrix} \xi_1 & \dots & \xi_{k+3} \end{pmatrix}, \dim\left({}^{k}\xi_e\right) = n+k+2, $$

and their respective dynamics

$$ {}^{k}f_e = \left(z(*), \xi_3, \dots, \xi_{k+2}, 0\right), $$

and

$$ {}^{k+1}f_e = \left(z(*), \xi_3, \dots, \xi_{k+2}, \xi_{k+3}, 0\right). $$

Proposition 2.5 *If ${}^{k}d\mathcal{O}_e$ has the following form:*

$$ {}^{k}d\mathcal{O}_e = span\left(\left[\begin{array}{cc} \left(\eta\left(\xi_1\right), 0\right) & 0 \\ \left(\boldsymbol{o}\left(\xi_1, \xi_2\right), \mathbf{0}\right) & 0 \\ \omega\left(\xi_1, \xi_2\right) & \alpha\left(\xi_1, \xi_2\right) \\ * & * \\ * & * \end{array}\right]\right), \tag{2.3} $$

then ${}^{k+1}d\mathcal{O}_e$ has the following form:

$$ {}^{k+1}d\mathcal{O}_e = span\left(\left[\begin{array}{ccc} \left(\eta\left(\xi_1\right), 0\right) & 0 & 0 \\ \left(\boldsymbol{o}\left(\xi_1, \xi_2\right), \mathbf{0}\right) & 0 & 0 \\ \omega\left(\xi_1, \xi_2\right) & \alpha\left(\xi_1, \xi_2\right) & 0 \\ * & * & \alpha\left(\xi_1, \xi_2\right) \\ * & * & * \end{array}\right]\right). $$

Proof 2.7 *If we apply the rules presented in section 2.4.2 to ${}^{k}d\mathcal{O}_e$ (as seen eq. 2.3), one may conclude that:*

$$ {}^{k}\mathcal{O}_e = span\left(\left[\begin{array}{cc} \left(\eta\left(\xi_1\right), 0\right) & 0 \\ \left(\boldsymbol{o}\left(\xi_1, \xi_2\right), \mathbf{0}\right) & 0 \\ \omega\left(\xi_1, \xi_2\right) & \alpha\left(\xi_1, \xi_2\right) \\ * & * \\ * & * \end{array}\right]\right) \rightarrow $$

$$\rightarrow {}^{k+1}\mathcal{O}_e = span\left(\left[\begin{array}{ccc} (\eta(\xi_1),0) & 0 & 0 \\ (\boldsymbol{o}(\xi_1,\xi_2),\mathbf{0}) & 0 & 0 \\ \omega(\xi_1,\xi_2) & \alpha(\xi_1,\xi_2) & 0 \\ * & * & \alpha(\xi_1,\xi_2) \\ * & * & * \end{array}\right]\right).$$

If we apply the induction defined in the proposition 2.5 to the observation space ${}^0\mathcal{O}_e$ (the one relative to the augmented state truncated in $N=0$) we obtain the generic codistribution ${}^N\Omega_e$ (the one relative to ${}^N\xi_e$):

$${}^N\Omega_e = \underbrace{\left(\begin{array}{ccccc} A(\xi_1,\xi_2) & 0 & 0 & \dots & 0 \\ b(\xi_1,\xi_2) & \alpha(\xi_1,\xi_2) & 0 & \dots & 0 \\ * & * & \alpha(\xi_1,\xi_2) & \dots & 0 \\ \vdots & \vdots & \vdots & \ddots & 0 \\ * & * & * & * & \alpha(\xi_1,\xi_2) \\ * & * & * & * & * \end{array}\right)}_{n+m+1}.$$

2.4.3 UIUSO Analisys

Let' s define the subspace ${}^0\mathcal{O}_{e*}$ of the observability codistribution ${}^0d\mathcal{O}_{e*}$ (eq. 2.2) as

$${}^0\mathcal{O}_{e*} = \text{span}\left(\left[\begin{array}{cc} A(\xi_1,\xi_2) & 0 \\ b(\xi_1,\xi_2) & \alpha(\xi_1,\xi_2) \end{array}\right]\right).$$

The particular problem we are going to study is the class of systems for which the analysis of the subspace ${}^0\mathcal{O}_{e*}$ is enough in order to conclude that the system ${}^0\xi_e$ is observable. This is true if

$$\text{rank}\left({}^0\mathcal{O}_{e*}\right) = n+1$$

and

$$\alpha(\xi_1,\xi_2) \neq 0,$$

which is true by definition.

Theorem 2.3 *If under the assumption that $\dot{u} = 0$, the subspace of the codistribution of observability ${}^{0}\mathcal{O}_{e*}$ is sufficient to show that ξ_Σ and u are observable, then ξ_Σ and u are observable for any $u = f(t)$, given that $f(t)$ is analytical.*

Proof 2.8 *Assuming that ${}^{k}\xi_e$ is observable, we will check if it implies that ${}^{k+1}\xi_e$ is observable.*

The codistribution ${}^{k}d\mathcal{O}_{e*}$ associated with ${}^{k}\xi_e$ is

$$ {}^{k}d\mathcal{O}_{e*} = span\left(\begin{bmatrix} A(\xi_1,\xi_2) & 0 & 0 & \dots & 0 \\ b(\xi_1,\xi_2) & \alpha(\xi_1,\xi_2) & 0 & \dots & 0 \\ \vdots & \vdots & \vdots & \ddots & 0 \\ * & * & * & * & \alpha(\xi_1,\xi_2) \end{bmatrix}\right). $$

If it is observable, then

$$ rank\left({}^{k}d\mathcal{O}_{e*}\right) = n + k + 1 = \dim\left({}^{k}\xi_e\right). $$

The codistribution matrix ${}^{k+1}\Omega_{e*}$ associated with ${}^{k+1}\xi_e$ is

$$ {}^{k+1}\Omega_{e*} = \begin{pmatrix} A(\xi_1,\xi_2) & 0 & 0 & \dots & 0 & 0 \\ b(\xi_1,\xi_2) & \alpha(\xi_1,\xi_2) & 0 & \dots & 0 & 0 \\ \vdots & \vdots & \vdots & \ddots & 0 & 0 \\ * & * & * & * & \alpha(\xi_1,\xi_2) & 0 \\ * & * & * & * & * & \alpha(\xi_1,\xi_2) \end{pmatrix}. $$

Therefore,as $\alpha \neq 0$, $rank\left({}^{k+1}\Omega_{e*}\right) = rank\left({}^{k}\Omega_{e*}\right)+1$. As $\dim\left({}^{k+1}\xi_e\right) = \dim\left({}^{k}\xi_e\right) + 1$, it is straightforward to see that ${}^{k}\xi_e$ observable implies in ${}^{k+1}\xi_e$ observable.

2.5 A nonlinear observer and sufficient conditions for asymptotically stability

Here we propose a nonlinear observer that can be adopted in order to reconstruct augmented states that may be composed of both system

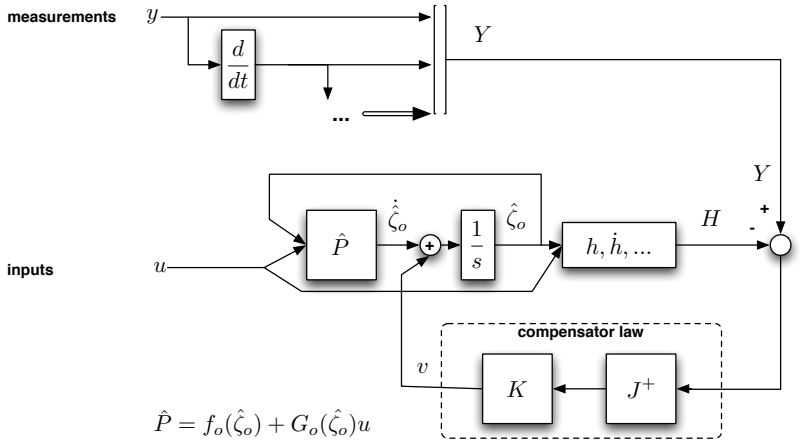

Figure 2.1: Proposed observer scheme.

original state and input disturbances as the ones presented along this chapter. We also discuss sufficient conditions to be met in order to guarantee the asymptotic stability of the observer.

Let's consider a control affine system that is already decomposed into observable and non observable subsystems, ζ_o and $\zeta_{\bar{o}}$ respectively. The observable subsystem dynamics is described in state form by $\dot{\zeta}_o = f_o(\zeta_o) + G_o(\zeta_o)u$ and system outputs can be described by $y = h_o(\zeta_o)$. The proposed observer dynamics is given by the auxiliary system (see [76] for a recent review on this topic):

$$\begin{cases} \dot{\hat{\zeta}}_o = f_o\left(\hat{\zeta}_o\right) + \sum_i g_{o_i}\left(\hat{\zeta}_o\right) u_i + v \\ \hat{y} = h_o\left(\hat{\zeta}_o\right) \end{cases} .$$

Let $e_o = \zeta_o - \hat{\zeta}_o$ be the observer error. Using the notation $\tilde{*}(x)$ to represent the symbolic operation $*(x) - *(\hat{x})$, e.g., $\tilde{f}_o(\zeta_o) = f_o(\zeta_o) - f_o(\hat{\zeta}_o)$, error dynamics is given by

$$\dot{e}_o = \tilde{f}_o(\zeta_o) + \sum_i \tilde{g}_{o_i}(\zeta_o)u_i - v\,, \tag{2.4}$$

where v is the observer compensator term. Let us choose

$$v = +KJ(\hat{\zeta_o})^{\dagger}(Y - H(\hat{\zeta_o})),$$

where $Y = \left(y^{(0)}, y^{(1)}, \ldots, y^{(l)}\right)$ is the extended output vector, $H\left(\hat{\zeta_o}\right) = \left(h_o\left(\hat{\zeta_o}\right), {h_o}^{(1)}\left(\hat{\zeta_o}\right), \ldots, {h_o}^{(l)}\left(\hat{\zeta_o}\right)\right)$ is the extended output function (l is at least the minimum order of the time derivatives required for the system to be observable), $J(\hat{\zeta_o})^{\dagger}$ is the pseudoinverse of extended output jacobian $J(\zeta_o) = \partial_{\zeta_o} H(\zeta_o)$ evaluated at $\hat{\zeta_o}$, and K is a positive definite constant gain matrix. If the system is locally weakly observable, the local approximation $J\left(\hat{\zeta_o}\right)^{\dagger}\left(Y - H\left(\hat{\zeta_o}\right)\right) = e_o + \epsilon\left(\zeta_o, \hat{\zeta_o}\right)$ is derived and the compensator term becomes $v = -K(e_o + \epsilon(\xi, \hat{\zeta_o}))$. $\epsilon(\xi, \hat{\zeta_o})$ (or simply ϵ) is the pseudoinverse approximation error. Assume that the observability codistribution associated to ζ_o is regular, i.e., not singular everywhere. An scheme of the proposed observer is presented in Fig. 2.1.

Proposition 2.6 *If* $\|\frac{e_o+\epsilon}{e_o}\|$, $\tilde{f}_o(\hat{\zeta_o})$ *and* $\tilde{G}_o(\hat{\zeta_o})$ *are bounded, the choice of a diagonal matrix* $K = diag\,(K_1, K_2, \ldots, K_h, \ldots)$, *is sufficient to guarantee asymptotic stability of the proposed observer error dynamics (please refer to eq.* (2.4)*) if*

$$K_h > \max\left(\left|\frac{e_{o_h}}{e_{o_h} + \epsilon_h}\right|\right)\left(\sup\left(\left\|\frac{\partial f_{o_h}(\zeta_o)}{\partial \zeta_o}\right\|\right) + \sum_i \sup\left(\left\|\frac{\partial g_{o_{i,h}}(\zeta_o)}{\partial \zeta_o} u_i\right\|\right)\right), \forall h, \tag{2.5}$$

where $g_{o_{i,h}}$ *corresponds to the element* h *of the vector* g_{o_i} *and* f_{o_h} *the element* h *of the vector* f_o.

Proof 2.9 *Letting* $V = \frac{1}{2} e_o^T e_o$ *be the Lyapunov candidate, we have*

$$\dot{V} = \sum_h \dot{V}_h = \sum_h e_{o_h} \dot{e_{oh}} = e_o^T \left(\tilde{f}_o(\zeta_o) + \sum_i \tilde{g}_{o_i}(\zeta_o) u_i - K(e_o + \epsilon)\right). \tag{2.6}$$

A sufficient condition for asymptotic stability is to have that $\dot{V}_h < 0, \forall h$*, i.e.,*

$$e_{o_h}\left(\tilde{f}_{o_h}\left(\zeta_o\right) + \sum_i \tilde{g}_{o_{i,h}} u_i - K_h\left(e_{o_h} - \epsilon_h\right)\right) < 0,$$

which can be rewritten as

$$K_h\left(1 + \frac{\epsilon_h}{e_{o_h}}\right) > \frac{\tilde{f}_{o_h}(\xi)}{e_{o_h}} + \sum_i \frac{\tilde{g}_{o_{i,h}}}{e_{o_h}} u_i. \tag{2.7}$$

Now, consider a state vector $x = (x_1, \ldots, x_n), x \in M \subseteq \mathbb{R}^n$*, and a scalar function* $z(x)$*, which partial derivative in direction of* x *is given by* $\frac{\partial z(x)}{\partial x} = \left[\frac{\partial z(x)}{\partial x_1}, \ldots, \frac{\partial z(x)}{\partial x_n}\right]$*. It is a direct consequence from the classical Cauchy mean value theorem that*

$$\frac{z(x) - z\left(\hat{x}\right)}{x_h - \hat{x}_h} \leq \sup_{x \in M}\left(norm\left(\frac{\partial z(x)}{\partial x}\right)\right).$$

Considering that $e_h = \zeta_{o_h} - \hat{\zeta}_{o_h}$ *and using the relation presented above together with eq.* (2.7)*, we may write*

$$K_h\left(1 + \frac{\epsilon_h}{e_{o_h}}\right) > \sup\left(\left\|\frac{\partial f_{o_h}\left(\zeta_o\right)}{\partial \zeta_o}\right\|\right) + \sum_i \sup\left(\left\|\frac{\partial g_{o_{i,h}}\left(\zeta_o\right)}{\partial \zeta_o} u_i\right\|\right).$$

If $\|\frac{e_o + \epsilon}{e_o}\|$ *is bounded by some arbitrary worst value, the relation described above can be rewriten as eq.* (2.5)*. The convergence for* $\hat{\zeta}_o(0)$ *in a local neighborhood of the real scaled state* $\zeta_o(0)$ *is guaranteed since the value of* ϵ *in the worst case is related to the maximum admissible* $\|e_o(0)\|$*.*

Chapter 3

On Appearance Localization, Mapping and Motion Reconstruction

In section 1.2.4 we investigated the use of the observability rank condition to study the left invertibility of a system. In this chapter we are interested in applying the observability analysis procedure described for control-affine non-linear systems to the problems of vehicle localization and simultaneous localization and mapping. We present results for unycicle and omnidirectional-like vehicles for which system outputs are comprised of bearing only measurements of stationary landmarks.

Using an unified framework with the control problem, results presented permit the construction of nonlinear observers with direct application in many problems from computer vision to autonomous navigation, such as feature tracking, visual odometry, input reconstruction, fault tolerant visual servoing, active perception, optimal control, model independent control and others.

Some of the results presented in this chapter were published in [77].

3.1 Problem Definition

In this chapter we will consider vehicles whose dynamics are slow enough to be neglected, and kinematics can be described by eq. (1.7):

$$\dot{\xi}_r = G(\xi_r)\, u_r + B(\xi_r)\, d_r\,, \tag{3.1}$$

where u_r are input controls, d_r is a generalized input disturbance, $G(\xi_r)$ contains the velocity fields that describe vehicle kinematics and $B(\xi_r)$ is a known disturbance input matrix. Generic movements on the plane can be described by $u_r = [v_f\ v_h\ \omega]^T$, $d_r = [d_f\ d_h\ d_\omega]^T$ and

$$G(\xi_r) = B(\xi_r) = [g_f\ g_h\ g_\omega] = \begin{bmatrix} \cos\theta_r & -\sin\theta_r & 0 \\ \sin\theta_r & \cos\theta_r & 0 \\ 0 & 0 & 1 \end{bmatrix}. \tag{3.2}$$

While generic movements could be represented by a 3×3 identity matrix I, such choice introduces the knowledge of the world reference frame: ν_f and d_f are assumed to be in the direction of axis ${}^W X$, while ν_h and d_h are in direction of ${}^W Z$. This leads to inconsistencies in the observability analysis. To illustrate the problem, consider an USO analysis with one marker only and $G = I$. This problem is completely observable whereas the same analysis using G defined as (3.2) is not. As a matter of fact, the unobservable space in the second problem is characterized by the reference frame orientation, which is assumed to be known when G is described using the identity matrix. Therefore, in order to achieve generic results and do not introduce any knowledge apart from the position of 3 markers, one should consider generic movements as described in (3.2).

Specific vehicle kinematics and disturbance models can be described by choosing G and B composed of subspaces of (3.2) and the proper choice of u_r and d_r. For example, a boat can be modeled as a unicycle vehicle with disturbance along the nonholonomic direction to represent the undesired lateral motion defining $G(\xi_r) = [g_f\ g_\omega]$, $B(\xi_r) = [g_h]$, $u_r = [v_f,\, \omega]^T$ and $d_r = d_\omega$.

We consider the analysis of vehicles equipped with a sensor head such that its measurements are angles in the horizontal plane between the line joining the obstacle features (landmarks) with the head position, and the forward direction of the vehicle (see fig. 4.1). The measurement process is modeled by equations of the form (1.21):

$$y_i = h_i(\xi_r, P_i) = \tan^{-1}\left(\frac{z_r - z_i}{x_r - x_i}\right) - \theta_r + \pi\,, \quad i = 1, \ldots, q\,, \qquad (3.3)$$

where $P_i = (x_i, z_i)$ describe the absolute position of landmark i and $q = N + M$ is the total number of landmarks (see figure 4.1). From these, N correspond to target observations and M correspond to measurements relating to markers. Note that equation (1.21) is not defined whenever vehicle and landmark positions coincide.

Observability Problems Consider a generic driftless control–affine system affected by the external disturbance vector d:

$$\dot{\xi}_\Sigma = G(\xi_\Sigma)u + B(\xi_\Sigma)d,\ \xi_\Sigma \in \mathbb{R}^n,\ u \in \mathbb{R}^m,\ d \in \mathbb{R}^\eta,$$

where $B(\xi_\Sigma)$ is a known disturbance input matrix.

Observability analysis will be done using two different approaches:

- **Unknown State Observability (USO)**: possibility of reconstructing state assuming that inputs are known.

$$\xi = (\xi_\Sigma)$$

- **Unknown Input Observability (UIO)**: possibility of reconstructing both state and inputs when inputs are not completely available or are uncertain, i.e., these are classified as input disturbances. In this case, we study the observability of an augmented system composed of system state and input disturbances:

$$\xi_e = \begin{pmatrix} \xi_\Sigma \\ d \\ \dot{d} \\ \vdots \end{pmatrix}$$

Observability Analysis In each of the problems studied, the observability codistribution filtration is iterated till the rank of the observability codistribution reaches its maximum. Then, a series of properties are investigated and characterized:

- **Observability codistribution**: the observability codistribution filtration is iterated till the rank of the observability codistribution reaches its maximum;
- **Minimum level of Lie Derivatives**: Minimum number of Lie bracketing required to cover the observable part of the state space;
- **Observable and non-observable dimensions**: Dimensions of observable and non-observable spaces;
- **Null space of the observability codistribution**: Whenever the system is not completely observable, the gradient of the set of states that are locally indistinguishable from an arbitrary initial configuration;
- **System Kalman form**: Whenever the system is not completely observable, one or more Kalman observable canonical form representations of the system with a local state decomposition of the state-space into observable and non-observable parts;

Moreover, we present the use of non-linear observers for the observable part of the state space in order to validate the theoretical results of the UIO problem.

Notations and definitions In order to simplify the following demonstrations we define the displacements $\Delta \mathrm{x}_{a,b} = x_a - x_b$ and $\Delta \mathrm{z}_{a,b} = z_a - z_b$, and the cartesian distance $\rho_{a,b} = \sqrt{(\Delta \mathrm{x}_{a,b})^2 + (\Delta \mathrm{z}_{a,b})^2}$.

3.2 Unknown State Observability - Unicycle Vehicle

In this section we will study the observability problem when inputs are available or assumed to be known. These results extend the ones presented in [11] because here we detail all possible cases from $3+N$ markers to $3+N$ targets, not only considering the completely observable cases. Moreover, a Kalman Form decomposition is presented for all non-observable cases.

Vehicle Kinematics In the following analysis we will consider a unicycle like mobile platform, whose dynamics is slow enough to be neglected, and kinematics can be described by a driftless kinematic model:

$$\dot{\xi}_r = G_r \; u_r,$$

where $u_r = (\nu_f, \omega)$ are the vehicle input controls: ν_f is the forward motion linear velocity and ω is the angular velocity. Moreover, $G(\xi_r)$ contains the velocity fields that describe vehicle kinematics:

$$G\left(\xi_r\right) = \left[\begin{array}{cc} g_f & g_\omega \end{array} \right] = \left[\begin{array}{cc} \cos\left(\theta_r\right) & 0 \\ \sin\left(\theta_r\right) & 0 \\ 0 & 1 \end{array} \right]. \tag{3.4}$$

System definition In the following analysis, we will study the observability problem under different characterizations regarding the number of known and unknown landmarks being observed (marker and targets). Wherever necessary, we use the notation $*_t$ to specify that the variable refers to a target and $*_m$ to specify that it refers to a marker.

The systems under investigation will be composed of the vehicle configuration and the unknown position of N targets:

$$\xi = \left(\xi_r, \xi_{t,1}, \ldots, \xi_{t,N}\right),$$

with corresponding system dynamics:

$$\dot{\xi} = \begin{bmatrix} \dot{\xi}_r \\ 0 \\ \vdots \\ 0 \end{bmatrix} = \begin{bmatrix} \cos(\theta_r) \\ \sin(\theta_r) \\ 0 \\ 0 \\ \vdots \\ 0 \end{bmatrix} \nu_f + \begin{bmatrix} 0 \\ 0 \\ 1 \\ 0 \\ \vdots \\ 0 \end{bmatrix} \omega.$$

Measurement process is modelled by $q = N + M$ equations of the form (1.21). From these, N correspond to target observations and M correspond to measurements relating to markers. System outputs are composed of measurements from both targets and markers:

$$y = \begin{bmatrix} y_{t,1} \\ y_{t,2} \\ \vdots \\ y_{t,N} \\ y_{m,N+1} \\ y_{m,N+2} \\ \vdots \\ y_{m,N+M} \end{bmatrix} = \begin{bmatrix} h_{t,1}(\xi_r, \xi_{t,1}) \\ h_{t,2}(\xi_r, \xi_{t,2}) \\ \vdots \\ h_{t,N}(\xi_r, \xi_{t,N}) \\ h_{m,N+1}(\xi_r, \xi_{m,N+1}) \\ h_{m,N+2}(\xi_r, \xi_{m,N+2}) \\ \vdots \\ h_{m,N+M}(\xi_r, \xi_{m,N+M}) \end{bmatrix},$$

and the position of landmarks are assumed not to be coincident, i.e., $\xi_i \neq \xi_j, \forall i \neq j$. Also, remember that equation (1.21) is not defined whenever vehicle and landmark positions coincide.

Codistribution form A generic form for the observability codistribution of the systems under investigation is

$$\Omega = \begin{bmatrix} \Omega^{(0)} \\ \Omega^{(1)} \\ \vdots \end{bmatrix} = \begin{bmatrix} \mathrm{dL}_\Delta{}^{(0)} h_1 \\ \mathrm{dL}_\Delta{}^{(0)} h_2 \\ \vdots \\ \mathrm{dL}_\Delta{}^{(1)} h_1 \\ \mathrm{dL}_\Delta{}^{(1)} h_2 \\ \vdots \end{bmatrix} = \begin{bmatrix} \partial_{\xi \mathrm{r}} L_\Delta{}^{(0)} h_1 & \partial_{\xi_t} L_\Delta{}^{(0)} h_1 \\ \vdots & \vdots \\ \partial_{\xi \mathrm{r}} L_\Delta{}^{(1)} h & \partial_{\xi_t} L_\Delta{}^{(0)} h_1 \\ \vdots & \vdots \end{bmatrix},$$

or

$$\Omega = \begin{bmatrix} \partial_{\xi_r} {L_\Delta}^{(0)} h_{t,1} & \partial_{\xi_{t,1}} {L_\Delta}^{(0)} h_{t,1} & 0 & 0 & 0 \\ \partial_{\xi_r} {L_\Delta}^{(0)} h_{t,2} & 0 & \partial_{\xi_{t,2}} {L_\Delta}^{(0)} h_{t,2} & 0 & 0 \\ \vdots & \vdots & \vdots & \ddots & \vdots \\ \partial_{\xi_r} {L_\Delta}^{(0)} h_{t,N} & 0 & 0 & 0 & \partial_{\xi_{t,N}} {L_\Delta}^{(0)} h_{t,N} \\ \hline \partial_{\xi_r} {L_\Delta}^{(0)} h_{m,N+1} & 0 & 0 & 0 & 0 \\ \vdots & \vdots & \vdots & \vdots & \vdots \\ \partial_{\xi_r} {L_\Delta}^{(0)} h_{m,N+M} & 0 & 0 & 0 & 0 \\ \hline \partial_{\xi_r} {L_\Delta}^{(1)} h_{t,1} & \partial_{\xi_t} {L_\Delta}^{(0)} h_{t,1} & 0 & 0 & 0 \\ \vdots & \vdots & \vdots & \vdots & \vdots \end{bmatrix} \begin{matrix} \left\{ \begin{matrix} \\ \\ \\ \\ \end{matrix} \right. N\text{targets} \\ \left\{ \begin{matrix} \\ \\ \\ \end{matrix} \right. M\text{markers} \\ \vdots \end{matrix} .$$

In all of the following analysis, the observability codistribution ranks reach their maximum within the first level of Lie differentiation. Codistributions Ω at this level will be composed of the following submatrices:

$$\frac{\partial h_i}{\partial \xi_r} = \left[\frac{\Delta \mathrm{z}_{r,i}}{{\rho_{r,i}}^2}, \frac{\Delta \mathrm{x}_{r,i}}{{\rho_{r,i}}^2}, -1 \right],$$

$$\partial_{\xi_r} L_\Delta^{(1)} h_i = \begin{bmatrix} \frac{2\Delta \mathrm{x}_{r,i} \Delta \mathrm{z}_{r,i} \cos(\theta_\mathrm{r}) + \left(\Delta \mathrm{z}_{r,i} - \Delta \mathrm{x}_{r,i}\right)\left(\Delta \mathrm{z}_{r,i} + \Delta \mathrm{x}_{r,i}\right) \sin(\theta_r)}{{\rho_{r,i}}^4} \\ -\frac{2\Delta \mathrm{x}_{r,i} \Delta \mathrm{z}_{r,i} \sin(\theta_r) + \left(\Delta \mathrm{z}_{r,i} - \Delta \mathrm{x}_{r,i}\right)\left(\Delta \mathrm{z}_{r,i} + \Delta \mathrm{x}_{r,i}\right) \cos(\theta_r)}{{\rho_{r,i}}^4} \\ \frac{\Delta \mathrm{x}_{r,i} \cos(\theta_\mathrm{r}) + \Delta \mathrm{z}_{r,i} \sin(\theta_\mathrm{r})}{{\rho_{r,i}}^2} \end{bmatrix}^T,$$

$$\partial_{\xi_i} h_i = \begin{bmatrix} \partial_{x_i} h_i & \partial_{z_i} h_i \end{bmatrix} = \begin{bmatrix} \frac{\Delta \mathrm{z}_{r,i}}{{\rho_{r,i}}^2} & \frac{-\Delta \mathrm{x}_{r,i}}{{\rho_{r,i}}^2} \end{bmatrix},$$

and

$$\partial_{\xi_i} L_\Delta^{(1)} h_i = \begin{bmatrix} \partial_{x_i} L_\Delta h_i & \partial_{z_i} L_\Delta h_i \end{bmatrix} =$$

$$\begin{bmatrix} \frac{-2\Delta \mathrm{x}_{r,i} \Delta \mathrm{z}_{r,i} \cos(\theta_r) - (\Delta \mathrm{z}_{r,i} + \Delta \mathrm{x}_{r,i})(\Delta \mathrm{z}_{r,i} - \Delta \mathrm{x}_{r,i}) \sin(\theta_r)}{{\rho_{r,i}}^4} \\ \frac{2\Delta \mathrm{x}_{r,i} \Delta \mathrm{z}_{r,i} \sin(\theta_r) - (\Delta \mathrm{z}_{r,i} + \Delta \mathrm{x}_{r,i})(\Delta \mathrm{z}_{r,i} - \Delta \mathrm{x}_{r,i}) \cos(\theta_r)}{{\rho_{r,i}}^4} \end{bmatrix} T$$

Extension of results Results presented in this section can be extended to problems involving any number of targets. Let's consider a generic system $\xi^* = (\xi_r, \xi_{t,1}, \ldots, \xi_{t,N})$. The system that describes the same problem with new $\bar{N}$ new targets will be written as $\xi = \left(\xi^*, \xi_{t,N+M+1}, \ldots, \xi_{t,N+M+\bar{N}}\right)$. We will use the notation * whenever we refer to to the original system ξ^*.

Proposition 3.1 *Consider a system* $\xi^* = (\xi_r, \xi_{t,1}, \ldots, \xi_{t,N})$*, for which the dimension of the observable space is given by* $\dim(\zeta_o{}^*) = K$*. Now, consider a system* $\xi = \left(\xi^*, \xi_{t,N+M+1}, \ldots, \xi_{t,N+M+\bar{N}}\right)$ *that is composed of* ξ^* *and* $\bar{N}$ *number of new targets. The dimension of the observable space of* ξ *is* $\dim(\zeta_o) \geq K + \bar{N}$*.*

Proof 3.1 *Given a generic observability codistribution* Ω^* *associated to* ξ^**:*

$$\Omega^* = \begin{pmatrix} \Omega^{*(0)} \\ \Omega^{*(1)} \\ \Omega^{*(2)} \end{pmatrix},$$

the correspondent Ω *(associated to* ξ*) that consider the same problem with* $\bar{N}$ *new targets can be written as*

$$\Omega = \begin{pmatrix} \Omega^{*(0)} & 0 \\ * & {\Omega_t}^{(0)} \\ \Omega^{*(1)} & 0 \\ * & {\Omega_t}^{(1)} \\ \Omega^{*(1)} & 0 \\ * & {\Omega_t}^{(1)} \\ \vdots & \vdots \end{pmatrix},$$

where

$${\Omega_t}^{(i)} = \begin{pmatrix} \partial_{\xi_{t,1}} {L_\Delta}^{(i)} h_{t,1} & 0 & \ldots \\ 0 & \partial_{\xi_{t,1}} {L_\Delta}^{(i)} h_{t,2} & \ldots \\ 0 & 0 & \ddots \end{pmatrix}.$$

Given that $\{{\Omega_t}^{(0)}, {\Omega_t}^{(1)}\}$ *has rank 2 (apart from when output is undefined, i.e.,* $P_r \to P_t$*), we can conclude that*

$$rank(\Omega) \geq rank(\Omega^*) + \bar{N},$$

that confirms proposition 3.1. This result does not depend on the number of new targets considered.

Remark 3.1 *It can be verified from proposition 3.1 that if* ξ^* *is completely observable then* ξ *is completely observable.*

3.2.1 3 or more markers

The state space under investigation is composed of the vehicle configuration only $\xi = (\xi_r)$ and system output consists of the measurement of three or more markers $y = (y_{m,1}, y_{m,2}, y_{m,3}, \ldots)$.

Observability analysis After 0 levels of Lie differentiation, the observability codistribution rank reaches its maximum of 3. Codistribution Ω for 0 levels of Lie bracketing is

$$\Omega = \begin{bmatrix} \partial_{\xi_r} h_1 \\ \partial_{\xi_r} h_2 \\ \partial_{\xi_r} h_3 \\ \vdots \end{bmatrix}.$$

Apart from configuration singularities, matrix rank of Ω is 3 and the system is locally weakly observable. The minimum number of Lie bracketing required to cover the observable part of the state space is 0, i.e., the problem is statically invertible and does not depend on the inputs. Given the complete observability of ξ, the set of indistinguishable states regarding a non singular initial configuration is empty.

3.2.2 2 markers

The state space under investigation is composed of the vehicle configuration only $\xi = (\xi_r)$ and system output consists of the measurement of two markers $y = (y_{m,1}, y_{m,2})$.

Observability analysis After 1 level of Lie differentiation, the observability codistribution rank reaches its maximum of 3. The codistribution filtration after 1 level of Lie bracketing is

$$\Omega = \begin{bmatrix} \partial_{\xi \mathrm{r}} h_1 \\ \partial_{\xi \mathrm{r}} h_2 \\ \partial_{\xi_r} L_\Delta h_1 \\ \partial_{\xi_r} L_\Delta h_2 \end{bmatrix}.$$

Apart from configuration singularities, the observable space dimension is given by matrix rank of Ω is 3 , i.e., the system is completely locally weakly and the non-observable space dimension is 0. The minimum number of Lie bracketing required to cover the observable part of the state space is is 1, i.e., the problem is not statically invertible, instead state reconstruction is only possible under vehicle motion. Given the complete observability of ξ, the nullspace of Ω is empty.

3.2.3 1 and a half markers

In this problem, we are interested in the investigation of a system which output consists of the measurement of two landmarks. From these one's position is completely known (marker) and the other landmark position is partially known (half marker), i.e., a one dimension space subsystem of the 2 dimensional position coordinates is assumed to be known while another one dimension space is assumed to be unknown. Without lost of generalization, we will assume that the coordinate z_1 is known while x_1 is unknown. Hence the state space under investigation is $\xi = (\xi_r, x_1)$ and system output is $y = (y_1, y_{m,2})$.

Observability analysis After 1 level of Lie differentiation, the observability codistribution rank reaches its maximum of 4:

$$\Omega = \begin{bmatrix} \partial_{\xi_r} h_1 & \partial_{x_1} h_1 \\ \partial_{\xi_r} h_2 & 0 \\ \partial_{\xi_r} L_\Delta h_1 & \partial_{x_1} L_\Delta h_1 \\ \partial_{\xi_r} L_\Delta h_2 & 0 \end{bmatrix}.$$

Apart from configuration singularities, the observable space dimension is given by matrix rank of Ω, which is 4. Hence, all state variables from ξ are locally weakly observable and the non-observable space dimension is 0. The minimum number of Lie bracketing required to cover the observable part of the state space is is 1. Given the complete observability of ξ, the nullspace of Ω is empty.

3.2.4 1 marker

The state space under investigation is composed of the vehicle configuration only, i.e., $\xi = (\xi_r, \xi_{t,1})$ and system output consists of the measurement of the marker $y = (y_{m,1})$.

Observability analysis After 1 level of Lie differentiation, the observability codistribution rank reaches its maximum of 2. The codistribution Ω at this level of Lie bracketing is

$$\Omega = \begin{bmatrix} \partial_{\xi_r} h_1 \\ \partial_{\xi_r} L_\Delta h_1 \end{bmatrix}.$$

Apart from configuration singularities, the observable space dimension is given by matrix rank of Ω, which is 2. Hence, ξ is not fully observable and the non-observable space dimension is 1. The minimum number of Lie bracketing required to cover the observable part of the state space is is 1. The nullspace of Ω is

$$\mathrm{Ker}(\Omega) = \mathrm{span}\left(\begin{bmatrix} -\Delta \mathrm{z}_{r,1} & \Delta \mathrm{x}_{r,1} & 1 \end{bmatrix}^T \right).$$

Kalman form decomposition Consider a reference frame $\langle P \rangle = \{{}^P O, {}^P X, {}^P Z\}$ (as seen in Fig. 3.1) such that its origin ${}^P O$ is coincident to the position of the feature $P_1 = (x_1, z_1)$ and axes ${}^P X$ and ${}^P Z$ are parallel to axes ${}^W X$ and ${}^W Z$ respectively.

Now, consider the pose displacement between ξ_r and ξ_i represented on polar coordinates w.r.t. $\langle P \rangle$, i.e.:

$$\xi_{\mathrm{rp}} = \Phi_p(\xi_r) = \begin{bmatrix} \rho \\ \beta \\ \phi \end{bmatrix} = \begin{bmatrix} \sqrt{(x_r - x_1)^2 + (z_r - z_1)^2} \\ \tan^{-1}\left(\frac{z_r - z_1}{x_r - x_1}\right) - \theta_r + \pi \\ \tan^{-1}\left(\frac{z_r - z_1}{x_r - x_1}\right) \end{bmatrix}, \qquad (3.5)$$

where ρ represents the cartesian distance from vehicle to point P_1, β represents the angle displacement between vehicle orientation and

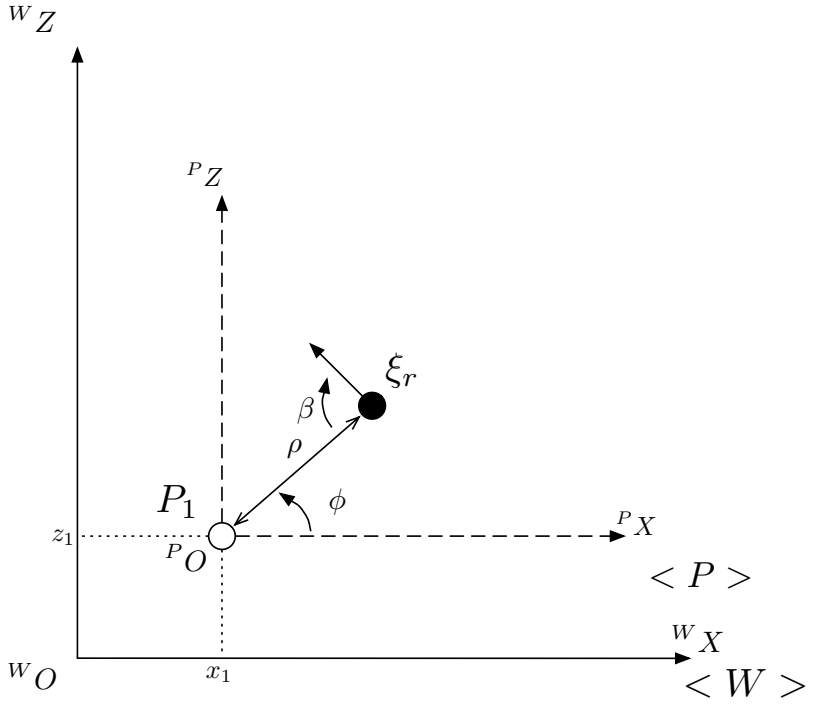

Figure 3.1: Reference frame $\langle P \rangle$ with axes parallel to $\langle W \rangle$ and vehicle configuration represented using polar coordinates.

the line that passes through point P_1 and vehicle position P_r and ϕ represents the angle formed by P_r with both axes ^{P}X and ^{W}X. Moreover, the notation $\Phi_p(*)$ is used to represent the transformation from cartesian to polar coordinates.

Vehicle kinematics on polar coordinates is given by

$$\dot{\xi_{\text{rp}}} = \begin{bmatrix} -\cos(\beta) \\ \frac{\sin(\beta)}{\rho} \\ \frac{\sin(\beta)}{\rho} \end{bmatrix} \nu_f + \begin{bmatrix} 0 \\ -1 \\ 1 \end{bmatrix} \omega. \tag{3.6}$$

Please note that the polar coordinates transformation is undefined for $\rho = 0$.

Now, in order to decouple observable and non-observable subsystems, let's consider the coordinate mapping $\zeta = \Phi(\xi) = \xi_{\text{rp}} = [\rho, \delta, \gamma]^T$ described by $\Phi : \mathbb{R}^2 \times S \to \mathbb{R}^+ \times S^2$. Under such coordinate transformation, system dynamics is given by $\dot{\zeta} = \dot{\xi}_{\text{rp}}$ and system output becomes $y = (\beta)$.

In order to verify if Φ is local diffeomorphism at ξ we compute its Jacobian:

$$J = J_{\xi_{\text{rp}}} = \begin{bmatrix} \frac{-x_1+x_r}{\sqrt{(x_1-x_r)^2+(z_1-z_r)^2}} & \frac{-z_1+z_r}{\sqrt{(x_1-x_r)^2+(z_1-z_r)^2}} & 0 \\ \frac{z_1-z_r}{(x_1-x_r)^2+(z_1-z_r)^2} & \frac{-x_1+x_r}{(x_1-x_r)^2+(z_1-z_r)^2} & -1 \\ \frac{z_1-z_r}{(x_1-x_r)^2+(z_1-z_r)^2} & \frac{-x_1+x_r}{(x_1-x_r)^2+(z_1-z_r)^2} & 0 \end{bmatrix}. \quad (3.7)$$

where the notation $J_{\xi_{\text{rp}}}$ is used to represent the jacobian associated to the description of vehicle coordinates using polar coordinates seen in eq. (3.6).

Matrix rank of J is 3 apart from $|J| = 0$, i.e., when

$$|J| = \frac{1}{\rho} = \frac{1}{\sqrt{(x_1 - x_r)^2 + (z_1 - z_r)^2}} = 0.$$

Hence, we conclude that Φ is not a global diffeomorphism and is not defined for $\rho = 0$, as expected. For $\rho \neq 0$, its inverse is given by

$$\xi = \Phi^{-1}(\zeta) = {\Phi_p}^{-1}(\xi_{\text{rp}}) = \begin{bmatrix} x_r \\ z_r \\ \theta_r \end{bmatrix} = \begin{bmatrix} x_1 + \rho\cos(\beta) \\ z_1 + \rho\sin(\beta) \\ \alpha - \beta + \pi \end{bmatrix},$$

where the notation ${\Phi_p}^{-1}(\xi_{\text{rp}})$ is used to represent the mapping from polar to cartesian coordinates., i.e., inverse of the mapping defined in eq.(3.6).

Observability analysis under local decomposition After 1 level of Lie differentiation, the observability codistribution for ζ is

$$\Omega = \begin{bmatrix} 0 & 1 & 0 \\ -\frac{\sin(\beta)}{\rho^2} & \frac{\cos(\beta)}{\rho} & 0 \end{bmatrix},$$

which nullspace is given by

$$\mathrm{Ker}(\Omega) = \mathrm{span}\left[\begin{array}{ccc} 0 & 0 & 1 \end{array}\right]^T,$$

and we may conclude that the observable subsystem is $\zeta_O = (\rho, \beta)$ and the non observable subsystem is $\zeta_{\bar{O}} = (\phi)$, i.e., distance ρ and angle displacement β from the vehicle to the target are observable while angle ϕ isn't.

3.2.5 Half marker and half target

In this problem, we are interested in the investigation of a system which output consists of the measurement of one landmarks for which position is partially known (half marker), i.e., a one dimension space subsystem of the 2 dimensional position coordinates is assumed to be known while another one dimension space is assumed to be unknown. Without lost of generalization, we will assume that the coordinate z_1 is known while x_1 is unknown. Hence the state space under investigation is $\xi = (\xi_r, x_1)$ and system output is $y = (y_1)$.

Observability analysis After 1 level of Lie differentiation, the observability codistribution rank reaches its maximum of 2. The codistribution filtration after 1 level of Lie bracketing is

$$\Omega = \begin{bmatrix} \partial_{\xi \mathrm{r}} h_1 & \partial_{x_1} h_1 \\ \partial_{\xi_r} L_\Delta h_1 & \partial_{x_1} L_\Delta h_1 \end{bmatrix}.$$

Apart from configuration singularities, matrix rank of Ω is 2. Hence, ξ is not fully observable and the both observable space and non-observable space dimension is 2. The minimum number of Lie bracketing required to cover the observable part of the state space is is 1. The nullspace of Ω is

$$\mathrm{Ker}(\Omega) = \mathrm{span}\left(\begin{bmatrix} 0 & 1 & 0 & 1 \\ -\Delta \mathrm{z}_{r,1} & \Delta \mathrm{x}_{r,1} & 1 & 0 \end{bmatrix}^T \right).$$

Kalman form decomposition Here we will consider the reference frame $\langle P \rangle$ presented in section 3.2.4 and seen in fig. 3.1.

Consider the coordinate transformation $\zeta = \Phi(\xi) = (\xi_{\mathrm{rp}}, x_1)$ described by $\Phi : \mathbb{R}^3 \times S \to \mathbb{R}^+ \times \mathbb{R}^1 \times S^2$. In this, ξ_{rp} represents the pose displacement of the vehicle on polar coordinates (as seen in eq. (3.5)) and x_1 corresponds to the unknown horizontal translation from origin O_P to origin O_W. The corresponding system dynamics is $\dot{\zeta} = \left(\dot{\xi}_{\mathrm{rp}}, 0\right)$ and system output is $y = (\beta)$.

In order to verify if Φ is local diffeomorphism at ξ we compute its Jacobian:

$$J = \begin{bmatrix} J_{\xi_{\text{rp}}} & J^* \\ 0 & 1 \end{bmatrix}, J^* = \begin{bmatrix} -\frac{\Delta \text{x}_{r,1}}{\rho_{r,1}} \\ \frac{\Delta \text{z}_{r,1}}{{\rho_{r,1}}^2} \\ \frac{\Delta \text{z}_{r,1}}{{\rho_{r,1}}^2} \end{bmatrix},$$

where $J_{\xi_{\text{rp}}}$ was seen in eq. (3.7). Matrix rank of J is 4 apart from $|J| = |J_{\xi_{\text{rp}}}| = 0$. Hence, we conclude while Φ represents a local diffeomorphism almost everywhere, it is not a global diffeomorphism and is not defined for $\rho = 0$, as expected. For $\rho \neq 0$, its inverse is given by

$$\xi = \Phi^{-1}(\zeta) = \begin{pmatrix} {\Phi_p}^{-1}(\xi_{\text{rp}}) \\ x_1 \end{pmatrix}.$$

Observability analysis under local decomposition After 1 level of Lie differentiation, the observability codistribution for ζ is

$$\Omega = \begin{bmatrix} 0 & 1 & 0 & 0 \\ -\frac{\sin(\beta)}{\rho^2} & \frac{\cos(\beta)}{\rho} & 0 & 0 \end{bmatrix},$$

which nullspace is given by

$$\text{Ker}(\Omega) = \text{span} \begin{bmatrix} 0 & 0 & 0 & 1 \\ 0 & 0 & 1 & 0 \end{bmatrix}^T$$

and we may conclude that the observable subsystem is $\zeta_o = (\rho, \beta)$ and the non observable subsystem is $\zeta_{\bar{o}} = (\phi, x_1)$, i.e., distance ρ and angle displacement β from the vehicle to the target are observable while angle ϕ and horizontal translation x_1 between O_W and O_P are not observable. Please note that the observable subsystem ζ_o is the same from the problem studied in section 3.2.4.

3.2.6 1 target

The state space under investigation is composed of the vehicle configuration and the position of one target, i.e., $\xi = (\xi_r, \xi_{t,1})$ and system output consists of the measurement of the target $y = (y_{t,1})$.

Observability analysis After 1 level of Lie differentiation, the observability codistribution rank reaches its maximum of 2, for which codistribution Ω is

$$\Omega = \begin{bmatrix} \partial_{\xi_\mathrm{r}} h_1 & \partial_{\xi_1} h_1 \\ \partial_{\xi_r} L_\Delta h_1 & \partial_{\xi_1} L_\Delta h_1 \end{bmatrix}.$$

Apart from configuration singularities, matrix rank of Ω is 2. Hence, ξ observable space dimension is 2 and non-observable space dimension is 3. The minimum number of Lie bracketing required to cover the observable part of the state space is is 1 and the nullspace of Ω is

$$\mathrm{Ker}(\Omega) = \mathrm{span}\left[\begin{bmatrix} 0 & 1 & 0 & 0 & 1 \\ 1 & 0 & 0 & 1 & 0 \\ -\Delta \mathrm{z}_{r,1} & \Delta \mathrm{x}_{r,1} & 1 & 0 & 0 \end{bmatrix}^T \right].$$

Kalman form decomposition Here we will consider the reference frame $\langle P \rangle$ presented in section 3.2.4 and seen in fig. 3.1. Consider the coordinate transformation $\zeta = \Phi(\xi) = (\xi_{\mathrm{rp}}, x_1, z_1)$ described by $\Phi : \mathbb{R}^4 \times S \to \mathbb{R}^+ \times \mathbb{R}^2 \times S^2$. In this, ξ_{rp} represents the pose displacement of the vehicle on polar coordinates (as seen in eq. (3.5)) and (x_1, z_1) corresponds to the position of the origin O_P w.r.t $\langle W \rangle$. The corresponding system dynamics is $\dot{\zeta} = \left(\dot{\xi}_{\mathrm{rp}}, 0, 0\right)$ and system output is $y = (\beta)$. In order to verify if Φ is local diffeomorphism at ξ we compute its Jacobian:

$$J = \begin{bmatrix} J_{\xi_{\mathrm{rp}}} & J^* \\ 0 & 1 \end{bmatrix}, J^* = \begin{bmatrix} -\frac{\Delta \mathrm{x}_{r,1}}{\rho_{r,1}} & \frac{\Delta \mathrm{z}_{r,1}}{\rho_{r,1}} \\ \frac{\Delta \mathrm{z}_{r,1}}{{\rho_{r,1}}^2} & -\frac{\Delta \mathrm{x}_{r,1}}{{\rho_{r,1}}^2} \\ \frac{\Delta \mathrm{z}_{r,1}}{{\rho_{r,1}}^2} & -\frac{\Delta \mathrm{x}_{r,1}}{{\rho_{r,1}}^2} \end{bmatrix},$$

where $J_{\xi_{\text{rp}}}$ was seen in eq. (3.7). Matrix rank of J is 5 apart from $|J| = |J_{\xi_{\text{rp}}}| = 0$. Hence, we conclude while Φ represents a local diffeomorphism almost everywhere, it is not a global diffeomorphism and is not defined for $\rho = 0$, as expected. For $\rho \neq 0$, its inverse is given by

$$\xi = \Phi^{-1}(\zeta) = \begin{pmatrix} {\Phi_p}^{-1}(\xi_{\text{rp}}) \\ x_1 \\ z_1 \end{pmatrix}.$$

Observability analysis under local decomposition After 1 level of Lie differentiation, the observability codistribution for ζ is

$$\Omega = \begin{bmatrix} 0 & 1 & 0 & 0 & 0 \\ -\frac{\sin(\beta)}{\rho^2} & \frac{\cos(\beta)}{\rho} & 0 & 0 & 0 \end{bmatrix},$$

which nullspace is given by

$$\text{Ker}(\Omega) = \text{span} \begin{bmatrix} 0 & 0 & 0 & 0 & 1 \\ 0 & 0 & 0 & 1 & 0 \\ 0 & 0 & 1 & 0 & 0 \end{bmatrix}^T$$

and we may conclude that the observable subsystem is $\zeta_o = (\rho, \beta)$ and the non observable subsystem is $\zeta_{\bar{o}} = (\phi, x_1, z_1)$, i.e., angle ϕ and origin ${}^P O$ w.r.t. world frame $\langle W \rangle$ are not observable. Once again the observable subsystem ζ_o is the same from the problem studied in section 3.2.4.

3.2.7 2 targets

The state space under investigation is composed of the vehicle configuration and the position of two targets, i.e., $\xi = (\xi_r, \xi_{t,1}, \xi_{t,2})$ and system output consists of the measurement of two targets $y = (y_{t,1}, y_{t,2})$.

Observability analysis After 1 level of Lie differentiation, the observability codistribution rank reaches its maximum of 4, for which codistribution Ω is

$$\Omega = \begin{bmatrix} \partial_{\xi \mathrm{r}} h_1 & \partial_{\xi_1} h_1 & 0 \\ \partial_{\xi \mathrm{r}} h_2 & 0 & \partial_{\xi \mathrm{r}} h_2 \\ \partial_{\xi_r} L_\Delta h_1 & \partial_{\xi_1} L_\Delta h_1 & 0 \\ \partial_{\xi_r} L_\Delta h_2 & 0 & \partial_{\xi_1} L_\Delta h_2 \end{bmatrix}.$$

Apart from configuration singularities, matrix rank of Ω is 4. Hence, ξ is not fully observable. Observable space dimension is 4 and non-observable space dimension is 2. The minimum number of Lie bracketing required to cover the observable part of the state space is is 1 and the nullspace of Ω is

$$\mathrm{Ker}(\Omega) = \mathrm{span}\left(\begin{bmatrix} \Delta \mathrm{z}_{r,2} & -\Delta \mathrm{x}_{r,1} & -1 & \Delta \mathrm{z}_{1,2} & 0 & 0 & \Delta \mathrm{x}_{1,2} \\ 1 & 0 & 0 & 1 & 0 & 1 & 0 \\ \Delta \mathrm{z}_{r,2} & \Delta \mathrm{x}_{r,2} & 1 & -\Delta \mathrm{z}_{1,2} & \Delta \mathrm{x}_{1,2} & 0 & 0 \end{bmatrix}^T \right).$$

Kalman form decomposition Consider a reference frame $\langle P \rangle = \{{}^P O, {}^P X, {}^P Z\}$ such that its origin ${}^P O$ is coincident to the position of the feature $P_1 = (x_1, z_1)$ and axis ${}^P X$ is coincident to the line that passes through P_1 and P_2, with direction from P_1 to P_2 (see Fig. 3.2). Orientation of $\langle P \rangle$ w.r.t. $\langle W \rangle$ will be denoted $\phi_{1,2}$. Position P_2 w.r.t. $\langle P \rangle$ will be described by ${}^P P_2 = \{{}^P x_2, 0\}$ and vehicle configuration will be described as ${}^P \xi_r = \left({}^P x_r, {}^P z_r, {}^P \theta_r\right)$.

Now, let's consider the coordinate transformation:

$$\zeta = ({}^P x_r, {}^P z_r, {}^P \theta_r, {}^P x_2, x_1, z_1, \phi_{1,2}),$$

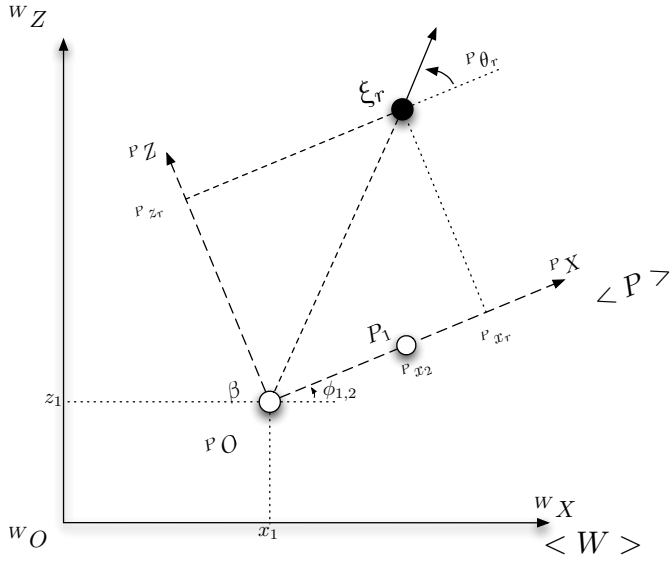

Figure 3.2: Reference frame $\langle P \rangle$.

given by $\Phi : \mathbb{R}^6 \times S \to \mathbb{R}^5 \times S^2$, i.e.,

$$\zeta = \begin{bmatrix} {}^{P}x_r \\ {}^{P}z_r \\ {}^{P}\theta_r \\ {}^{P}x_2 \\ x_1 \\ z_1 \\ \phi_{1,2} \end{bmatrix} = \begin{bmatrix} (x_r - x_1)\cos\left(\tan^{-1}\left(\frac{z_2-z_1}{x_2-x_1}\right)\right) + (z_r - z_1)\sin\left(\tan^{-1}\left(\frac{z_2-z_1}{x_2-x_1}\right)\right) \\ (z_r - z_1)\cos\left(\tan^{-1}\left(\frac{z2-z1}{x2-x1}\right)\right) - (x_r - x_1)\sin\left(\tan^{-1}\left(\frac{z_2-z_1}{x_2-x_1}\right)\right) \\ \theta\mathrm{r} - \tan^{-1}\left(\frac{z_2-z_1}{x_2-x_1}\right) \\ (\mathrm{x2}-\mathrm{x1})\cos(\phi 12) + (\mathrm{z2}-\mathrm{z1})\sin(\phi 12) \\ x_1 \\ z_1 \\ \tan^{-1}\left(\frac{z_2-z_1}{x_2-x_1}\right) \end{bmatrix},$$

for which system dynamics yields:

$$\dot{\zeta} = \begin{bmatrix} \cos\left({}^{P}\theta_r\right)\nu_f \\ \sin\left({}^{P}\theta_r\right)\nu_f \\ \omega \\ 0 \\ 0 \\ 0 \\ 0 \end{bmatrix},$$

and system output becomes

$$y = \begin{bmatrix} \pi - {}^{P}\theta_r + \tan^{-1}\left(\frac{{}^{P}z_r}{{}^{P}x_r}\right) \\ \pi - {}^{P}\theta_r + \tan^{-1}\left(\frac{{}^{P}z_r}{{}^{P}x_r - {}^{P}x_2}\right) \end{bmatrix}.$$

In order to verify if Φ is local diffeomorphism at ξ we compute its Jacobian. Matrix rank of J is 7 apart from $|J| = 0$, i.e., when

$$|\mathrm{J}| = \frac{{}^{P}x_2}{{\rho_{1,2}}^2}.$$

Hence, we conclude that Φ is not a global diffeomorphism and is not defined for $\rho = 0$, as expected. Moreover, Φ is not a local diffeomorphism if ${}^{P}x_2 = 0$, however that would be the case only if P_1 and P_2 are coincident, i.e., $P_1 = P_2$, which is not the case here.

Observability analysis under local decomposition After 1 level of Lie differentiation, the observability codistribution for ζ is

$$\Omega = \begin{bmatrix} \partial_{\zeta_r} h_1 & 0 & 0 & 0 & 0 \\ \partial_{\zeta_r} h_2 & \partial_{\zeta_4} h_2 & 0 & 0 & 0 \\ \partial_{\zeta_r} L_\Delta h_1 & 0 & 0 & 0 & 0 \\ \partial_{\zeta_r} L_\Delta h_2 & \partial_{\zeta_4} L_\Delta h_2 & 0 & 0 & 0 \end{bmatrix},$$

where

$$\partial_{\zeta_r} h_i = \begin{bmatrix} \frac{{}^{P}\Delta \mathrm{z}_{r,i}}{{\rho_{r,i}}^2} & \frac{{}^{P}\Delta \mathrm{x}_{r,i}}{{\rho_{r,i}}^2} & -1 \end{bmatrix},$$

$$\partial_{\zeta_r} L_\Delta h_i = \begin{bmatrix} \frac{2\,{}^{P}\Delta \mathrm{x}_{r,i}\,{}^{P}\Delta \mathrm{z}_{r,i}\cos({}^{P}\theta_r) + ({}^{P}\Delta \mathrm{z}_{r,i} + {}^{P}\Delta \mathrm{x}_{r,i})\,({}^{P}\Delta \mathrm{z}_{r,i} - {}^{P}\Delta \mathrm{x}_{r,i})\sin({}^{P}\theta_r)}{{\rho_{r,i}}^4} \\ -\frac{2\,{}^{P}\Delta \mathrm{x}_{r,i}\,{}^{P}\Delta \mathrm{z}_{r,i}\sin({}^{P}\theta_r) + ({}^{P}\Delta \mathrm{z}_{r,i} + {}^{P}\Delta \mathrm{x}_{r,i})\,({}^{P}\Delta \mathrm{z}_{r,i} - {}^{P}\Delta \mathrm{x}_{r,i})\cos({}^{P}\theta_r)}{{\rho_{r,i}}^4} \\ \frac{{}^{P}\Delta \mathrm{x}_{r,i}\,\cos({}^{P}\theta_r) + {}^{P}\Delta \mathrm{z}_{r,i}\sin({}^{P}\theta_r)}{{\rho_{r,i}}^2} \end{bmatrix}^T,$$

$$\partial_{\zeta_4} h_2 = \frac{{}^{P}\Delta \mathrm{z}_{r,2}}{{\rho_{r,2}}^2},$$

and

$$\partial_{\zeta_4} L_\Delta h_2 = \frac{\left(-2\,{}^{P}\Delta \mathrm{x}_{r,2}\,{}^{P}\Delta \mathrm{z}_{r,2}\cos(\theta_r) - ({}^{P}\Delta \mathrm{z}_{r,2} + {}^{P}\Delta \mathrm{x}_{r,2})\,({}^{P}\Delta \mathrm{z}_{r,2} - {}^{P}\Delta \mathrm{x}_{r,2})\sin(\theta_r)\right)}{{\rho_{r,2}}^4}.$$

Nullspace of Ω is given by:

$$\mathrm{Ker}(\Omega) = \mathrm{span}\left(\left[\begin{array}{ccccccc} 0 & 0 & 0 & 0 & 0 & 0 & 1 \\ 0 & 0 & 0 & 0 & 0 & 1 & 0 \\ 0 & 0 & 0 & 0 & 1 & 0 & 0 \end{array}\right]\right),$$

and we may conclude that the observable subsystem is given by $\zeta_o = \left({}^P x_r, {}^P z_r, {}^P \theta_r, {}^P x_2\right)$ and the non observable subsystem is

$$\zeta_{\bar{o}} = (\mathrm{x1}, \mathrm{z1}, \phi_{1,2}).$$

Remark 3.2 *The observable subsystem ζ_o of the 2 targets problem is equivalent to the system investigated in the 1 and a half marker problem if one considers the z position of the* half marker *as zero.*

Table 3.1: Summary of results.

M	0	0	0	0	1	$1+\frac{1}{2}$	$1+\frac{1}{2}$	2	$3+\bar{M}$
N	$2+\bar{N}$	2	1	$\frac{1}{2}$	0	0	$\bar{N}$	0	$\bar{N}$
k	1	1	1	1	1	1	0	1	0
$\dim(\xi)$	$7+2\bar{N}$	7	5	4	3	4	$4+\bar{N}$	3	$3+2\bar{M}+2\bar{N}$
$\dim(\zeta_o)$	$4+2\bar{N}$	4	2	2	2	4	$4+\bar{N}$	3	$3+2\bar{M}+2\bar{N}$
$\dim(\zeta_{\bar{o}})$	3	3	3	2	1	0	0	0	0

3.2.8 Conclusions

Table 3.2.8 presents an overview of the results obtained in this section and also extends this results as already described. The table presents the following details:

- M: Number of markers;
- N: Number of targets;
- k: Minimum level of lie-bracketing required to cover observable space;
- $\dim(\xi)$: System dimension;
- $\dim(\zeta_o)$: Observable space dimension;
- $\dim(\zeta_{\bar{o}})$: Non-observable space dimension;

The most relevant results can be summarised as follows.

1 landmark If only one landmark is being observed, the observable subsystem is

$$\zeta_o = (\rho, \beta),$$

where ρ represents the cartesian distance from the vehicle to the landmark and β represents the bearing angle between vehicle orientation and the landmark.

The non observable space is composed of ϕ (the angle formed by the vehicle position and any arbitrary reference frame) and of the position of the landmark in case it is not known (target).

2, 3 or more landmarks When at least two landmarks are being observed, the observable subsystem is

$$\zeta_o = \left({}^P x_r,\, {}^P z_r,\, {}^P \theta_r,\, {}^P x_1,\, {}^P z_1,\, {}^P x_2,\, {}^P z_2,\, {}^P x_3,\, {}^P z_3, \ldots \right),$$

where P is a coordinate frame arbitrary chosen w.r.t. of the landmarks,e.g., with origin coincident to the position of P_1 and axis ${}^P X$ parallel to the line that passes through P_1 and P_2. If 3 or more landmarks are known (markers), the observable subsystem is observable at 0 levels of Lie bracketing, otherwise it becomes observable after 1 level of Lie differentiation.

The non observable space regards the coordinate transformation between frame $\langle P \rangle$ and world frame $\langle W \rangle$. This coordinate transformation is completely non observable if all landmarks are unknown (targets) and becomes completely observable when a 3-dimensional space subsystem of the positions of the landmarks w.r.t. $\langle W \rangle$ is previously known (a problem named the 1 and a half marker problem here), e.g., position of P_1 and orientation of the line passing through P_1 and P_2 w.r.t. $\langle W \rangle$ are previously known.

3.3 Unknown Input Observability

In this section we will study the observability problem when inputs are not completely available, i.e., input disturbances can affect the system.

Disturbance model Consider a vehicle described by $\xi_r = (x_r, z_r, \theta_r)$ (see fig. 1.5), for which dynamics is slow enough to be neglected and inputs are completely unknown, i.e., inputs are treated as a disturbance itself. We can represent disturbances on all directions of the plane by considering the following dynamics:

$$\dot{\xi}_r = f_r(\xi_r, d_r) = [g_f \ g_h \ g_\omega]\, d_r = \begin{bmatrix} \cos(\theta_r) & -\sin(\theta_r) & 0 \\ \sin(\theta_r) & \cos(\theta_r) & 0 \\ 0 & 0 & 1 \end{bmatrix} d_r, \quad (3.8)$$

that corresponds to a disturbance input matrix $B(\xi_r)$ chosen to describe omnidirectional kinematics and a disturbance vector

$$d_r = (d_f, d_h, d_\omega)$$

that comprehends all the possible planar generalized velocities.

In order to study system left-invertibility and state observability problems concurrently, i.e., the possibility of reconstructing system state and an unknown input (or disturbance) from the knowledge of the outputs [75], we consider the augmented system composed of vehicle state and all input disturbances derivatives $\xi_e = (\xi_{e,r}, \xi_{e,d1}, \xi_{e,d2}, \ldots) = \left(\xi_r, d_r, d_r^{(1)}, \ldots\right)$.

System definition In this section we will investigate the disturbance observability problem for different configurations regarding the number of M markers and N targets being measured. We will refer to ξ_t as a vector with all targets and ξ_m as a vector with all markers:

$$\xi_t = [\xi_{t,M+1}, \ldots, \xi_{t,M+N}]^T,$$

and

$$\xi_m = [\xi_{t,1}, \ldots, \xi_{t,M}]^T.$$

A generic augmented system state will be composed of vehicle configuration, position of targets and disturbance d_r:

$$\xi_e =$$

$$= (\xi_{e,r}, \xi_{e,f1}, \xi_{e,f2}, \ldots, \xi_{e,d1}, \xi_{e,d2}, \ldots) =$$
$$= \left(\xi_r, \xi_{t,M+1}, \ldots, \xi_{t,M+N}, d_r, d_r^{(1)}, \ldots\right),$$

with corresponding system dynamics:

$$\dot{\xi} = \begin{bmatrix} \dot{\xi}_r \\ 0 \\ \vdots \\ 0 \\ \xi_{e,d2} \\ \vdots \end{bmatrix} = \begin{bmatrix} g_f \\ 0 \\ \vdots \\ 0 \\ 0 \\ \vdots \end{bmatrix} d_f + \begin{bmatrix} g_h \\ 0 \\ \vdots \\ 0 \\ 0 \\ \vdots \end{bmatrix} d_h + \begin{bmatrix} g_\omega \\ 0 \\ \vdots \\ 0 \\ 0 \\ \vdots \end{bmatrix} d_\omega.$$

Given that we apply the procedure proposed in section 2.4 to study the disturbance observability analysis, we are interested in investigating the observability problem for $\dot{d}_r = 0$ and then to verify if results can be extended for any analytic $d_r(t)$.

Measurement process is modeled by $q = N + M$ equations of the form (1.21), yielding:

$$Y = \begin{bmatrix} y_{m,1} \\ y_{m,2} \\ \vdots \\ y_{m,M} \\ y_{t,M+1} \\ \vdots \\ y_{t,M+N} \end{bmatrix} = \begin{bmatrix} h_{m,1}(\xi_r, \xi_{m,1}) \\ h_{m,2}(\xi_r, \xi_{m,2}) \\ \vdots \\ h_{m,M}(\xi_r, \xi_{m,M}) \\ h_{t,M+1}(\xi_r, \xi_{t,M+1}) \\ \vdots \\ h_{t,M+N}(\xi_r, \xi_{t,M+N}) \end{bmatrix}.$$

Codistribution form In section 2.4 we presented a procedure for investigating the disturbance observability problem that consists in studying the rank of codistribution codistribution ${}^0\Omega$ associated with constant disturbances, and then, extending results to any analytic disturbances. A generic form for the observability codistribution ${}^0\Omega$ of the systems under investigation is

$$
{}^0\Omega = \begin{bmatrix} {}^0\Omega^{(0)} \\ {}^0\Omega^{(1)} \\ \vdots \end{bmatrix} = \begin{bmatrix} \mathrm{dL_\Delta}^{(0)} h_1 \\ \mathrm{dL_\Delta}^{(0)} h_2 \\ \vdots \\ \mathrm{dL_\Delta}^{(1)} h_1 \\ \mathrm{dL_\Delta}^{(1)} h_2 \\ \vdots \end{bmatrix} = \begin{bmatrix} \partial_{\xi_r} {L_\Delta}^{(0)} h_1 & \partial_{\xi_t} {L_\Delta}^{(0)} h_1 & \partial_{d_r} {L_\Delta}^{(0)} h_1 \\ \vdots & \vdots & \vdots \\ \partial_{\xi_r} {L_\Delta}^{(1)} h_1 & \partial_{\xi_t} {L_\Delta}^{(1)} h_1 & \partial_{d_r} {L_\Delta}^{(1)} h_1 \\ \vdots & \vdots & \vdots \end{bmatrix}
$$

or

$$
{}^0\Omega = \begin{bmatrix} {}^0\Omega^0_{\xi_r} & {}^0\Omega^0_{\xi_t} & {}^0\Omega^0_{d_r} \\ {}^0\Omega^1_{\xi_r} & {}^0\Omega^1_{\xi_t} & {}^0\Omega^1_{d_r} \\ \vdots & \vdots & \vdots \end{bmatrix},
$$

where

$$
\begin{bmatrix} {}^0\Omega^0_{\xi_r} \\ {}^0\Omega^1_{\xi_r} \\ \vdots \end{bmatrix} = \begin{bmatrix} \partial_{\xi_r} {L_\Delta}^{(0)} h_{m,1} \\ \vdots \\ \partial_{\xi_r} {L_\Delta}^{(0)} h_{m,M} \\ \partial_{\xi_r} {L_\Delta}^{(0)} h_{t,M+1} \\ \partial_{\xi_r} {L_\Delta}^{(0)} h_{t,M+2} \\ \vdots \\ \partial_{\xi_r} {L_\Delta}^{(0)} h_{t,M+N} \\ \partial_{\xi_r} {L_\Delta}^{(1)} h_{m,1} \\ \vdots \end{bmatrix},
$$

$$
\begin{bmatrix} \Omega^0_{\xi_t} \\ \Omega^1_{\xi_t} \\ \vdots \end{bmatrix} = \begin{bmatrix} 0 & 0 & 0 & 0 \\ \vdots & \vdots & \vdots & \vdots \\ 0 & 0 & 0 & 0 \\ \partial_{\xi_{t,M+1}} {L_\Delta}^{(0)} h_{t,M+1} & 0 & 0 & 0 \\ 0 & \partial_{\xi_{t,M+2}} {L_\Delta}^{(0)} h_{t,M+2} & 0 & 0 \\ \vdots & \vdots & \ddots & \vdots \\ 0 & 0 & 0 & \partial_{\xi_{t,M+N}} {L_\Delta}^{(0)} h_{t,M+N} \\ 0 & 0 & 0 & 0 \\ \vdots & \vdots & \vdots & \vdots \end{bmatrix} \begin{matrix} \\ \\ \\ \left.\begin{matrix} \\ \\ \end{matrix}\right\} M\text{markers} \\ \left.\begin{matrix} \\ \\ \\ \end{matrix}\right\} N\text{markers} \\ \\ \vdots \end{matrix},
$$

and

$$\begin{bmatrix} \Omega^0_{dr} \\ \Omega^1_{dr} \\ \vdots \end{bmatrix} = \begin{bmatrix} \partial_{\mathrm{dr}} {L_\Delta}^{(0)} h_{m,1} \\ \vdots \\ \partial_{\mathrm{dr}} {L_\Delta}^{(0)} h_{m,M} \\ \partial_{\mathrm{dr}} {L_\Delta}^{(0)} h_{t,M+1} \\ \partial_{\mathrm{dr}} {L_\Delta}^{(0)} h_{t,M+2} \\ \vdots \\ \partial_{\mathrm{dr}} {L_\Delta}^{(0)} h_{t,M+N} \\ \partial_{\mathrm{dr}} {L_\Delta}^{(1)} h_{m,1} \\ \vdots \end{bmatrix}.$$

Codistribution ${}^0\Omega$ submatrices In order to simplify the following demonstrations let's define the disturbances d_f and d_h on polar coordinates:

$$\begin{bmatrix} d_\rho \\ d_\phi \end{bmatrix} = \Phi_p\left(d_h, d_f\right) = \begin{bmatrix} \sqrt{{d_f}^2 + {d_h}^2} \\ \tan^{-1}\left(\frac{d_f}{d_h}\right) \end{bmatrix},$$

which inverse is given by

$$\begin{bmatrix} d_h \\ d_f \end{bmatrix} = {\Phi_p}^{-1}\left[d_\rho, d_\phi\right) = \begin{bmatrix} d_\rho \cos\left(d_\phi\right) \\ d_\rho \sin\left(d_\phi\right) \end{bmatrix}.$$

We will also use the following notations: $\Delta \mathrm{x}_i = \Delta \mathrm{x}_{r,i}, \Delta \mathrm{z}_i = \Delta \mathrm{z}_{r,i}, \rho_i = \rho_{r,i}$, $\Delta_\phi = \mathrm{d}\phi - \theta \mathrm{r}$, $S(*) = \sin(*)$ and $C(*) = \cos(*)$.

Note that this coordinate transformation is not defined for $d_\rho = 0$.

In all of the following analysis, the observability codistribution ranks reach their maximum within the third level of Lie differentiation. Codistributions Ω till this level will be composed of the following sub-matrices $\partial_{\xi_r} {L_\Delta}^{(*)} h_i$:

$$\partial_{\xi_r} {L_\Delta}^{(0)} h_i = \begin{bmatrix} -\frac{\Delta \mathrm{z}_i}{\rho_i^2} \\ \frac{\Delta \mathrm{x}_i}{\rho_i^2} \\ -1 \end{bmatrix}^T, \; \partial_{\xi_r} {L_\Delta}^{(1)} h_i = \begin{bmatrix} \frac{\mathrm{d}\rho\left(2S\left[\Delta_\phi\right]\Delta \mathrm{x}_i \Delta \mathrm{z}_i + C\left[\Delta_\phi\right]\left(-\Delta \mathrm{x}_i^2 + \Delta \mathrm{z}_i^2\right)\right)}{\rho_i^4} \\ \frac{\mathrm{d}\rho\left(-2C\left[\Delta_\phi\right]\Delta \mathrm{x}_i \Delta \mathrm{z}_i + S\left[\Delta_\phi\right]\left(-\Delta \mathrm{x}_i^2 + \Delta \mathrm{z}_i^2\right)\right)}{\rho_i^4} \\ \frac{\mathrm{d}\rho\left(S\left[\Delta_\phi\right]\Delta \mathrm{x}_i + C\left[\Delta_\phi\right]\Delta \mathrm{z}_i\right)}{\rho_i^2} \end{bmatrix}^T,$$

$$\partial_{\xi_r} {L_\Delta}^{(2)} h_i =$$

$$= \begin{bmatrix} -\frac{\mathrm{d}\rho\left(2\mathrm{d}\rho C\left[2\Delta_\phi\right]\Delta z_i\left(-3\Delta x_i^2+\Delta z_i^2\right)+d_\omega S\left[\Delta_\phi\right]\left(\Delta x_i^4-\Delta z_i^4\right)+2C\left[\Delta_\phi\right]\Delta x_i\left(-2\mathrm{d}\rho S\left[\Delta_\phi\right]\left(\Delta x_i^2-3\Delta z_i^2\right)+d_\omega \Delta z_i\rho_i^2\right)\right)}{\rho_i^6} \\ -\frac{\mathrm{d}\rho\left(C\left[\Delta_\phi\right]\left(4\mathrm{d}\rho S\left[\Delta_\phi\right]\Delta z_i\left(-3\Delta x_i^2+\Delta z_i^2\right)+d\omega\left(-\Delta x_i^4+\Delta z_i^4\right)\right)+2\Delta x_i\left(\mathrm{d}\rho C\left[2\Delta_\phi\right]\left(\Delta x_i^2-3\Delta z_i^2\right)+d_\omega S\left[\Delta_\phi\right]\Delta z_i\rho_i^2\right)\right)}{\rho_i^6} \\ \frac{\mathrm{d}\rho\left(-4\mathrm{d}\rho S\left[2\Delta_\phi\right]\Delta x_i\Delta z_i+2\mathrm{d}\rho C\left[2\Delta_\phi\right](\Delta x_i-\Delta z_i)(\Delta x_i+\Delta z_i)-d_\omega C\left[\Delta_\phi\right]\Delta x_i\rho_i^2+d_\omega S\left[\Delta_\phi\right]\Delta z_i\rho_i^2\right)}{\rho_i^4} \end{bmatrix}^T,$$

and

$$\partial_{\xi_r} {L_\Delta}^{(3)} h_i =$$

$$= \begin{bmatrix} \frac{\mathrm{d}\rho\left(6\mathrm{d}\rho^2 C\left[3\Delta_\phi\right]\left(\Delta x_i^4-6\Delta x_i^2\Delta z_i^2+\Delta z_i^4\right)+d_\omega^2 C\left[\Delta_\phi\right](\Delta x_i-\Delta z_i)(\Delta x_i+\Delta z_i)\rho_i^4\right)}{\rho_i^8} \\ \frac{\mathrm{d}\rho\left(24\mathrm{d}\rho^2 C\left[3\Delta_\phi\right]\Delta x_i^3\Delta z_i-24\mathrm{d}\rho^2 C\left[3\Delta_\phi\right]\Delta x_i\Delta z_i^3+6\mathrm{d}\rho^2 S\left[3\Delta_\phi\right]\left(\Delta x_i^4-6\Delta x_i^2\Delta z_i^2+\Delta z_i^4\right)-6\mathrm{d}\rho d_\omega S\left[2\Delta_\phi\right]\Delta x_i^3\rho_i^2\right)}{\rho_i^8} \\ \frac{\mathrm{d}\rho\left(S\left[\Delta_\phi\right]\Delta x_i+C\left[\Delta_\phi\right]\Delta z_i\right)\left(12\mathrm{d}\rho^2 C\left[2\Delta_\phi\right]\left(-\Delta x_i^2+\Delta z_i^2\right)\right)}{\rho_i^6} \end{bmatrix}^T +$$

$$+ \begin{bmatrix} \frac{-2\mathrm{d}\rho\ \left(12\mathrm{d}\rho^2 S\left[3\Delta_\phi\right]\Delta x_i(\Delta x_i-\Delta z_i)\Delta z_i(\Delta x_i+\Delta z_i)\right)}{\rho_i^8} \\ \frac{\mathrm{d}\rho\left(+18\mathrm{d}\rho d_\omega S\left[2\Delta_\phi\right]\Delta x_i\Delta z_i^2\rho_i^2+6\mathrm{d}\rho d_\omega C\left[2\Delta_\phi\right]\Delta z_i\left(-3\Delta x_i^2+\Delta z_i^2\right)\rho_i^2+d_\omega^2 S\left[\Delta_\phi\right]\Delta x_i^2\rho_i^4\right)}{\rho_i^8} \\ \frac{\mathrm{d}\rho\left(12\mathrm{d}\rho C\left[\Delta_\phi\right]\Delta x_i\left(4\mathrm{d}\rho S\left[\Delta_\phi\right]\Delta z_i+d_\omega\rho_i^2\right)\right)}{\rho_i^6} \end{bmatrix}^T +$$

$$+ \begin{bmatrix} \frac{-2\mathrm{d}\rho\left(d_\omega\rho_i^2\left(3\mathrm{d}\rho C\left[2\Delta_\phi\right]\Delta x_i\left(\Delta x_i^2-3\Delta z_i^2\right)+3\mathrm{d}\rho S\left[2\Delta_\phi\right]\Delta z_i\left(-3\Delta x_i^2+\Delta z_i^2\right)+d_\omega S\left[\Delta_\phi\right]\Delta x_i\Delta z_i\rho_i^2\right)\right)}{\rho_i^8} \\ \frac{\mathrm{d}\rho\left(+2d_\omega^2 C\left[\Delta_\phi\right]\Delta x_i\Delta z_i\rho_i^4-d_\omega^2 S\left[\Delta_\phi\right]\Delta z_i^2\rho_i^4\right)}{\rho_i^8} \\ \frac{-\mathrm{d}\rho\left(\rho_i^2\left(6\mathrm{d}\rho^2+12\mathrm{d}\rho d_\omega S\left[\Delta_\phi\right]\Delta z_i+d_\omega^2\rho_i^2\right)\right)}{\rho_i^6} \end{bmatrix}^T$$

Codistributions Ω till second level of bracketing will be composed of the following sub-matrices $\partial_{\xi_i} {L_\Delta}^{(*)} h_i$:

$$\partial_{\xi_i} {L_\Delta}^{(0)} h_i = \begin{bmatrix} \frac{\Delta z_i}{\rho_i^2} \\ -\frac{\Delta x_i}{\rho_i^2} \end{bmatrix}^T,\ \partial_{\xi_i} {L_\Delta}^{(1)} h_i = \begin{bmatrix} \frac{\mathrm{d}\rho(-2S[\Delta\phi]\Delta x_i\Delta z_i+C[\Delta\phi](\Delta x_i-\Delta z_i)(\Delta x_i+\Delta z_i))}{\rho_i^4} \\ \frac{\mathrm{d}\rho(2C[\Delta\phi]\Delta x_i\Delta z_i+S[\Delta\phi](\Delta x_i-\Delta z_i)(\Delta x_i+\Delta z_i))}{\rho_i^4} \end{bmatrix}^T,$$

$$\partial_{\xi_i} {L_\Delta}^{(2)} h_i =$$
$$\begin{bmatrix} \frac{\mathrm{d}\rho\left(2\mathrm{d}\rho C[2\Delta\phi]\Delta z_i\left(-3\Delta x_i^2+\Delta z_i^2\right)+d_\omega S[\Delta\phi]\left(\Delta x_i^4-\Delta z_i^4\right)+2C[\Delta\phi]\Delta x_i\left(-2\mathrm{d}\rho S[\Delta\phi]\left(\Delta x_i^2-3\Delta z_i^2\right)+d_\omega\Delta z_i\rho_i^2\right)\right)}{\rho_i^6} \\ \frac{\mathrm{d}\rho\left(C[\Delta\phi]\left(4\mathrm{d}\rho S[\Delta\phi]\Delta z_i\left(-3\Delta x_i^2+\Delta z_i^2\right)+d_\omega\left(-\Delta x_i^4+\Delta z_i^4\right)\right)+2\Delta x_i\left(\mathrm{d}\rho C[2\Delta\phi]\left(\Delta x_i^2-3\Delta z_i^2\right)+d_\omega S[\Delta\phi]\Delta z_i\rho_i^2\right)\right)}{\rho_i^6} \end{bmatrix}^T,$$

and

$$\partial_{\xi_i} {L_\Delta}^{(3)} h_i =$$

$$\left[\begin{array}{c} \frac{\mathrm{d}\rho\left(-6\mathrm{d}\rho^2 C[3\Delta\phi]\left(\Delta \mathrm{x}_i^4-6\Delta \mathrm{x}_i^2\Delta \mathrm{z}_i^2+\Delta \mathrm{z}_i^4\right)+d_\omega^2 C[\Delta\phi]\left(-\Delta \mathrm{x}_i^2+\Delta \mathrm{z}_i^2\right)\rho_i^4\right)}{\rho_i^8} \\ \frac{\mathrm{d}\rho\left(-24\mathrm{d}\rho^2 C[3\Delta\phi]\Delta \mathrm{x}_i^3\Delta \mathrm{z}_i+24\mathrm{d}\rho^2 C[3\Delta\phi]\Delta \mathrm{x}_i\Delta \mathrm{z}_i^3-6\mathrm{d}\rho^2 S[3\Delta\phi]\left(\Delta \mathrm{x}_i^4-6\Delta \mathrm{x}_i^2\Delta \mathrm{z}_i^2+\Delta \mathrm{z}_i^4\right)+6\mathrm{d}\rho d_\omega S[2\Delta\phi]\Delta \mathrm{x}_i^3\rho_i^2\right)}{\rho_i^8} \end{array}\right]^T +$$

$$+\left[\begin{array}{c} \frac{2\mathrm{d}\rho\left(12\mathrm{d}\rho^2 S[3\Delta\phi]\Delta \mathrm{x}_i(\Delta \mathrm{x}_i-\Delta \mathrm{z}_i)\Delta \mathrm{z}_i(\Delta \mathrm{x}_i+\Delta \mathrm{z}_i)\right)}{\rho_i^8} \\ \frac{\mathrm{d}\rho\left(-18\mathrm{d}\rho d_\omega S[2\Delta\phi]\Delta \mathrm{x}_i\Delta \mathrm{z}_i^2\rho_i^2-6\mathrm{d}\rho d_\omega C[2\Delta\phi]\Delta \mathrm{z}_i\left(-3\Delta \mathrm{x}_i^2+\Delta \mathrm{z}_i^2\right)\rho_i^2\right)}{\rho_i^8} \end{array}\right]^T +$$

$$+\left[\begin{array}{c} \frac{2\mathrm{d}\rho\left(+d_\omega\rho_i^2\left(3\mathrm{d}\rho C[2\Delta\phi]\Delta \mathrm{x}_i\left(\Delta \mathrm{x}_i^2-3\Delta \mathrm{z}_i^2\right)+3\mathrm{d}\rho S[2\Delta\phi]\Delta \mathrm{z}_i\left(-3\Delta \mathrm{x}_i^2+\Delta \mathrm{z}_i^2\right)+d_\omega S[\Delta\phi]\Delta \mathrm{x}_i\Delta \mathrm{z}_i\rho_i^2\right)\right)}{\rho_i^8} \\ \frac{\mathrm{d}\rho\left(-d_\omega^2 S[\Delta\phi]\Delta \mathrm{x}_i^2\rho_i^4-2d_\omega^2 C[\Delta\phi]\Delta \mathrm{x}_i\Delta \mathrm{z}_i\rho_i^4+d_\omega^2 S[\Delta\phi]\Delta \mathrm{z}_i^2\rho_i^4\right)}{\rho_i^8} \end{array}\right]^T$$

Codistributions Ω till second third of bracketing will be composed of the following sub-matrices $\partial_d {L_\Delta}^{(*)} h_i$:

$$\partial_d {L_\Delta}^{(0)} h_i = \left[\begin{array}{c} 0 \\ 0 \\ 0 \end{array}\right]^T,\ \partial_d {L_\Delta}^{(1)} h_i = \left[\begin{array}{c} \frac{S[\theta\mathrm{r}]\Delta \mathrm{x}_i-C[\theta\mathrm{r}]\Delta \mathrm{z}_i}{\rho_i^2} \\ \frac{C[\theta\mathrm{r}]\Delta \mathrm{x}_i+S[\theta\mathrm{r}]\Delta \mathrm{z}_i}{\rho_i^2} \\ -1 \end{array}\right]^T,$$

$$\partial_d {L_\Delta}^{(2)} h_i = \left[\begin{array}{c} \frac{4\mathrm{d}\rho S[\mathrm{d}\phi-2\theta\mathrm{r}]\Delta \mathrm{x}_i\Delta \mathrm{z}_i+2\mathrm{d}\rho C[\mathrm{d}\phi-2\theta\mathrm{r}]\left(-\Delta \mathrm{x}_i^2+\Delta \mathrm{z}_i^2\right)+d_\omega C[\theta\mathrm{r}]\Delta \mathrm{x}_i\rho_i^2+d_\omega S[\theta\mathrm{r}]\Delta \mathrm{z}_i\rho_i^2}{\rho_i^4} \\ \frac{-4\mathrm{d}\rho C[\mathrm{d}\phi-2\theta\mathrm{r}]\Delta \mathrm{x}_i\Delta \mathrm{z}_i+2\mathrm{d}\rho S[\mathrm{d}\phi-2\theta\mathrm{r}]\left(-\Delta \mathrm{x}_i^2+\Delta \mathrm{z}_i^2\right)-d_\omega S[\theta\mathrm{r}]\Delta \mathrm{x}_i\rho_i^2+d_\omega C[\theta\mathrm{r}]\Delta \mathrm{z}_i\rho_i^2}{\rho_i^4} \\ \frac{\mathrm{d}\rho(S[\Delta\phi]\Delta \mathrm{x}_i+C[\Delta\phi]\Delta \mathrm{z}_i)}{\rho_i^2} \end{array}\right]^T,$$

and

$$\partial_d {L_\Delta}^{(3)} h_i =$$

$$= \left[\begin{array}{c} \frac{6\mathrm{d}\rho^2 S[2\mathrm{d}\phi-3\theta\mathrm{r}]\Delta \mathrm{x}_i^3-18\mathrm{d}\rho^2 S[2\mathrm{d}\phi-3\theta\mathrm{r}]\Delta \mathrm{x}_i\Delta \mathrm{z}_i^2-6\mathrm{d}\rho^2 C[2\mathrm{d}\phi-3\theta\mathrm{r}]\Delta \mathrm{z}_i\left(-3\Delta \mathrm{x}_i^2+\Delta \mathrm{z}_i^2\right)-6\mathrm{d}\rho d_\omega S[\mathrm{d}\phi-2\theta\mathrm{r}]\Delta \mathrm{x}_i^2\rho_i^2}{\rho_i^6} \\ -\frac{-18\mathrm{d}\rho^2 S[2\mathrm{d}\phi-3\theta\mathrm{r}]\Delta \mathrm{x}_i^2\Delta \mathrm{z}_i+6\mathrm{d}\rho^2 S[2\mathrm{d}\phi-3\theta\mathrm{r}]\Delta \mathrm{z}_i^3+6\mathrm{d}\rho^2 C[2\mathrm{d}\phi-3\theta\mathrm{r}]\Delta \mathrm{x}_i\left(\Delta \mathrm{x}_i^2-3\Delta \mathrm{z}_i^2\right)}{\rho_i^6} \\ \frac{\mathrm{d}\rho(3\mathrm{d}\rho C[2\Delta\phi](\Delta \mathrm{x}_i-\Delta \mathrm{z}_i)(\Delta \mathrm{x}_i+\Delta \mathrm{z}_i))}{\rho_i^4} \end{array}\right]^T +$$

$$+\left[\begin{array}{c} \frac{-12\mathrm{d}\rho d_\omega C[\mathrm{d}\phi-2\theta\mathrm{r}]\Delta \mathrm{x}_i\Delta \mathrm{z}_i\rho_i^2+6\mathrm{d}\rho d_\omega S[\mathrm{d}\phi-2\theta\mathrm{r}]\Delta \mathrm{z}_i^2\rho_i^2-d_\omega^2 S[\theta\mathrm{r}]\Delta \mathrm{x}_i\rho_i^4+d_\omega^2 C[\theta\mathrm{r}]\Delta \mathrm{z}_i\rho_i^4}{\rho_i^6} \\ \frac{+12\mathrm{d}\rho d_\omega S[\mathrm{d}\phi-2\theta\mathrm{r}]\Delta \mathrm{x}_i\Delta \mathrm{z}_i\rho_i^2+6\mathrm{d}\rho d_\omega C[\mathrm{d}\phi-2\theta\mathrm{r}]\left(-\Delta \mathrm{x}_i^2+\Delta \mathrm{z}_i^2\right)\rho_i^2+d_\omega^2 C[\theta\mathrm{r}]\Delta \mathrm{x}_i\rho_i^4+d_\omega^2 S[\theta\mathrm{r}]\Delta \mathrm{z}_i\rho_i^4}{\rho_i^6} \\ \frac{+\mathrm{d}\rho\left(2d_\omega S[\Delta\phi]\Delta \mathrm{z}_i\rho_i^2-2C[\Delta\phi]\Delta \mathrm{x}_i\left(6\mathrm{d}\rho S[\Delta\phi]\Delta \mathrm{z}_i+d_\omega\rho_i^2\right)\right)}{\rho_i^4} \end{array}\right]^T$$

Extension of results Results can be extended for problems of partially known inputs on the state form

$$\dot{\xi}_r = f_r\left(\xi_r, d_r\right) + G(\xi_r)u_r, \tag{3.9}$$

where vehicle kinematics is described by $G(\xi_r)$ and known inputs by u_r. As a matter of fact, given a generic observability matrix O^*_Σ that describes the original problem (equation (3.8)), the correspondent O_Σ that describes the partially known input problem (equation (3.9)) is composed of O^*_Σ and new lines described by covectors $L^{(k)}_{g_*} h_i$, $g_* \in G$. Hence, $rank(O_\Sigma) \geq rank(O^*_\Sigma)$ and we can conclude that if O^*_Σ is full rank, then O_Σ is also full rank and hence observable, independently of vehicle kinematics G and known inputs u_r considered.

Remark 3.3 *The various possible input observability analysis for an unicycle vehicle are particular cases of the more general unknown input observability analysis for an omnidirectional vehicle presented here, i.e.,* $d_h = 0$.

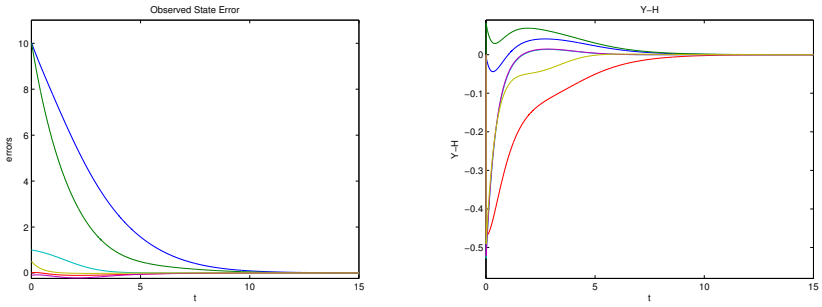

(1) (b)

Figure 3.3: Observer errors: (a) observed state error; (b) Y-H.

3.3.1 3 or more markers

The state space under investigation is composed of the vehicle configuration and disturbance $\xi_e = (\xi_r, d_r, d_r^{(1)}, \ldots)$ and system output consists of the measurement of three or more markers

$$y = (y_{m,1}, y_{m,2}, y_{m,3}, \ldots).$$

Observability analysis For constant disturbances, after 1 levels of Lie differentiation, the observability codistribution rank reaches its maximum of 6. Codistribution ${}^0\Omega$ for 1 levels of Lie bracketing is

$${}^0\Omega = \begin{bmatrix} \Omega^0_{\xi_r} & 0 \\ \Omega^1_{\xi_r} & \Omega^1_{d_r} \end{bmatrix} = \begin{bmatrix} \partial_{\xi_r} {L_\Delta}^{(0)} h_{m,1} & 0 \\ \partial_{\xi_r} {L_\Delta}^{(0)} h_{m,2} & 0 \\ \partial_{\xi_r} {L_\Delta}^{(0)} h_{m,3} & 0 \\ \vdots & \vdots \\ \partial_{\xi_r} {L_\Delta}^{(1)} h_{m,1} & \partial_{d_r} {L_\Delta}^{(1)} h_{m,1} \\ \partial_{\xi_r} {L_\Delta}^{(1)} h_{m,2} & \partial_{d_r} {L_\Delta}^{(1)} h_{m,2} \\ \partial_{\xi_r} {L_\Delta}^{(1)} h_{m,3} & \partial_{d_r} {L_\Delta}^{(1)} h_{m,3} \\ \vdots & \vdots \end{bmatrix}.$$

Apart from configuration singularities, $rank({}^0\Omega) = 6$ and system is locally weakly observable.Apart from singularities, both vehicle state

and constant input disturbances are locally weakly observable if 3 landmark positions are known. The minimum number of Lie bracketing required to cover the observable part of the state space ${}^0\xi_e$ is 1. Given the complete observability of ξ_e, the set of indistinguishable states regarding a non singular initial configuration is empty.

We evaluate these results through simulation using the implementation of the non-linear observer described in section 2.5 to reconstruct the observable space ζ_o. Initial conditions and system parameters are arbitrary. It is seen in Fig. 3.3 that the observer state converges to ζ_o.

Extension of results Now, we investigate if this result can be extended to any analytic d_f, d_h and d_ω. As ${}^0\xi_e$ is observable, we must verify if ${}^k\xi_e$ observable $\rightarrow$ ${}^{k+1}\xi_e$ observable. Therefore, let's analyze what happens with ${}^k\Omega$ when we apply the inductive step from ${}^k\xi_e$ to ${}^{k+1}\xi_e$:

$$ {}^k\Omega = \begin{bmatrix} * & 0 \\ * & \Omega^1_{d_r} \end{bmatrix} \rightarrow^{k+1} O_\Sigma = \begin{bmatrix} * & 0 & 0 \\ * & \Omega^1_{d_r} & 0 \\ * & * & \Omega^1_{d_r} \end{bmatrix}. $$

Notice that $rank({}^{k+1}\Omega) = rank({}^k\Omega) + rank(\Omega^1_{d_r})$. If ${}^k\Omega$ is observable, then

$$ rank\left({}^{k+1}\Omega\right) = dim\left({}^k\xi_e\right) + 3 = dim\left({}^{k+1}\xi_e\right), $$

and we can conclude that ${}^k\xi_e$ observable implies in ${}^{k+1}\xi_e$ being also observable. Hence, for analytic unknown disturbances d_f, d_h and d_ω, both vehicle state and input disurbances are locally weakly observable if 3 landmark positions are known.

3.3.2 2 markers

The state space under investigation is composed of the vehicle configuration and disturbance $\xi_e = (\xi_r, d_r, d_r^{(1)}, \ldots)$ and system output consists of the measurement of two markers $y = (y_{m,1}, y_{m,2})$.

Observability analysis For constant disturbances, after 2 levels of Lie differentiation, the observability codistribution rank reaches its maximum of 6. Codistribution ${}^0\Omega$ for 2 levels of Lie bracketing is

$$
{}^0\Omega = \begin{bmatrix} \Omega^0_{\xi_r} & 0 \\ \Omega^1_{\xi_r} & \Omega^1_{d_r} \\ \Omega^2_{\xi_r} & \Omega^2_{d_r} \end{bmatrix} = \begin{bmatrix} \partial_{\xi_\mathrm{r}} {L_\Delta}^{(0)} h_{m,1} & 0 \\ \partial_{\xi_\mathrm{r}} {L_\Delta}^{(0)} h_{m,2} & 0 \\ \partial_{\xi_\mathrm{r}} {L_\Delta}^{(1)} h_{m,1} & \partial_{d_r} {L_\Delta}^{(1)} h_{m,1} \\ \partial_{\xi_\mathrm{r}} {L_\Delta}^{(1)} h_{m,2} & \partial_{d_r} {L_\Delta}^{(1)} h_{m,2} \\ \partial_{\xi_\mathrm{r}} {L_\Delta}^{(2)} h_{m,1} & \partial_{d_r} {L_\Delta}^{(2)} h_{m,1} \\ \partial_{\xi_\mathrm{r}} {L_\Delta}^{(2)} h_{m,2} & \partial_{d_r} {L_\Delta}^{(2)} h_{m,2} \end{bmatrix}.
$$

Apart from configuration singularities, $rank({}^0\Omega) = 6$ and system is locally weakly observable, i.e., both vehicle state and constant input disturbances are observable if 2 landmark positions are known (markers). The minimum number of Lie bracketing required to cover the observable part of the state space ${}^0\xi_e$ is 2. Given the complete observability of ξ_e, the set of indistinguishable states regarding a non singular initial configuration is empty.

We evaluate these results through simulation using the implementation of the non-linear observer described in section 2.5 to reconstruct the observable space ζ_o. Initial conditions and system parameters are arbitrary. It is seen in Fig. 3.4 that the observer state converges to ζ_o.

Extension of results Now, let's investigate if this result can be extended to any analytic d_r. As ${}^0\xi_e$ is observable, we must verify if ${}^k\xi_e$ observable $\rightarrow$ ${}^{k+1}\xi_e$ observable. Therefore, let's analyze what

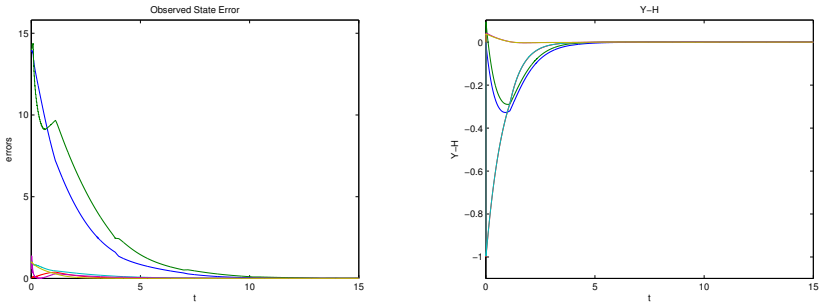

(1) (b)

Figure 3.4: Observer errors: (a) observed state error; (b) Y-H.

happens with ${}^{k}\Omega$ when we apply the inductive step from ${}^{k}\xi_e$ to ${}^{k+1}\xi_e$:

$$ {}^{k}\Omega = \begin{bmatrix} * & 0 \\ * & \Omega^1_{d_r} \\ * & \Omega^2_{d_r} \end{bmatrix} \rightarrow {}^{k+1}\Omega = \begin{bmatrix} * & 0 & 0 \\ * & \Omega^1_{d_r} & 0 \\ * & * & \Omega^1_{d_r} \\ * & * & \Omega^2_{d_r} \end{bmatrix}. $$

From the above all we can conclude is that $rank({}^{k+1}\Omega) \geq rank({}^{k}\Omega)$. Hence, ${}^{k}\xi_e$ does not necessarily imply in the observability of ${}^{k+1}\xi_e$ and we can't conclude on the observability of any analytic d_r using the induction presented.

3.3.3 1 and a half markers

In this problem, we are interested in the investigation of a system which output consists of the measurement of two landmarks, of which one is a marker (P_1) and the other one's position is partially known (half marker P_2), i.e., a one dimension space subsystem of the 2 dimensional position P_2 is assumed to be known while another one dimension space is unknown. We will assume that the known component of P_2 is z_2 while x_2 is unknown. Moreover, we will define $z_2 = z_1$ (what could be obtained through a proper rotation of the reference frame $\langle W \rangle$). The state space under investigation is composed of vehicle configuration, the unknown component of the position of P_2 represented by x_2 and the disturbance $\xi_e = (\xi_r, x_2, d_r, d_r^{(1)}, \ldots)$. System output consists of the measurement of the two landmarks $y = (y_{m,1}, y_2)$.

Observability analysis The codistribution ${}^0\Omega$ reaches its maximum rank after 2 levels of Lie differentiation:

$$
{}^0\Omega = \begin{bmatrix} \Omega^0_{\xi_r} & \Omega^0_{x_2} & 0 \\ \Omega^1_{\xi_r} & \Omega^0_{x_2} & \Omega^1_{d_r} \\ \Omega^2_{\xi_r} & \Omega^0_{x_2} & \Omega^2_{d_r} \end{bmatrix} = \begin{bmatrix} \partial_{\xi_r} {L_\Delta}^{(0)} h_1 & 0 & 0 \\ \partial_{\xi_r} {L_\Delta}^{(0)} h_2 & \partial_{x_2} {L_\Delta}^{(0)} h_2 & 0 \\ \partial_{\xi_r} {L_\Delta}^{(1)} h_1 & 0 & \partial_{d_r} {L_\Delta}^{(1)} h_1 \\ \partial_{\xi_r} {L_\Delta}^{(1)} h_2 & \partial_{x_2} {L_\Delta}^{(1)} h_2 & \partial_{d_r} {L_\Delta}^{(1)} h_2 \\ \partial_{\xi_r} {L_\Delta}^{(2)} h_1 & 0 & \partial_{d_r} {L_\Delta}^{(2)} h_1 \\ \partial_{\xi_r} {L_\Delta}^{(2)} h_2 & \partial_{x_2} {L_\Delta}^{(2)} h_2 & \partial_{d_r} {L_\Delta}^{(2)} h_2 \end{bmatrix}
$$

Apart from configuration singularities, the observable space dimension is 6 and the non-observable space dimension is 1. The minimum number of Lie bracketing required to cover the observable part of the state space is is 2 and the nullspace of ${}^0\Omega$ is

$$
\text{Ker } ({}^0\Omega) = \text{span} \left(\begin{bmatrix} \Delta \mathrm{x}_{1,2} \Delta \mathrm{x}_{r,1} + \Delta \mathrm{z}_{1,2} \Delta \mathrm{z}_{r,1} \\ -x_r \Delta \mathrm{z}_{1,2} - x_2 \Delta \mathrm{z}_{r,1} + x_1 \Delta \mathrm{z}_{r,1} \\ -\Delta \mathrm{z}_{1,2} \\ d_f \Delta \mathrm{x}_{1,2} \\ d_h \Delta \mathrm{x}_{1,2} \\ 0 \\ \rho^2_{1,2} \end{bmatrix}^T \right).
$$

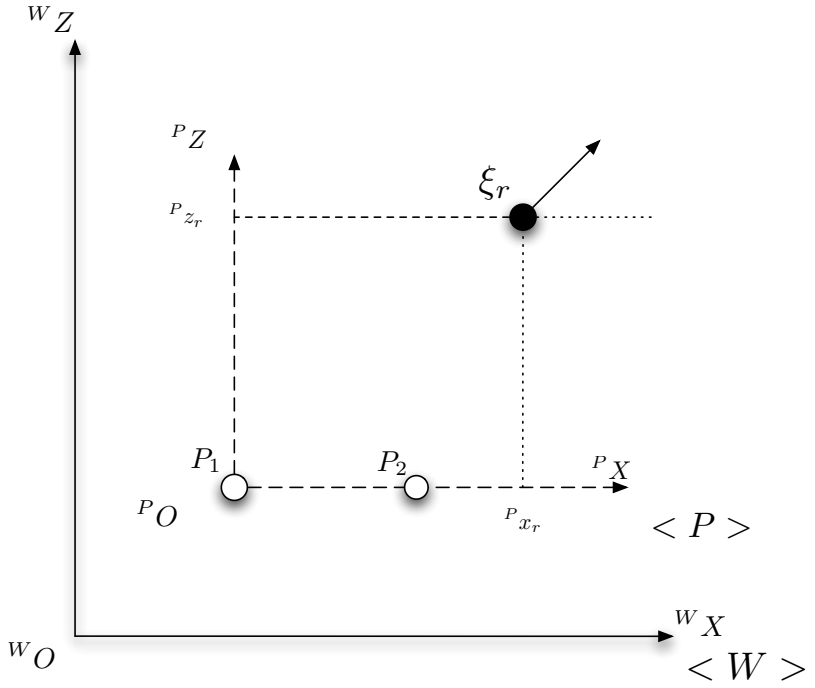

Figure 3.5: Reference frame $\langle P \rangle$.

Kalman form decomposition Consider a reference frame $\langle P \rangle = \{^{P}O, ^{P}X, ^{P}Z\}$ such that its origin ^{P}O is coincident to the position of the marker $P_1 = (x_1, z_1)$ and axis ^{P}X and ^{P}Z are parallel to ^{W}X and ^{W}Z respectively (see Fig. 3.5). Let's also define the notation $\bar{*}$ to describe the scaling operation $\bar{*} = */\lambda$, where λ is an arbitrarily chosen scale factor such that $\lambda \neq 0$. Please note that while this notation was already used in this thesis to represent homogeneous point coordinates, this will not be the case from here on.

Now, let's consider the coordinate transformation $^{0}\zeta = \left(^{P}\bar{\xi}_r, \bar{d}_r, \lambda\right)$ where a scaled version of the vehicle configuration is given by $^{P}\bar{\xi}_r = \left(^{P}\bar{x}_r, ^{P}\bar{z}_r, ^{P}\theta_r\right)$ and a scaled version of input disturbances is given by $\bar{d}_r = \left(\bar{d}_f, \bar{d}_h, d_\omega\right)$. It is straightforward to check that independently of λ system dynamics for the couple ξ_r, d_r are equivalent to that of

$\bar{\xi}_r$, $\bar{d}_r$, i.e., for $\dot{\xi}$ described by $\dot{\xi}_r = f(\xi_r, d_r)$, we have $\dot{\bar{\xi}}_r$ described by $\dot{\bar{\xi}}_r = f\left(\bar{\xi}_r, \bar{d}_r\right)$

If we choose the scale factor as $\lambda = x_2 - x_1$. The coordinate transformation is described in depth as

$$
{}^0\zeta = \Phi({}^0\xi_e) = \begin{bmatrix} {}^P\bar{x}_r \\ {}^P\bar{z}_r \\ {}^P\theta_r \\ \overline{d_f} \\ \overline{d_h} \\ d_\omega \\ \lambda \end{bmatrix} = \begin{bmatrix} \frac{\Delta \mathrm{x}_{r,1}}{\Delta \mathrm{x}_{2,1}} \\ \frac{\Delta \mathrm{z}_{r,1}}{\Delta \mathrm{x}_{2,1}} \\ \theta_r \\ d_f / \lambda \\ d_h / \lambda \\ d_\omega \\ \Delta \mathrm{x}_{2,1} \end{bmatrix} = \begin{bmatrix} \frac{x_r - x_1}{x_2 - x_1} \\ \frac{z_r - z_1}{x_2 - x_1} \\ \theta_r \\ d_f / (x_2 - x_1) \\ d_h / (x_2 - x_1) \\ d_\omega \\ (x_2 - x_1) \end{bmatrix},
$$

which system dynamics yields:

$$
{}^0\dot{\zeta} = \begin{bmatrix} \dot{\bar{\xi}}_r \\ 0 \\ \vdots \\ 0 \end{bmatrix} = \begin{bmatrix} \overline{d_f}\cos(\theta_r) - \overline{d_h}\sin(\theta_r) \\ \overline{d_h}\cos(\theta_r) + \overline{d_f}\sin(\theta_r) \\ d_\omega \\ 0 \\ \vdots \\ 0 \end{bmatrix}.
$$

In order to verify if Φ is local diffeomorphism at ${}^0\xi_e$ we compute its Jacobian:

$$
J = \begin{bmatrix} \frac{1}{\lambda} & 0 & 0 & 0 & 0 & 0 & -\frac{\Delta \mathrm{x}_{r,1}}{\lambda^2} \\ 0 & \frac{1}{\lambda} & 0 & 0 & 0 & 0 & -\frac{\Delta \mathrm{z}_{r,1}}{\lambda^2} \\ 0 & 0 & 1 & 0 & 0 & 0 & 0 \\ 0 & 0 & 0 & \frac{1}{\lambda} & 0 & 0 & -\frac{d_f}{\lambda^2} \\ 0 & 0 & 0 & 0 & \frac{1}{\lambda} & 0 & -\frac{d_h}{\lambda^2} \\ 0 & 0 & 0 & 0 & 0 & 1 & 0 \\ 0 & 0 & 0 & 0 & 0 & 0 & 1 \end{bmatrix}.
$$

Matrix rank of J is 7 apart from $|J| = \frac{1}{\lambda^4} = 0$. Given that $\lambda = \Delta_2, 1$, $|J|$ would be undefined whenever landmarks P_1 and P_2 coincide,

which is not the case here given that we assume $P_i \neq P_j, \forall i \neq j$. Hence, we conclude that Φ does represents a global diffeomorphism and its inverse is given by

$$
{}^0\xi_e = \begin{bmatrix} x_r \\ z_r \\ \theta_r \\ d_r \\ d_h \\ d_\omega \\ x_2 \end{bmatrix} = \Phi^{-1}({}^0\zeta) = \begin{bmatrix} \lambda\Delta \mathrm{x}_{r,1} + x_1 \\ \lambda\Delta \mathrm{z}_{r,1} + z_1 \\ \theta_r \\ d_f\lambda \\ d_h\lambda \\ d_\omega \\ \lambda + x_1 \end{bmatrix}.
$$

Finally, system output is given by

$$
y = \begin{bmatrix} h_1({}^0\zeta) \\ h_2({}^0\zeta) \end{bmatrix},
$$

where $h_i({}^0\zeta)$ is given by

$$
h_i({}^0\zeta) = \pi - \theta_r + \tan^{-1}\left(\frac{{}^P\Delta\bar{z}_{r,i}}{{}^P\Delta\bar{x}_{r,i}}\right),
$$

and $\Delta\bar{x}_{r,2} = {}^P\bar{x}_r - 1$, $\Delta\bar{x}_{r,1} = {}^P\bar{x}_r$, $\Delta\bar{z}_{r,1} = \Delta\bar{z}_{r,2} = {}^P\bar{z}_r$.

Observability analysis under local decomposition After 2 levels of Lie differentiation, the observability codistribution for ${}^0\zeta$ is

$$
\Omega = \begin{bmatrix} \Omega^0_{P\bar{\xi}_r} & \Omega^0_{\bar{d}_r} & \Omega^0_{\lambda} \\ \Omega^1_{P\bar{\xi}_r} & \Omega^1_{\bar{d}_r} & \Omega^1_{\lambda} \\ \Omega^2_{P\bar{\xi}_r} & \Omega^2_{\bar{d}_r} & \Omega^2_{\lambda} \end{bmatrix} = \begin{bmatrix} \Omega^0_{P\bar{\xi}_r} & \Omega^1_{\bar{d}_r} & 0 \\ \Omega^1_{P\bar{\xi}_r} & \Omega^1_{\bar{d}_r} & 0 \\ \Omega^2_{P\bar{\xi}_r} & \Omega^2_{\bar{d}_r} & 0 \end{bmatrix}.
$$

Given the equivalence of $\dot{\xi}_r$ and $\dot{\bar{\xi}}_r$ we also have the equivalence of the following submatrices: $\Omega^0_{P\bar{\xi}_r} \Longleftrightarrow \Omega^0_{\xi_r}$ and $\Omega^0_{\bar{d}_r} \Longleftrightarrow \Omega^0_{d_r}$.

Nullspace of Ω is given by

$$
\mathrm{Ker}(\Omega) = \mathrm{span}\left(\begin{bmatrix} 0 & 0 & 0 & 0 & 0 & 0 & 1 \end{bmatrix}^T\right),
$$

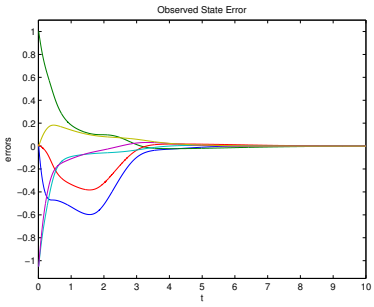

(1)

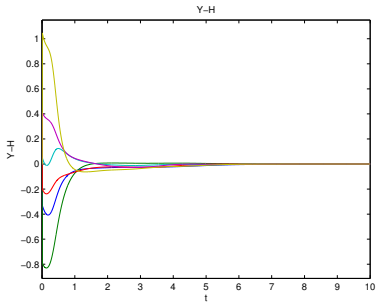

(b)

Figure 3.6: Observer errors: (a) observed state error; (b) Y-H.

and we may conclude that the observable subsystem is ${}^0\zeta_o = \left(\bar{\xi}_r, \bar{d}_r\right)$ and the non observable subsystem is the scale factor ${}^0\zeta_{\bar{o}} = (\lambda) = (\Delta x_{2,1})$.

We evaluate these results through simulation using the implementation of the non-linear observer described in section 2.5 to reconstruct the observable space ζ_o. Initial conditions and system parameters are arbitrary. It is seen in Fig. 3.6 that the observer state converges to ζ_o.

Extension of results Following the same reasoning presented 2, one can conclude that the observable space ${}^k\zeta_o$ does not necessarily imply in the same observable space for ${}^{k+1}\zeta_o$ and we can't discuss the observability of any analytic d_r.

3.3.4 1 marker

The state space under investigation is composed of vehicle configuration and input disturbance $\xi_e = (\xi_r, d_r, d_r^{(1)}, \ldots)$ and system output consists of the measurement of one marker only $y = (y_{m,1})$.

Observability analysis After 3 levels of Lie differentiation, the rank of the observability codistribution ${}^0\Omega$ reaches its maximum of 4. At this level, codistribution ${}^0\Omega$ is

$$ {}^0\Omega = \begin{bmatrix} \Omega^0_{\xi_r} & 0 \\ \Omega^1_{\xi_r} & \Omega^1_{d_r} \\ \Omega^2_{\xi_r} & \Omega^2_{d_r} \\ \Omega^3_{\xi_r} & \Omega^3_{d_r} \end{bmatrix} = \begin{bmatrix} \partial_{\xi_\mathrm{r}} {L_\Delta}^{(0)} h_{m,1} & 0 \\ \partial_{\xi_\mathrm{r}} {L_\Delta}^{(1)} h_{m,1} & \partial_{d_r} {L_\Delta}^{(1)} h_{m,1} \\ \partial_{\xi_\mathrm{r}} {L_\Delta}^{(2)} h_{m,1} & \partial_{d_r} {L_\Delta}^{(2)} h_{m,1} \\ \partial_{\xi_\mathrm{r}} {L_\Delta}^{(3)} h_{m,1} & \partial_{d_r} {L_\Delta}^{(3)} h_{m,1} \end{bmatrix}. $$

Apart from configuration singularities, the observable space dimension is 4 and the non-observable space dimension is 2. The minimum number of Lie bracketing required to cover the observable part of the state space is 3 and the nullspace of ${}^0\Omega$ is

$$ \mathrm{Ker}\left({}^0\Omega\right) = \mathrm{span}\left(\begin{bmatrix} \Delta \mathrm{x}_{r,1} & \Delta \mathrm{z}_{r,1} & 0 & d_f & d_h & 0 \\ -\Delta \mathrm{z}_{r,1} & \Delta \mathrm{x}_{r,1} & 1 & 0 & 0 & 0 \end{bmatrix} \right) $$

Kalman form decomposition Consider a reference frame $\langle P \rangle = \{{}^P O, {}^P X, {}^P Z\}$ as presented in section 3.2.4: origin ${}^P O$ is coincident to the position of the feature $P_1 = (x_1, z_1)$ and axes ${}^P X$ and ${}^P Z$ are parallel to axes ${}^W X$ and ${}^W Z$ respectively (please refer to Fig. 3.1). Consider also the polar representation of vehicle configuration $(\rho, \beta, \phi) = \Phi_p(\xi_r)$ and disturbances $(d_\rho, d_\phi) = \Phi_p(d_f, d_h)$.

In order to decouple observable and non-observable subsystems,

let's consider the coordinate mapping described by

$$
{}^0\zeta = \Phi({}^0\xi_e) = \left(\overline{\xi_{\mathrm{rp}}}, d_p\right) = \begin{bmatrix} \bar{\rho} \\ \beta \\ \phi \\ d_\rho \\ d_\phi \\ d_\omega \end{bmatrix} = \begin{bmatrix} \frac{\rho}{d_\rho} \\ \beta \\ \phi \\ d_\rho \\ d_\phi \\ d_\omega \end{bmatrix} = \begin{bmatrix} \frac{\sqrt{(x_r - x_1)^2 + (z_r - z_1)^2}}{\sqrt{{d_f}^2 + {d_h}^2}} \\ \tan^{-1}\left(\frac{z_r - z_1}{x_r - x_1}\right) - \theta_r + \pi \\ \tan^{-1}\left(\frac{z_r - z_1}{x_r - x_1}\right) \\ \sqrt{{d_f}^2 + {d_h}^2} \\ \tan^{-1}\left(\frac{d_f}{d_h}\right) \\ d_\omega \end{bmatrix},
$$

where the notation $\left(\overline{\xi_{\mathrm{rp}}}, d_p\right)$ is used to explicit the scaled polar coodinates of the vehicle $\overline{\xi_{\mathrm{rp}}}$ and the polar coordinates of the disturbance d_p.

Under such coordinate transformation system output becomes $y = (\beta)$ and system dynamics is given by

$$
{}^0\dot{\zeta} = \begin{bmatrix} -\sin\left(d_\phi + \beta\right) \\ -\frac{\bar{\rho} d_\omega + \cos\left(d_\phi + \beta\right)}{\bar{\rho}} \\ -\frac{\cos\left(d_\phi + \beta\right)}{\bar{\rho}} \\ 0 \\ 0 \\ 0 \end{bmatrix}.
$$

In order to verify if Φ is local diffeomorphism at ${}^0\xi_e$ we compute its Jacobian:

$$
J = J_{\left(\overline{\xi_{\mathrm{rp}}}, d_p\right)} = \begin{bmatrix} \frac{\Delta \mathrm{x}_{r,1}}{\rho_{r,1} d_\rho} & \frac{\Delta \mathrm{z}_{r,1}}{\rho_{r,1} d_\rho} & 0 & -\frac{\rho_{r,1} d_f}{d_\rho^3} & -\frac{\rho_{r,1} d_h}{d_\rho^3} & 0 \\ -\frac{\Delta \mathrm{z}_{r,1}}{{\rho_{r,1}}^2} & \frac{\Delta \mathrm{x}_{r,1}}{{\rho_{r,1}}^2} & -1 & 0 & 0 & 0 \\ -\frac{\Delta \mathrm{z}_{r,1}}{{\rho_{r,1}}^2} & \frac{\Delta \mathrm{x}_{r,1}}{{\rho_{r,1}}^2} & 0 & 0 & 0 & 0 \\ 0 & 0 & 0 & \frac{d_h}{d_\rho^2} & -\frac{d_f}{d_\rho^2} & 0 \\ 0 & 0 & 0 & \frac{d_f}{d_\rho^2} & \frac{d_h}{d_\rho^2} & 0 \\ 0 & 0 & 0 & 0 & 0 & 1 \end{bmatrix},
$$

where the notation $J_{\left(\overline{\xi_{\mathrm{rp}}},\, d_p\right)}$ is used to represent the jacobian associated to $\left(\overline{\xi_{\mathrm{rp}}}, d_p\right)$. Matrix rank of J is 6 apart from $|J| = 0$, i.e., when

$$|\mathrm{J}| = \frac{1}{\rho_{r,1} {d_\rho}^2} = 0.$$

Hence, we conclude while Φ is a local diffeomorphism almost everywhere, it is not a global diffeomorphism as is it not defined for $\rho = 0$ or $d_\rho = 0$, as expected.

Observability analysis under local decomposition After 3 levels of Lie differentiation, the observability codistribution for ${}^0\zeta$ is

$${}^0\Omega = \left[\begin{array}{cccc|cccc} 0 & 1 & 0 & 0 & 0 & 0 & 0 & 0 \\ \frac{C\left[\beta+d_\phi\right]}{\bar{\rho}^2} & \frac{S\left[\beta+d_\phi\right]}{\bar{\rho}} & 0 & 0 & 0 & \frac{S\left[\beta+d_\phi\right]}{\bar{\rho}} & 0 & 0 \\ \frac{\left(4C\left[\beta+d_\phi\right]+d_\omega\bar{\rho}\right)S\left[\beta+d_\phi\right]}{\bar{\rho}^3} & -\frac{2C\left[2\left(\beta+d_\phi\right)\right]+d_\omega C\left[\beta+d_\phi\right]\bar{\rho}}{\bar{\rho}^2} & 0 & 0 & 0 & -\frac{2C\left[2\left(\beta+d_\phi\right)\right]+d_\omega C\left[\beta+d_\phi\right]\bar{\rho}}{\bar{\rho}^2} & 0 & 0 \\ -\frac{6C\left[3\left(\beta+d_\phi\right)\right]+d_\omega\bar{\rho}\left(6C\left[2\left(\beta+d_\phi\right)\right]+d_\omega C\left[\beta+d_\phi\right]\bar{\rho}\right)}{\bar{\rho}^4} & -\frac{d_\omega\bar{\rho}\left(12C\left[\beta+d_\phi\right]+d_\omega\bar{\rho}\right)S\left[\beta+d_\phi\right]+6S\left[3\left(\beta+d_\phi\right)\right]}{\bar{\rho}^3} & 0 & 0 & 0 & -\frac{d_\omega\bar{\rho}\left(12C\left[\beta+d_\phi\right]+d_\omega\bar{\rho}\right)S\left[\beta+d_\phi\right]+6S\left[3\left(\beta+d_\phi\right)\right]}{\bar{\rho}^3} & 0 & 0 \end{array}\right],$$

$$\left[\begin{array}{cccc} 0 & 0 & 0 & 0 \\ 0 & \frac{S\left[\beta+d_\phi\right]}{\bar{\rho}} & 0 & 0 \\ 0 & -\frac{2C\left[2\left(\beta+d_\phi\right)\right]+d_\omega C\left[\beta+d_\phi\right]\bar{\rho}}{\bar{\rho}^2} & -1 & -\frac{S\left[\beta+d_\phi\right]}{\bar{\rho}} \\ 0 & -\frac{d_\omega\bar{\rho}\left(12C\left[\beta+d_\phi\right]+d_\omega\bar{\rho}\right)S\left[\beta+d_\phi\right]+6S\left[3\left(\beta+d_\phi\right)\right]}{\bar{\rho}^3} & \frac{3C\left[2\left(\beta+d_\phi\right)\right]+2d_\omega C\left[\beta+d_\phi\right]\bar{\rho}}{\bar{\rho}^2} & \end{array}\right]$$

which nullspace is given by

$$\mathrm{Ker}\left({}^0\Omega\right) = \left(\left[\begin{array}{cccccc} 0 & 0 & 0 & 1 & 0 & 0 \\ 0 & 0 & 1 & 0 & 0 & 0 \end{array}\right]\right),$$

and we may conclude that the observable subsystem is ${}^0\zeta_o = (\bar{\rho}, \beta, d_\phi, d_\omega)$ and the non observable subsystem is ${}^0\zeta_{\bar{o}} = (d_\rho, \phi)$.

We evaluate these results through simulation using the implementation of the non-linear observer described in section 2.5 to reconstruct the observable space ζ_o. Initial conditions and system parameters are arbitrary. It is seen in Fig. 3.7 that the observer state converges to ζ_o.

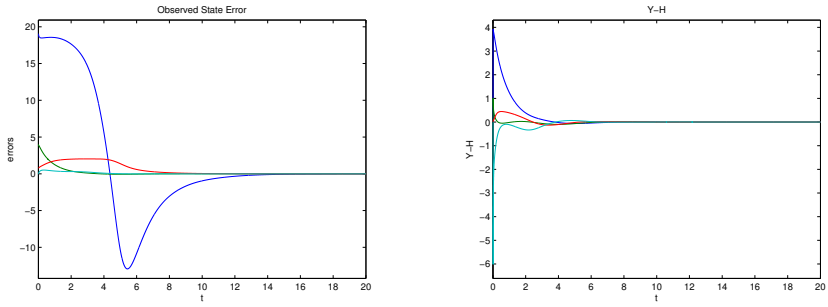

(1) (b)

Figure 3.7: Observer errors: (a) observed state error; (b) Y-H.

Extension of results Following the same reasoning presented 2, one can conclude that the observable space ${}^{k}\zeta_o$ does not necessarily imply in the same observable space for ${}^{k+1}\zeta_o$ and we can't discuss the observability of any analytic d_r.

3.3.5 Half marker

In this problem, we are interested in the investigation of a system which output consists of the measurement of one landmark for which position is partially known (half marker), i.e., a one dimension space subsystem of the 2 dimensional position coordinates is assumed to be known while another one dimension space is assumed to be unknown. Without lost of generalization, we will assume that the coordinate z_1 is known while x_1 is unknown. The state space under investigation is composed of vehicle configuration, the unknown component of the position of P_1 represented by x_1 and disturbance $\xi_e = (\xi_r, x_1, d_r, , d_r^{(1)}, \ldots)$. System output consists of the measurement of one landmark only $y = (y_1)$.

Observability analysis After 3 levels of Lie differentiation, the rank of the observability codistribution ${}^0\Omega$ reaches its maximum of 4. At this level, codistribution ${}^0\Omega$ is

$$ {}^0\Omega = \begin{bmatrix} \Omega^0_{\xi_r} & \Omega^0_{x_1} & 0 \\ \Omega^1_{\xi_r} & \Omega^1_{x_1} & \Omega^1_{d_r} \\ \Omega^2_{\xi_r} & \Omega^2_{x_1} & \Omega^2_{d_r} \\ \Omega^3_{\xi_r} & \Omega^3_{x_1} & \Omega^3_{d_r} \end{bmatrix} = \begin{bmatrix} \partial_{\xi \mathrm{r}} {L_\Delta}^{(0)} h_1 & \partial_{x_1} {L_\Delta}^{(0)} h_1 & 0 \\ \partial_{\xi \mathrm{r}} {L_\Delta}^{(1)} h_1 & \partial_{x_1} {L_\Delta}^{(1)} h_1 & \partial_{d_r} {L_\Delta}^{(1)} h_1 \\ \partial_{\xi \mathrm{r}} {L_\Delta}^{(2)} h_1 & \partial_{x_1} {L_\Delta}^{(2)} h_1 & \partial_{d_r} {L_\Delta}^{(2)} h_1 \\ \partial_{\xi \mathrm{r}} {L_\Delta}^{(3)} h_1 & \partial_{x_1} {L_\Delta}^{(3)} h_1 & \partial_{d_r} {L_\Delta}^{(3)} h_1 \end{bmatrix}. $$

Apart from configuration singularities, the observable space dimension is 4 and the non-observable space dimension is 3. The minimum number of Lie bracketing required to cover the observable part of the state space is 3 and the nullspace of ${}^0\Omega$ is

$$ \mathrm{Ker}\left({}^0\Omega\right) = \mathrm{span}\left(\begin{bmatrix} 0 & 1 & 0 & 0 & 0 & 0 & 1 \\ \Delta \mathrm{x}_{r,1} & \Delta \mathrm{z}_{r,1} & 0 & d_f & d_h & 0 & 0 \\ -\Delta \mathrm{z}_{r,1} & \Delta \mathrm{x}_{r,1} & 1 & 0 & 0 & 0 & 0 \end{bmatrix} \right). $$

Kalman form decomposition Consider the reference frame $\langle P \rangle$ as described in section 3.2.4 and seen in Fig. 3.1.

Consider the coordinate transformation ${}^0\zeta = \Phi({}^0\xi_e) = \left(\overline{\xi_{\text{rp}}}, d_p, x_1\right)$ where $\overline{\xi_{\text{rp}}} = (\bar{\rho}, \beta, \phi) = (\rho\,/d_\rho\,, \beta, \phi)$, d_p describes the input disturbance using polar coordinates, and x_1 is the unknown horizontal translation of origin ${}^PO$ w.r.t. origin $\langle W \rangle$. Corresponding system dynamics is ${}^0\dot{\zeta} = \left(\dot{\overline{\xi_{\text{rp}}}}, 0, 0, \ldots\right)$ and system output is $y = (\beta)$.

In order to verify if Φ is local diffeomorphism at ${}^0\xi_e$ we compute its Jacobian:

$$J = \begin{bmatrix} J_{\left(\overline{\xi_{\text{rp}}}, d_p\right)} & J^* \\ 0 & 1 \end{bmatrix}, J^* = \begin{bmatrix} -\frac{\Delta \text{x}_{r,1}}{\rho_{r,1} d_\rho} \\ \frac{-\text{z1}+\text{zr}}{{\rho_{r,1}}^2} \\ \frac{\Delta \text{z}_r}{{\rho_{r,1}}^2} \\ 0 \\ 0 \\ 0 \end{bmatrix}.$$

Matrix rank of J is 7 apart from $|J| = 0$, i.e., when

$$|\text{J}| = \frac{1}{\rho_{r,1} {d_\rho}^2} = 0.$$

Hence, we conclude while Φ is a local diffeomorphism almost everywhere it is not a global diffeomorphism and is it not defined for $\rho = 0$ or $d_\rho = 0$, as expected.

Observability analysis under local decomposition After 3 levels of Lie differentiation, the observability codistribution for ${}^0\zeta$ is

$${}^0\Omega = \left[\begin{array}{cccc} 0 & 1 & 0 \\ \frac{C\left[\beta+d_\phi\right]}{\bar{\rho}^2} & \frac{S\left[\beta+d_\phi\right]}{\bar{\rho}} & 0 \\ \frac{\left(4C\left[\beta+d_\phi\right]+d_\omega\bar{\rho}\right)S\left[\beta+d_\phi\right]}{\bar{\rho}^3} & -\frac{2C\left[2\left(\beta+d_\phi\right)\right]+d_\omega C\left[\beta+d_\phi\right]\bar{\rho}}{\bar{\rho}^2} & 0 \\ -\frac{6C\left[3\left(\beta+d_\phi\right)\right]+d_\omega\bar{\rho}\left(6C\left[2\left(\beta+d_\phi\right)\right]+d_\omega C\left[\beta+d_\phi\right]\bar{\rho}\right)}{\bar{\rho}^4} & -\frac{d_\omega\bar{\rho}\left(12C\left[\beta+d_\phi\right]+d_\omega\bar{\rho}\right)S\left[\beta+d_\phi\right]+6S\left[3\left(\beta+d_\phi\right)\right]}{\bar{\rho}^3} & 0 \end{array}\right],$$

$$\left[\begin{array}{cccc} 0 & 0 & 0 & 0 \\ 0 & \frac{S\left[\beta+d_\phi\right]}{\bar{\rho}} & -1 & 0 \\ 0 & -\frac{2C\left[2\left(\beta+d_\phi\right)\right]+d_\omega C\left[\beta+d_\phi\right]\bar{\rho}}{\bar{\rho}^2} & -\frac{S\left[\beta+d_\phi\right]}{\bar{\rho}} & 0 \\ 0 & -\frac{d_\omega\bar{\rho}\left(12C\left[\beta+d_\phi\right]+d_\omega\bar{\rho}\right)S\left[\beta+d_\phi\right]+6S\left[3\left(\beta+d_\phi\right)\right]}{\bar{\rho}^3} & \frac{3C\left[2\left(\beta+d_\phi\right)\right]+2d_\omega C\left[\beta+d_\phi\right]\bar{\rho}}{\bar{\rho}^2} & 0 \end{array}\right]$$

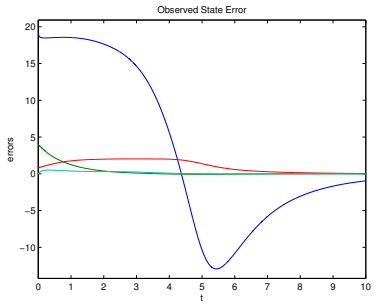

(1)

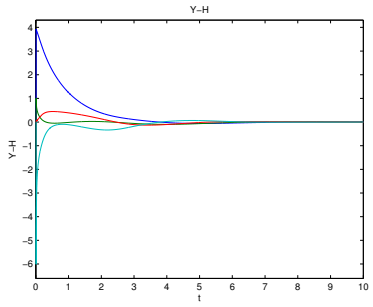

(b)

Figure 3.8: Observer errors: (a) observed state error; (b) Y-H.

which nullspace is given by

$$\text{Ker}\left({}^{0}\Omega\right) = \left(\begin{bmatrix} 0 & 0 & 0 & 0 & 0 & 0 & 1 \\ 0 & 0 & 0 & 0 & 0 & 0 & 0 \\ 0 & 0 & 1 & 0 & 0 & 0 & 0 \\ 0 & 0 & 0 & 1 & 0 & 0 & 0 \end{bmatrix}^{T} \right),$$

and we may conclude that the observable subsystem is

$${}^{0}\zeta_{o} = \left(\bar{\rho}, \beta, d_{\phi}, d_{\omega}\right),$$

and the non observable subsystem is ${}^{0}\zeta_{\bar{o}} = (d_{\rho}, \phi, x_1, z_1)$.

We evaluate these results through simulation using the implementation of the non-linear observer described in section 2.5 to reconstruct the observable space ζ_o. Initial conditions and system parameters are arbitrary. It is seen in Fig. 3.8 that the observer state converges to ζ_o.

Extension of results Following the same reasoning presented 2, one can conclude that the observable space ${}^{k}\zeta_{o}$ does not necessarily imply in the same observable space for ${}^{k+1}\zeta_{o}$ and we can't discuss the observability of any analytic d_r.

3.3.6 1 target

The state space under investigation is composed of vehicle configuration, the position of one target and input disturbance:

$$\xi_e = (\xi_r, \xi_1, d_r, d_r^{(1)}, \ldots),$$

where we are using the notation $\xi_1 = \xi_{t,1}$ for its simplicity. System output consists of the measurement of one target only $y = (y_{t,1})$.

Observability analysis After 3 levels of Lie differentiation, the rank of the observability codistribution ${}^0\Omega$ reaches its maximum of 4. At this level, codistribution ${}^0\Omega$ is

$${}^0\Omega = \begin{bmatrix} \Omega^0_{\xi_r} & \Omega^0_{\xi_1} & 0 \\ \Omega^1_{\xi_r} & \Omega^1_{\xi_1} & \Omega^1_{d_r} \\ \Omega^2_{\xi_r} & \Omega^2_{\xi_1} & \Omega^2_{d_r} \\ \Omega^3_{\xi_r} & \Omega^3_{\xi_1} & \Omega^3_{d_r} \end{bmatrix} = \begin{bmatrix} \partial_{\xi_\mathrm{r}} {L_\Delta}^{(0)} h_{t,1} & \partial_{\xi_1} {L_\Delta}^{(0)} h_{t,1} & 0 \\ \partial_{\xi_\mathrm{r}} {L_\Delta}^{(1)} h_{t,1} & \partial_{\xi_1} {L_\Delta}^{(1)} h_{t,1} & \partial_{d_r} {L_\Delta}^{(1)} h_{t,1} \\ \partial_{\xi_\mathrm{r}} {L_\Delta}^{(2)} h_{t,1} & \partial_{\xi_1} {L_\Delta}^{(2)} h_{t,1} & \partial_{d_r} {L_\Delta}^{(2)} h_{t,1} \\ \partial_{\xi_\mathrm{r}} {L_\Delta}^{(3)} h_{t,1} & \partial_{\xi_1} {L_\Delta}^{(3)} h_{t,1} & \partial_{d_r} {L_\Delta}^{(3)} h_{t,1} \end{bmatrix}.$$

Apart from configuration singularities, the observable space dimension is 4 and the non-observable space dimension is 4. The minimum number of Lie bracketing required to cover the observable part of the state space is 3 and the nullspace of ${}^0\Omega$ is

$$\mathrm{Ker}\left({}^0\Omega\right) = \mathrm{span}\left(\begin{bmatrix} 1 & 0 & 0 & 1 & 0 & 0 & 0 & 0 \\ 0 & 1 & 0 & 0 & 1 & 0 & 0 & 0 \\ \Delta \mathrm{x}_{r,1} & \Delta \mathrm{z}_{r,1} & 0 & 0 & 0 & d_f & d_h & 0 \\ -\Delta \mathrm{z}_{r,1} & \Delta \mathrm{x}_{r,1} & 1 & 0 & 0 & 0 & 0 & 0 \end{bmatrix} \right).$$

Kalman form decomposition Consider the reference frame $\langle P \rangle$ as described in section 3.2.4 and seen in Fig. 3.1.

Consider the coordinate transformation ${}^0\zeta = \Phi({}^0\xi_e) = \left(\overline{\xi_{\mathrm{rp}}}, d_p, \xi_1\right)$ where $\overline{\xi_{\mathrm{rp}}} = (\bar{\rho}, \beta, \phi) = (\rho\,/d_\rho\,, \beta, \phi)$, d_p describes the input disturbance using polar coordinates, and ξ_1 is the position of the target, i.e., the position of the origin ${}^PO$. Corresponding system dynamics is ${}^0\dot{\zeta} = \left(\dot{\overline{\xi_{\mathrm{rp}}}}, 0, 0, \ldots\right)$ and system output is $y = (\beta)$.

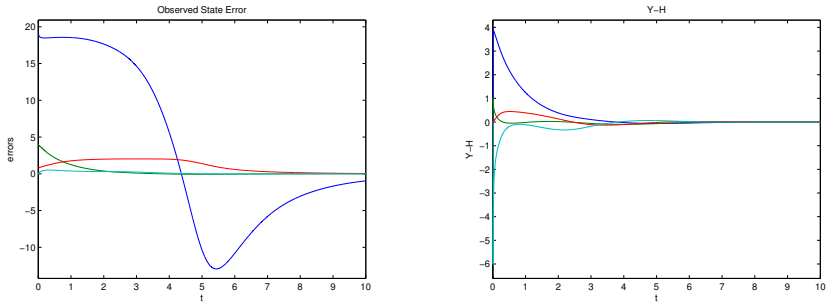

(1) (b)

Figure 3.9: Observer errors: (a) observed state error; (b) Y-H.

In order to verify if Φ is local diffeomorphism at ${}^0\xi_e$ we compute its Jacobian:

$$J = \begin{bmatrix} J_{(\overline{\xi_{\mathrm{rp}}}, d_p)} & J^* \\ 0 & I \end{bmatrix}, J^* = \begin{bmatrix} -\frac{\Delta \mathrm{x}_{r,1}}{\rho_{r,1} d_\rho} & -\frac{\Delta \mathrm{z}_{r,1}}{\rho_{r,1} d_\rho} \\ \frac{-\mathrm{z1}+\mathrm{zr}}{{\rho_{r,1}}^2} & \frac{\mathrm{x1}-\mathrm{xr}}{{\rho_{r,1}}^2} \\ \frac{\Delta \mathrm{z}_r}{{\rho_{r,1}}^2} & -\frac{\Delta \mathrm{x}_r}{{\rho_{r,1}}^2} \\ 0 & 0 \\ 0 & 0 \\ 0 & 0 \end{bmatrix}.$$

Matrix rank of J is 8 apart from $|J| = 0$, i.e., when:

$$|\mathrm{J}| = \frac{1}{\rho_{r,1} {d_\rho}^2} = 0$$

Hence, we conclude while Φ is a local diffeomorphism almost everywhere it is not a global diffeomorphism and is it not defined for $\rho = 0$ or $d_\rho = 0$, as expected.

We evaluate these results through simulation using the implementation of the non-linear observer described in section 2.5 to reconstruct the observable space ζ_o. Initial conditions and system parameters are arbitrary. It is seen in Fig. 3.9 that the observer state converges to ζ_o.

Observability analysis under local decomposition After 3 levels of Lie differentiation, the observability codistribution for ${}^0\zeta$ is

$$
{}^0\Omega =
$$

$$
\left[\begin{array}{cccc}
0 & 1 & 0 & \\
\frac{C\left[\beta+d_\phi\right]}{\bar{\rho}^2} & \frac{S\left[\beta+d_\phi\right]}{\bar{\rho}} & 0 & \\
\frac{\left(4C\left[\beta+d_\phi\right]+d_\omega\bar{\rho}\right)S\left[\beta+d_\phi\right]}{\bar{\rho}^3} & -\frac{2C\left[2\left(\beta+d_\phi\right)\right]+d_\omega C\left[\beta+d_\phi\right]\bar{\rho}}{\bar{\rho}^2} & 0 & \\
-\frac{6C\left[3\left(\beta+d_\phi\right)\right]+d_\omega\bar{\rho}\left(6C\left[2\left(\beta+d_\phi\right)\right]+d_\omega C\left[\beta+d_\phi\right]\bar{\rho}\right)}{\bar{\rho}^4} & -\frac{d_\omega\bar{\rho}\left(12C\left[\beta+d_\phi\right]+d_\omega\bar{\rho}\right)S\left[\beta+d_\phi\right]+6S\left[3\left(\beta+d_\phi\right)\right]}{\bar{\rho}^3} & 0 &
\end{array}\right],
$$

$$
\left[\begin{array}{ccccc}
0 & 0 & 0 & 0 & 0 \\
0 & \frac{S\left[\beta+d_\phi\right]}{\bar{\rho}} & -1 & 0 & 0 \\
0 & -\frac{2C\left[2\left(\beta+d_\phi\right)\right]+d_\omega C\left[\beta+d_\phi\right]\bar{\rho}}{\bar{\rho}^2} & -\frac{S\left[\beta+d_\phi\right]}{\bar{\rho}} & 0 & 0 \\
0 & -\frac{d_\omega\bar{\rho}\left(12C\left[\beta+d_\phi\right]+d_\omega\bar{\rho}\right)S\left[\beta+d_\phi\right]+6S\left[3\left(\beta+d_\phi\right)\right]}{\bar{\rho}^3} & \frac{3C\left[2\left(\beta+d_\phi\right)\right]+2d_\omega C\left[\beta+d_\phi\right]\bar{\rho}}{\bar{\rho}^2} & 0 & 0
\end{array}\right]
$$

which nullspace is given by

$$
\text{Ker}\left({}^0\Omega\right) = \left(\left[\begin{array}{cccccccc}
0 & 0 & 0 & 0 & 0 & 0 & 1 & 0 \\
0 & 0 & 0 & 0 & 0 & 0 & 0 & 1 \\
0 & 0 & 1 & 0 & 0 & 0 & 0 & 0 \\
0 & 0 & 0 & 1 & 0 & 0 & 0 & 0
\end{array}\right]^T\right),
$$

and we may conclude that the observable subsystem is

$$
{}^0\zeta_o = (\bar{\rho}, \beta, d_\phi, d_\omega)
$$

and the non observable subsystem is ${}^0\zeta_{\bar{o}} = (d_\rho, \phi, x_1, z_1)$.

Extension of results Following the same reasoning presented 2, one can conclude that the observable space ${}^k\zeta_o$ does not necessarily imply in the same observable space for ${}^{k+1}\zeta_o$ and we can't discuss the observability of any analytic d_r.

3.3.7 2 targets

The state space under investigation is composed of vehicle configuration, the position of two targets and disturbance:

$$\xi_e = (\xi_r, \xi_1, \xi_2, d_r, d_r^{(1)}, \ldots),$$

where we are using the notation $\xi_1 = \xi_{t,1}$ and $\xi_1 = \xi_{t,2}$ for its simplicity .System output consists of the measurement of two markers $y = (y_{t,1}, y_{t,2})$.

Observability analysis After 2 levels of Lie differentiation, the observability codistribution rank reaches its maximum of 6. Codistribution ${}^0\Omega$ at the second level of Lie bracketing is

$${}^0\Omega = \begin{bmatrix} \Omega^0_{\xi_r} & \Omega^0_{\xi_1} & \Omega^0_{\xi_2} & 0 \\ \Omega^1_{\xi_r} & \Omega^1_{\xi_1} & \Omega^1_{\xi_2} & \Omega^1_{d_r} \\ \Omega^2_{\xi_r} & \Omega^2_{\xi_1} & \Omega^2_{\xi_2} & \Omega^2_{d_r} \end{bmatrix} =$$

$$= \begin{bmatrix} \partial_{\xi_r} {L_\Delta}^{(0)} h_{m,1} & \partial_{\xi_{t,1}} {L_\Delta}^{(0)} h_{t,1} & 0 & 0 \\ \partial_{\xi_r} {L_\Delta}^{(0)} h_{m,2} & 0 & \partial_{\xi_{t,2}} {L_\Delta}^{(0)} h_{t,2} & 0 \\ \partial_{\xi_r} {L_\Delta}^{(1)} h_{m,1} & \partial_{\xi_{t,1}} {L_\Delta}^{(1)} h_{t,1} & 0 & \partial_{d_r} {L_\Delta}^{(1)} h_{m,1} \\ \partial_{\xi_r} {L_\Delta}^{(1)} h_{m,2} & 0 & \partial_{\xi_{t,2}} {L_\Delta}^{(1)} h_{t,2} & \partial_{d_r} {L_\Delta}^{(1)} h_{m,2} \\ \partial_{\xi_r} {L_\Delta}^{(2)} h_{m,1} & \partial_{\xi_{t,1}} {L_\Delta}^{(2)} h_{t,1} & 0 & \partial_{d_r} {L_\Delta}^{(2)} h_{m,1} \\ \partial_{\xi_r} {L_\Delta}^{(2)} h_{m,2} & 0 & \partial_{\xi_{t,2}} {L_\Delta}^{(2)} h_{t,2} & \partial_{d_r} {L_\Delta}^{(2)} h_{m,2} \end{bmatrix}.$$

Apart from configuration singularities, the observable space dimension is 6 and the non-observable space dimension is 4. The minimum number of Lie bracketing required to cover the observable part of the state space is 2. The nullspace of ${}^0\Omega$ is omitted here for brevity.

Kalman form decomposition Consider a reference frame $\langle P \rangle = \{{}^P O, {}^P X, {}^P Z\}$ as presented in section 3.2.7, i.e., its origin ${}^P O$ is coincident to the position of the feature $P_1 = (x_1, z_1)$ and axis ${}^P X$ is coincident to the line that passes through P_1 and P_2, with direction

from P_1 to P_2 (see Fig. 3.2). Orientation of $\langle P\rangle$ w.r.t. $\langle W\rangle$ will be denoted $\phi_{1,2}$. Position P_2 w.r.t. $\langle P\rangle$ will be described by ${}^{P}P_2 = \{{}^{P}x_2, 0\}$ and vehicle configuration will be described as ${}^{P}\xi_r = \left({}^{P}x_r, {}^{P}z_r, {}^{P}\theta_r\right)$.

Now, let's consider the coordinate transformation

$$ {}^{0}\zeta = \left({}^{P0}\bar{\xi}_{er}, \bar{d}_r, \lambda, \xi_1, \phi_{1,2}\right), $$

which is composed of a scaled version of the vehicle configuration is given by ${}^{P}\bar{\xi}_r = \left({}^{P}\bar{x}_r, {}^{P}\bar{z}_r, {}^{P}\theta_r\right)$, a scaled version of input disturbances is given by $\bar{d}_r = \left(\bar{d}_f, \bar{d}_h, d_\omega\right)$, orientation of $\langle P\rangle$ w.r.t. $\langle W\rangle$ is denoted by $\phi_{1,2}$ and origin ${}^{P}O$ position is given by ξ_1. Once again ,it is straightforward to check that independently of λ, for $\dot{\xi}$ described by $\dot{\xi}_r = f\left(\xi_r, d_r\right)$, we have $\dot{\bar{\xi}}_r$ described by $\dot{\bar{\xi}}_r = f\left(\bar{\xi}_r, \bar{d}_r\right)$.

If we choose the scale factor as $\lambda = {}^{P}x_2 = (x_2 - x_1)\cos(\phi_{1,2}) + (z_2 - z_1)\sin(\phi_{1,2})$ The coordinate transformation is described in depth as

$$ {}^{0}\zeta = \Phi({}^{0}\xi_e) = \begin{bmatrix} {}^{P}\bar{x}_r \\ {}^{P}\bar{z}_r \\ {}^{P}\theta_r \\ \bar{d}_f \\ \bar{d}_h \\ d_\omega \\ \lambda \\ \phi_{1,2} \\ x_1 \\ z_1 \end{bmatrix} = \begin{bmatrix} \frac{{}^{P}x_r}{\lambda} \\ \frac{{}^{P}z_r}{\lambda} \\ {}^{P}\theta_r \\ d_f/\lambda \\ d_h/\lambda \\ d_\omega \\ {}^{P}x_2 \\ \tan^{-1}\left(\frac{z_2 - z_1}{x_2 - x_1}\right) \\ x_1 \\ z_1 \end{bmatrix}, $$

and system dynamics is

$$ {}^{0}\dot{\zeta} = \begin{bmatrix} \dot{\bar{\xi}}_r \\ 0 \\ \vdots \\ 0 \end{bmatrix} = \begin{bmatrix} \bar{d}_f \cos\left({}^{P}\theta_r\right) - \bar{d}_h \sin\left({}^{P}\theta_r\right) \\ \bar{d}_h \cos\left({}^{P}\theta_r\right) + \bar{d}_f \sin\left({}^{P}\theta_r\right) \\ d_\omega \\ 0 \\ \vdots \end{bmatrix}. $$

Please note that this transformation is similar to the one proposed in section 3.3.3 apart from the new elements $\phi_{1,2}$, x_1 and z_1. Once again, computing the jacobian of ${}^0\zeta$, one can verify that the transformation is undefined whenever landmarks P_1 and P_2 coincide, which is not the case here given that we assume $P_i \neq P_j, \forall i \neq j$. Hence, we conclude that Φ does represents a global diffeomorphism.

Observability analysis under local decomposition After 2 levels of Lie differentiation, the observability codistribution for ${}^0\zeta$ is

$${}^0\Omega = \begin{bmatrix} \Omega^0_{P\bar{\xi}_r} & \Omega^0_{\bar{d}_r} & \Omega^0_{\lambda} & \Omega^0_{\phi_{1,2}} & \Omega^0_{\xi_1} \\ \Omega^1_{P\bar{\xi}_r} & \Omega^1_{\bar{d}_r} & \Omega^1_{\lambda} & \Omega^1_{\phi_{1,2}} & \Omega^1_{\xi_1} \\ \Omega^2_{P\bar{\xi}_r} & \Omega^2_{\bar{d}_r} & \Omega^2_{\lambda} & \Omega^2_{\phi_{1,2}} & \Omega^2_{\xi_1} \end{bmatrix} = \begin{bmatrix} \Omega^0_{P\bar{\xi}_r} & \Omega^0_{\bar{d}_r} & 0 & 0 & 0 & 0 \\ \Omega^1_{P\bar{\xi}_r} & \Omega^1_{\bar{d}_r} & 0 & 0 & 0 & 0 \\ \Omega^2_{P\bar{\xi}_r} & \Omega^2_{\bar{d}_r} & 0 & 0 & 0 & 0 \end{bmatrix}.$$

Matrix rank of ${}^0\Omega$ is 6 and the observable subsystem is ${}^0\zeta_o = \left({}^P\bar{x}_r, {}^P\bar{z}_r, {}^P\theta_r, \bar{d}_f, \bar{d}_h, d_\omega\right)$ and non-observable subsystem is

$${}^0\zeta_{\bar{o}} = \left(\lambda, x_1, z_1, \phi_{1,2}\right).$$

This can be verified checking the nullspace of ${}^0\Omega$:

$$\text{Ker}\left({}^0\Omega\right) = \text{span}\left(\begin{bmatrix} 0 & 0 & 0 & 0 & 0 & 0 & 1 & 0 & 0 & 0 \\ 0 & 0 & 0 & 0 & 0 & 0 & 0 & 1 & 0 & 0 \\ 0 & 0 & 0 & 0 & 0 & 0 & 0 & 0 & 1 & 0 \\ 0 & 0 & 0 & 0 & 0 & 0 & 0 & 0 & 0 & 1 \end{bmatrix}\right).$$

We evaluate these results through simulation using the implementation of the non-linear observer described in section 2.5 to reconstruct the observable space ζ_o. Initial conditions and system parameters are arbitrary. It is seen in Fig. 3.10 that the observer state converges to ζ_o.

Extension of results Following the same reasoning presented 2, one can conclude that the observable space ${}^k\zeta_o$ does not necessarily imply in the same observable space for ${}^{k+1}\zeta_o$ and we can't discuss the observability of any analytic d_r.

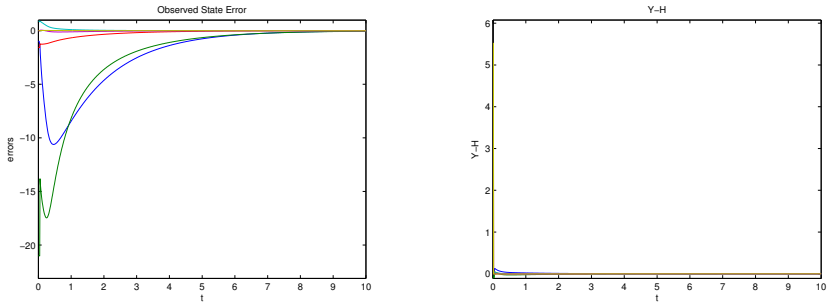

(1) (b)

Figure 3.10: Observer errors: (a) observed state error; (b) Y-H.

3.3.8 Conclusions

Table 3.3.8 presents an overview of the results obtained in this section and also extends this results for problems involving any number of targets as already described. The table presents the following details:

- M: Number of markers;
- N: Number of targets;
- k: Minimum level of lie-bracketing required to cover observable space;
- $\dim(\xi)$: System dimension;
- $\dim(\zeta_o)$: Observable space dimension;
- $\dim(\zeta_{\bar{o}})$: Non-observable space dimension;

The most relevant results can be summarised as follows.

2, 3 or more markers If 2 markers are being observed, results are sufficient to show that the problem is completely observable if input disturbances are constant. If 3 or more markers are being observed

Table 3.2: Summary of results.

M	0	0	0	0	1	$1+\frac{1}{2}$	$1+\frac{1}{2}$	2	$3+\bar{M}$
N	$2+\bar{N}$	2	1	$\frac{1}{2}$	0	0	$\bar{N}$	0	$\bar{N}$
k	2	2	3	3	3	2	2	2	1
$\dim(\xi)$	$10+2\bar{N}$	10	8	7	6	7	$7+\bar{N}$	6	$6+2\bar{M}+2\bar{N}$
$\dim(\zeta_o)$	$6+2\bar{N}$	6	4	4	4	6	$*$	6	$6+2\bar{M}+2\bar{N}$
$\dim(\zeta_{\bar{o}})$	4	4	4	3	2	1	$*$	0	0

then the problem is completely observable for any analytic input disturbance.

1 landmark If only one landmark is being observed, the observable subsystem is $\zeta_o = (\bar{\rho}, \beta, d_\phi, d_\omega)$, where $\bar{\rho}$ represents the scaled cartesian distance from the vehicle to the landmark, β represents the bearing angle between vehicle orientation and the landmark, d_ϕ is the polar coordinate of the input disturbance and d_ω is the orientation component of the input disturbance.

The non observable subsystem is composed of the radial coordinate of the input disturbance d_ρ, ϕ (the angle formed by the vehicle position and any arbitrary reference frame) and the position of the landmark in case it is not known (target).

1 and a half marker, and 2, 3 or more targets When two or more landmarks are being observed and all of them are targets, or only one is a marker, then the observable subsystem is

$$\zeta_o = \left({}^P\bar{x}_r, {}^P\bar{z}_r, {}^P\theta_r, \bar{d}_f, \bar{d}_h, d_\omega, {}^P\bar{x}_1, {}^P\bar{z}_1, {}^P\bar{x}_2, {}^P\bar{z}_2, ...\right),$$

where P is a coordinate frame arbitrary chosen w.r.t. the landmarks,e.g., with origin coincident to the position of P_1 and axis ${}^PX$ parallel to the line that passes through P_1 and P_2. Hence, w.r.t $\langle P\rangle$ the observable

subsystem is composed of the scaled configuration of the vehicle, the scaled positions of the features and the scaled disturbance inputs.

The non observable space is composed of the scale factor λ and the coordinate transformation between frame $\langle P \rangle$and world frame $\langle W \rangle$. In the results presented, frame $\langle P \rangle$ is assumed to be coincident to the position of the first feature P_1. This coordinate transformation is completely non observable if all landmarks are unknown (targets) and becomes observable in the case in which 1 and a half or more markers are available.

Results presented regard constant input disturbances, however it is straightforward to verify that if 3 or more landmarks are being observed, then results can be extended to the case of analytical input disturbances by the application of theorem 2.3.

3.4 An illustrative comparison of USO and UIO under simulations

During simulations an unicycle-like vehicle performs an arbitrary trajectory and receives external disturbance characterized by a constant input acting along its nonholonomic direction. In order to localize the robot while reconstructing input disturbances we present a comparison of different cases that illustrate different observability problems that were presented or discussed here. We chose the case where 3 markers are being observed for simplicity given that the system is completely observable on both USO or UIO problems. The different cases presented here are:

- **Case 1 - USO using unicycle kinematics**: in this case results regard the observer reconstruction of vehicle state ξ_r considering unicycle-like vehicle kinematics. System input u is completely known and disturbance reconstruction is not an output of the observer. Results can be seen in figures 3.11-b, 3.12-b, 3.13-b and 3.14-b;

- **Case 2 - UIO considering unicycle kinematics for disturbance**: in this case results regard the observer reconstruction of vehicle state and vehicle input, i.e. $\xi = \{\xi_r, d_r\}$. System input is completely unknown and is considered a disturbance itself. However, here we consider that $B(\xi_r)$ describe the kinematics of an unicycle–like vehicle. Results can be seen in figures 3.11-c, 3.12-c, 3.13-c and 3.14-c;

- **Case 3 - UIO with partially known inputs (using unicycle kinematics) and omnidirectional kinematics for disturbance**: in this case results regard the observer reconstruction of state and disturbance with partially known inputs. Here consider the generic disturbance input matrix $B(\xi) = I$ and $d \in \mathbb{R}^3$, permitting us to reconstruct disturbances in all directions of the input space. Partially known input $u_r = (\nu_f, \omega)^T$ and velocity vectors in G corresponding to the unicycle-like vehicle kinematics. Results can be seen in figures 3.11-d, 3.12-d, 3.13-d and 3.14-d;

For completeness, we also report the use of the triangulation method for direct computation of the state–output inverse $y \to \xi_r$ using 3 measurements. In this case only vehicle localization is performed as direct disturbance reconstruction is not a direct output of the method. An approximate reconstruction of inputs can be roughly obtained considering the derivative of the vehicle configuration.

All observers are realized as described in section 2.5 and simulations are performed using the following system parameters:

- Observers initial estimated state is $\bar{\xi}_r(0) = (0\,\mathrm{m}, 0\,\mathrm{m}, 0\,\mathrm{rad})^T$.

- During simulations we consider a triangular K. To present a fair comparison between problems, all observers use the same gains: $K_1 = K_2 = 1.5$ and $K_i = 0.5, \forall i \neq 1, 2$.

- We consider a choice of $\left(1 + \frac{\epsilon}{e}\right) \simeq 1$ and $\max(\|d\|) = 1$.

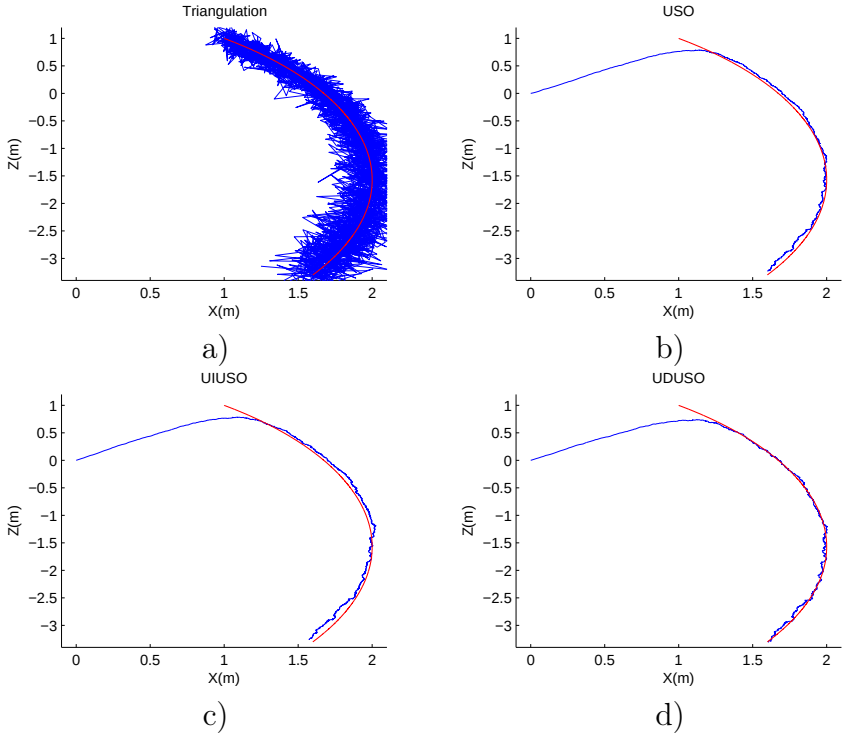

Figure 3.11: Estimated trajectories: (a) triangulation; (b) case 1; (c) case 2; and (d) case 3.

- Real vehicle trajectory is described by inputs

$$(\nu, \omega)^T = (0.1\,\text{m/s}, -0.1\,\text{rad/s})^T$$

  and input disturbance $B(x)d = (0\,\text{m/s}, -0.1\,\text{m/s}, 0\,\text{rad/s})^T$.

- Output y_i, $\forall i$ is affected by a measurement noise that is described by a random Gaussian variable with standard deviation $\sigma = 0.005\,\text{rad}$.

- No pre-filtering is used.

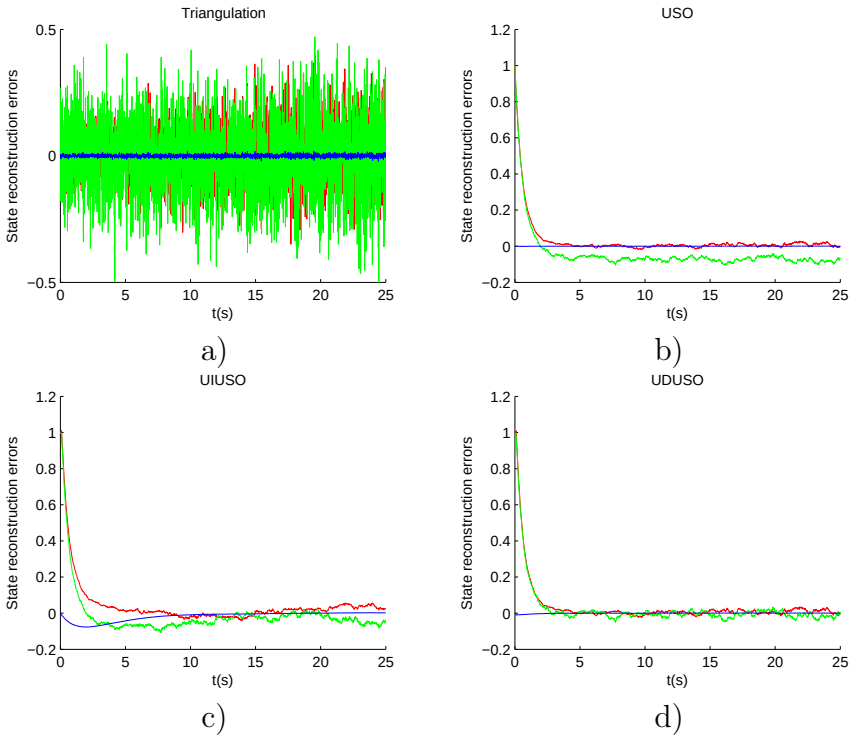

Figure 3.12: Estimation errors: (a) triangulation; (b) case 1; (c) case 2; and (d) case 3.

In these simulations the number of landmarks used is $q = 3$. For the sake of simplicity, the number of targets is $N = 0$. Results are presented as follows:

- figure 3.11 shows time history of real and estimated vehicle positions P_r; Real trajectory is represented with a red line and estimated trajectory with a blue line.
- figure 3.12 shows time history of estimation errors for variables x_r (red), z_r (green) and θ_r (blue).
- figure 3.13 shows time history of velocity reconstruction estimation errors $\dot{\tilde{x}}_r$ (red), $\dot{\tilde{z}}_r$ (green) and $\tilde{\omega}$. Given that velocity re-

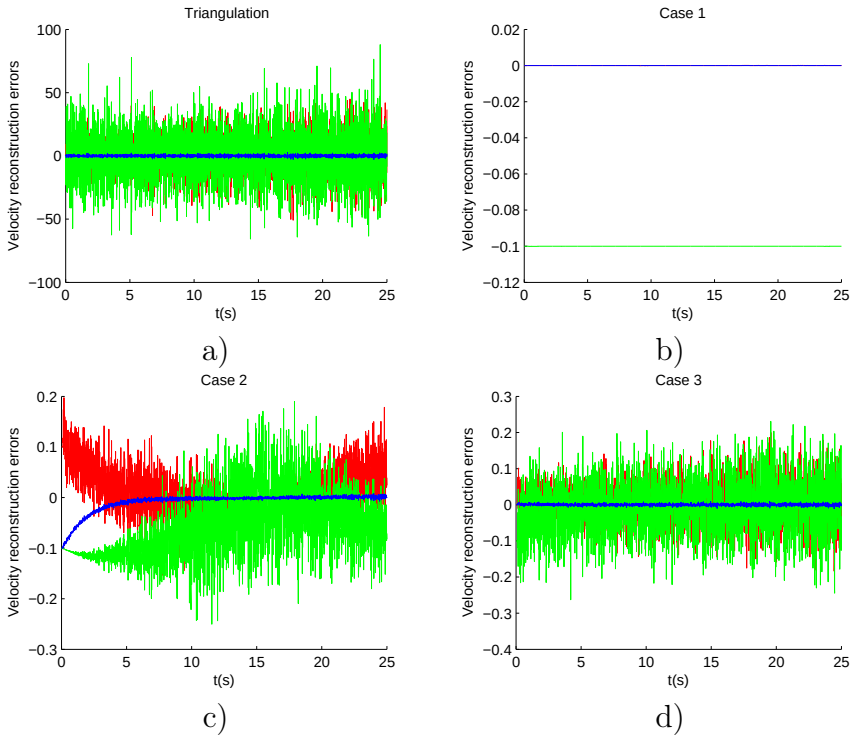

Figure 3.13: Velocity reconstruction errors: (a) triangulation; (b) case 1; (c) case 2; and (d) case 3.

construction is not a direct output of the triangulation method, figure 3.13-a shows the derivative of vehicle estimated state with the method. Similarly, for case 1, figure 3.13-b represent the constant error between known velocities and real ones.

- figure 3.14 shows time history of bearing tracking errors, i.e., the difference between estimated measurement and real ones. Figure 3.14-a shows the time history of measurement noise.

Please note that different scales are used in each figure for each case studied. E.g. in figure 3.13, the order of errors for the triangulation case is 10^2 while for cases 1,2 and 3 it is 10^{-1}.

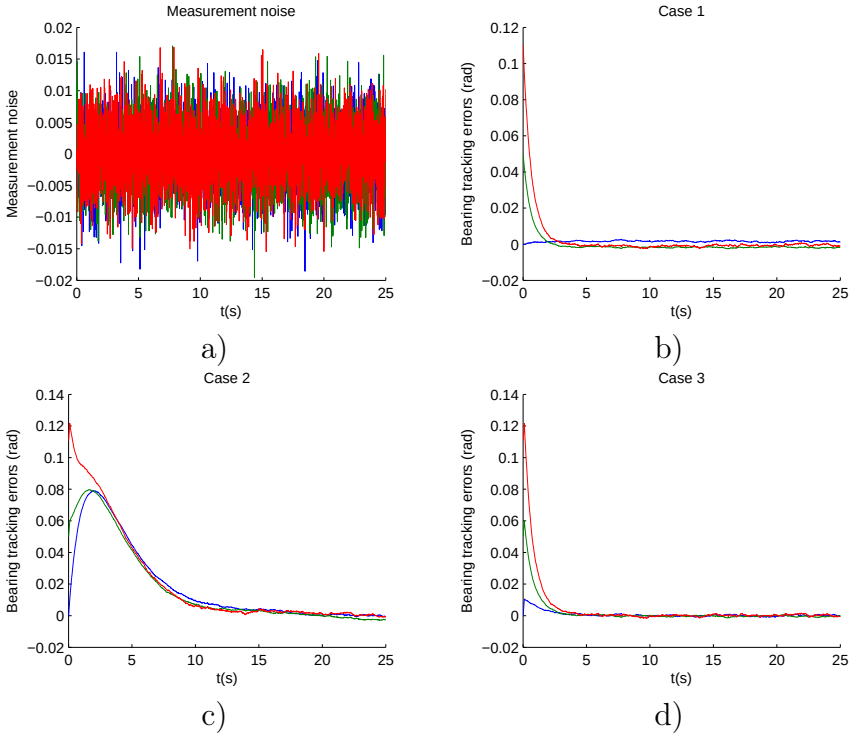

Figure 3.14: Bearing tracking errors: (a) measurement noise; (b) case 1; (c) case 2; and (d) case 3.

It can be observed that triangulation results are the ones most affected by measurement noise. This is a consequence from the fact that no filter is applied to measurements or results. The use of an observer constitute a filter itself, what explains the results obtained in the cases where an observer is applied.

In case 2, vehicle drift is not considered as a disturbance and, as expected, errors do not converge to zero. However, it performs much better than the USO observer (case 1), that presents the worst convergence case. As expected, case 3 presents the best results, and is the only observer for which errors converge to zero.

Presented simulations illustrate some advantages of using Disturbance Observers (DO): DO can compensate modeling uncertainties, as a matter of fact, observers can be constructed without considering any specific model at all; DO can be used to robustly track measurements (feature tracking) without requiring any previous knowledge of inputs or the system; disturbance reconstruction can guarantee convergence of constant gain observers; DO makes robust controllers with disturbance rejection a possibility; finally, disturbance observers can be applied even in cases where no input knowledge is available, e.g. visual odometry. However, disturbance observers may be used with caution, e.g. during transitory behavior the reconstruction of disturbance introduces oscillations in estimated state and equivalent observers may take longer to converge.

Chapter 4

On Appearance Servoing

In this chapter we define appearance servoing, investigate its feasibility and propose different possibilities for retrieving the system observable state.

4.1 Appearance Servoing Definition

In section in section 1.1.2 we discussed many limitations regarding the classical classifications of visual servoing into Position Based and Image Based. These limitations ask for different classifications of the servoing problem that may be more adequate to certain applications. In particular, if one think of robotic tasks on unstructured environments, where robust modeling, or fault detection, or online parameter identification, or disturbance rejection play a crucial role concerning performance and convergence of systems under feedback control, a stronger definition regarding the construction of stabilizing control laws is required. One particular robotic task that is the primary basis of this thesis is the pose regulation of a robot in a desired position expressed with a desired image, a task coherent with the navigation of a vehicle that uses *Appearance Maps* as reference.

Hence, here the *appearance servoing* is proposed as a classification that takes input disturbances in consideration, explicitly restricts the

construction of adequate stabilizing control laws and do not depend on proprioceptive measurements. Moreover, it does not exclude the coexistence with a PBVS or IBVS classification as it does not depend on the way the error is defined.

Definition 4.1 Appearance Servoing -

Appearance Servoing concerns the pose regulation of a robot in a desired position expressed with a desired image. A stabilizing control law z for system state ξ (or a subsystem of) is defined as static appearance servoing *if it has the following form:*

$$u(t) = z\left(y_{ext}[t], \lambda_{int}\right) ,$$

and is defined as dynamic appearance servoing *if it has the following form:*

$$\begin{cases} \Phi\left(\hat{\xi}_r, \hat{\lambda}_{ext}, \hat{d}\right) = o\left(y_{ext}[0,t], v[0,t], \lambda_{int}\right) \\ u(t) = z\left(\phi\left(\hat{\xi}_r, \hat{\lambda}_{ext}, \hat{d}\right), \lambda_{int}\right) \end{cases} ,$$

where Φ describes a observable and reachable subspace of the estimates $\hat{\xi}, \hat{\lambda}_{ext}, \hat{d}$ and is given by the observer o and $\partial u / \partial \lambda_{ext} = \partial u / \partial \xi = \partial u / \partial d = 0$.

As highlighted by the *appearance servoing* definition here introduced, it does not exclude the use of observers in the control scheme. It is also worthwhile to note that these definitions do not depend on proprioceptive measurements: lack of such information is modelled using the unknown disturbance model. We also consider unstructured environments, however intrinsic parameters can be assumed to be known a priori (through parameter identification/calibration procedures) while extrinsic parameters can not.

4.2 Appearance Servoing Observability

This section is devoted to the observability analysis and to the vehicle inputs reconstruction issues. Again, no information apart from

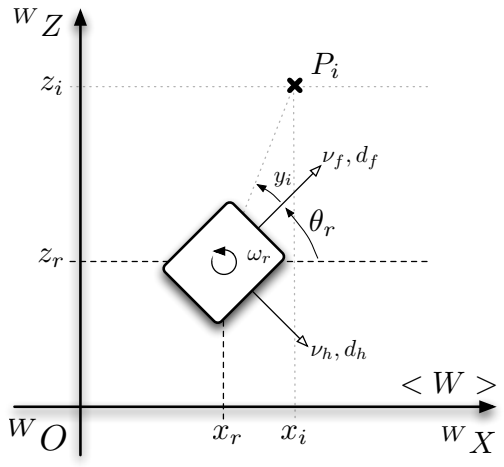

Figure 4.1: Fixed frame $\langle W \rangle$, vehicle state $(x_r,\ z_r,\ \theta_r)$, generalized velocities (ν_f, ν_h, ω), input disturbances (d_f, d_h, d_ω) and i_{th} landmark position $P_i = (x_i,\ z_i)$.

calibration parameters are assumed to be known a priori. In order to simplify notations, we define: the coordinate displacement between two points a and b as $\Delta *_{a,b} = *_a - *_b$; the Euclidean distance on the $^W X \times^W Z$ plane as $\rho_{a,b} = \sqrt{\Delta x_{a,b}{}^2 + \Delta z_{a,b}{}^2}$.

4.2.1 Dynamic Appearance Servoing

Consider a vehicle with unknown inputs[1], i.e., $G(\xi_r) = 0$ in (3.2). Without loss of generality, we further assume the origin of the world frame $\langle W \rangle$ to be coincident with the desired position of the robot, with $^C Z \equiv {}^W X$, i.e., $\xi_{rd} = (0, 0, 0)$ (see Fig. 4.1), defined by a desired image.

Let $d_{r,h}$ be the h–th element of the input vector d_r. $d_{r,h}(t)$ can be expressed using an infinite Taylor expansion around $d_{r,h,0} = d_{r,h}(0)$

[1]As discussed in section 3, the results can be extended to any type of vehicle with known inputs and unknown disturbance.

as $d_{r,h}(t) = \sum_{i=0}^{+\infty} {d_{r,h,0}}^{(i)} \frac{t^i}{i!}$. This way, an augmented system state is easily derived as $\xi_e = \left[\xi_{e,r}^T, \xi_{e,f}^T, \xi_{e,\mathrm{d1}}^T, \xi_{e,\mathrm{d2}}^T, \ldots\right]^T$, i.e., composing the vehicle state $\xi_{e,r} = \xi_r$, the motion–less landmark positions $\xi_{e,f} = [{}^W P_1^T, {}^W P_2^T, \ldots, , {}^W P_{n_f}^T]^T$, the input disturbances $\xi_{e,\mathrm{d1}} = {d_r}^{(0)}$ and its derivatives $\xi_{e,\mathrm{dn}} = {d_r}^{(n-1)}$, whose dynamics is given by $\dot{\xi}_e = \left[\dot{\xi}_{e,r}^T, 0, \xi_{e,\mathrm{d2}}^T, \xi_{e,\mathrm{d3}}^T, \ldots\right]^T$.

It is assumed in this context that the feature correspondence between the current and desired image is granted, hence the output of the system is a vector $y = [y_{\mathrm{cur}}^T, y_{\mathrm{des}}^T]^T$ of current and desired image point positions. The n_f landmark measurements (with $n_f > 2$) on the current (or desired) image are modelled using equation (1.21) and described by the vector $y_{\mathrm{cur}} = \left[y_{\mathrm{cur},1}^T, \ldots, y_{\mathrm{cur},n_f}^T\right]^T$. The i-th feature measurement on the current image is given by

$$y_{\mathrm{cur},i} = h_{\mathrm{cur},i}({}^W\xi_r, {}^W P_i) =$$

$$\begin{bmatrix} \mathrm{atan2}\left(-\Delta z_{i,r} C_{\theta_r} + \Delta x_{i,r} S_{\theta_r}, \Delta x_{i,r} C_{\theta_r} + \Delta z_{i,r} S_{\theta_r}\right) \\ \mathrm{atan2}\left({}^W y_i, \Delta x_{i,r} C_{\theta_r} + \Delta z_{i,r} S_{\theta_r}\right) \end{bmatrix}, \tag{4.1}$$

while the measurements in the desired image are

$$y_{\mathrm{des},i} = h_{\mathrm{des},i}({}^W\xi_r, {}^W P_i) = \begin{bmatrix} \mathrm{atan2}\left(-z_i, x_i\right) \\ \mathrm{atan2}\left(y_i, x_i\right) \end{bmatrix}. \tag{4.2}$$

The system thus derived is given by

$$\Sigma_e = \begin{cases} \dot{\xi}_e = \left[{\dot{\xi}_r}^T, 0, \xi_{e,\mathrm{d2}}^T, \xi_{e,\mathrm{d3}}^T, \ldots\right]^T \\ y = h(\xi_e) = \left[y_{\mathrm{cur},1}^T, \ldots, y_{\mathrm{cur},n_f}^T, y_{\mathrm{des},1}^T, \ldots, y_{\mathrm{des},n_f}^T\right]^T. \end{cases}$$

Let us define the polynomial disturbance ${}^K d_{r,h}(t)$ as the partial Taylor expansion of $d_{r,h}(t)$ around $d_{r,h,0} = d_{r,h}(0)$ as ${}^K d_{r,h}(t) = \sum_{i=0}^{K} {d_0}^{(i)} \frac{t^i}{i!}$ and $d_{r,h}^{(K+1)} = 0$. In such a case, the augmented system state is ${}^k\xi_e =$

$\left[\xi_{e,r}^T,\, \xi_{e,f}^T,\, \xi_{e,\mathrm{d}1}^T,\, \xi_{e,\mathrm{d}2}^T,\, \ldots,\, \xi_{e,\mathrm{dk}}^T\right]^T$, with corresponding system dynamics ${}^k\dot{\xi}_e = \left[\dot{\xi}_{e,r}^T,\, 0,\, \xi_{e,\mathrm{d}2}^T,\, \xi_{e,\mathrm{d}3}^T,\, \ldots, 0\right]^T$.

The observability analysis of ${}^k\xi_e$ is carried out applying the rank condition to the observability matrix ${}^kO$. However, the following question arises: if ${}^k\xi_e$ is observable under the assumption of $d_{r,h}^{(k+1)} = 0, \forall h$, does it implies that ξ_e is observable for any analytic $d_{r,h}$?

To investigate the extension of the observability analysis of ${}^k\xi_e$, it is possible to apply the mathematical induction method starting from the base case ${}^0\xi_e$ and studying the inductive step from ${}^k\xi_e$ to ${}^{k+1}\xi_e$. The procedure can be summarized as follows:

- ${}^0\xi_e$ is observable: investigate the observability problem for ${}^0\xi$;
- ${}^k\xi_e$observable $\rightarrow$ ${}^{k+1}\xi_e$observable: investigate if ${}^k\xi_e$ being observable implies in the observability of ${}^{k+1}\xi_e$;

Satisfying the above conditions implies that ξ_e is observable for any analytic $d_{r,h}(t)$. It is important to note that the logical induction presents sufficient, but not necessary, conditions for system observability.

Disturbance Observability Analysis

In this section the problem rank condition property is analyzed and a discussion on the local decomposition into observable and non observable subsystems is presented.

The system ${}^0\Sigma_e$ is not completely observable, its unobservable space is one dimensional and the null space of the observability codistribution is given by

$$\left(x_r, z_r, 0, {}^W x_1, {}^W y_1, {}^W z_1, \ldots, {}^W x_{n_f}, {}^W y_{n_f}, {}^W z_{n_f}, d_f, d_h, 0\right) .$$

With the aim of writing the appearance servoing problem under an observable canonical form, let $\lambda \in \left\{{}^W y_1, \ldots, {}^W y_{n_f}\right\}$ be a scaling

factor. For instance, if $\lambda = {}^{W}y_i$, a new coordinates mapping is defined as

$$\zeta = \Phi\left(\xi_e\right) = \left\{\bar{\xi}_r, {}^{W}\bar{P}_1, \ldots, {}^{W}\hat{P}_i, \ldots, {}^{W}\bar{P}_{n_f}, \bar{d}_r, \bar{d}^{(1)}{}_r, \ldots, \lambda\right\},$$

where $\bar{\xi}_r = (\bar{x}_r,\, \bar{z}_r,\, \theta_r)$, ${}^{W}\hat{P}_i = \left({}^{W}\bar{x}_i,\, {}^{W}\bar{z}_i\right)$ and $\overline{*}$ defines the operation $\overline{*} = */\lambda$. Striclty speaking, ζ contains a scaled version of ξ_e, except for the variables θ_r and ${}^{W}y_i = \lambda$. This way, $dim(\zeta) = dim(\xi_e)$ and $\Phi\left(\xi_e\right)$ is a global diffeomorphism for $\lambda \neq 0$. The vector representation of the new state is

$$\begin{aligned}\zeta &= \left[\bar{\xi}_r^T,\, {}^{W}\bar{P}_1^T, \ldots,\, {}^{W}\bar{P}_{n_f}^T,\, \bar{d}_r^T,\, \bar{d}_r{}^{(1)^T}, \ldots,\, \lambda\right]^T \\ &= \left[\zeta_r^T,\, \zeta_f^T,\, \zeta_d^T,\, \lambda\right]^T,\end{aligned}$$

where $\zeta_r = \bar{\xi}_r$ and $\dot{\zeta}_r = (g_f, g_h, g_w)\,\bar{d}_r$ (see (3.2)),

$$\zeta_f = \left[{}^{W}\bar{P}_1^T,\, \ldots,\, {}^{W}\bar{P}_{n_f}^T\right]^T = \left[\zeta_1^T,\, \ldots,\, \zeta_{n_f}^T\right]^T$$

with $\dot{\zeta}_f = 0$, and finally $\zeta_d = \left[\bar{d}_r^T,\, \bar{d}_r{}^{(1)^T}, \ldots\right]^T$ with $\dot{\zeta}_d = \left[\zeta_{d,2}^T, \zeta_{d,3}^T, \ldots\right]^T$. Hence,

$$\dot{\zeta} = \left[\dot{\zeta_r}^T, 0, \ldots, 0, \zeta_{\mathrm{d2}}^T, \zeta_{\mathrm{d3}}^T, \ldots, 0\right]^T,$$

with measurements still described by both the vector $y_{\mathrm{des},i}$, given in the new set of coordinates by

$$\begin{aligned}y_{\mathrm{des},i} &= h_{\zeta\mathrm{des},i}(\zeta) = \\ &= \begin{pmatrix} \mathrm{atan2}\left(-\mathrm{sign}(\lambda)\bar{z}_i, \mathrm{sign}(\lambda)\bar{x}_i\right) \\ \mathrm{atan2}\left(\mathrm{sign}(\lambda)\bar{y}_i, \mathrm{sign}(\lambda)\bar{x}_i\right) \end{pmatrix},\end{aligned}$$

and by the vector $y_{\mathrm{cur},i}$, obtained from (4.2.1) in a similar way. Notice that $\mathrm{sign}(\lambda)$ can be obtained from the desired image.

As a result, the appearance servoing problem is fully described by the auxiliary system

$$\Psi = \begin{cases} \dot{\zeta} = \left[\dot{\zeta_r}^T, 0, \ldots, 0, \zeta_{\mathrm{d2}}^T, \zeta_{\mathrm{d3}}^T, \ldots, 0\right]^T \\ y = h_\zeta(\zeta) = h(\Phi^{-1}(\zeta)) \end{cases}$$

in canonical form.

Proposition 4.1 *The local decomposition of the appearance servoing problem for constant $\bar{d}_r$ is given by:*

$$
{}^0\Psi = \begin{cases} {}^0\dot{\zeta} = \left[\dot{\zeta_r}^T, 0, \ldots, 0\right]^T \\ y = h_\zeta({}^0\zeta)\,, \end{cases}
$$

where, apart from singularities, the observable state is $\zeta_o = (\zeta_r, \zeta_f, \zeta_d)$, while the unobservable subsystem is $\zeta_{\bar{o}} = \lambda$, whereas the number of landmarks being observed is $n_f > 2$.

Proof 4.1 *After 1 level of Lie differentiation, the observability codistribution rank reaches its maximum and codistribution ${}^0\Omega$ can be written as:*

$$
\begin{aligned}
{}^0\Omega &= \begin{bmatrix} \Omega^{(0)} \\ \Omega^{(1)} \end{bmatrix} = \begin{bmatrix} \Omega_{\zeta_r}{}^{(0)} & \Omega_{\zeta_f}{}^{(0)} & \Omega_{\zeta_d}{}^{(0)} & \Omega_{\lambda}{}^{(0)} \\ \Omega_{\zeta_r}{}^{(1)} & \Omega_{\zeta_f}{}^{(1)} & \Omega_{\zeta_d}{}^{(1)} & \Omega_{\lambda}{}^{(1)} \end{bmatrix} = \\
&= \begin{bmatrix} \Omega_{\zeta_r}{}^{(0)} & \Omega_{\zeta_f}{}^{(0)} & 0 & 0 \\ \Omega_{\zeta_r}{}^{(1)} & \Omega_{\zeta_f}{}^{(1)} & \Omega_{\zeta_d}{}^{(1)} & 0 \end{bmatrix} = \\
&= \begin{bmatrix} \partial_{\zeta_r} L_f{}^{(0)} h_1 & \partial_{\zeta_1} L_f{}^{(0)} h_1 & \ldots & 0 & 0 & 0 \\ \vdots & \vdots & \ddots & \vdots & \vdots & \vdots \\ \partial_{\zeta_r} L_f{}^{(0)} h_n & 0 & \ldots & \partial_{\zeta_n} L_f{}^{(0)} h_n & 0 & 0 \\ \partial_{\zeta_r} L_f{}^{(1)} h_1 & \partial_{\zeta_n} L_f{}^{(1)} h_1 & \ldots & 0 & \partial_{\zeta_d} L_f{}^{(1)} h_1 & 0 \\ \vdots & \vdots & \vdots & \ddots & \vdots & \vdots \\ \partial_{\zeta_r} L_f{}^{(1)} h_n & 0 & \ldots & \partial_{\zeta_n} L_f{}^{(1)} h_n & \partial_{\zeta_d} L_f{}^{(1)} h_n & 0 \end{bmatrix}.
\end{aligned} \tag{4.3}
$$

The terms $\partial_* L_*{}^{(*)} h_* \neq 0$ are not explicitly reported here for space limits. Apart from configuration singularities, the rank of ${}^0\Omega$ is $dim({}^0\zeta) - 1$ and the null space of ${}^0\Omega$ is $(0, \ldots, 0, 1)$, hence the proof.

Corollary 4.1 *Follows from Proposition 4.1 that the ratios $x_r : z_r : x_1 : y_1 : z_1 : \ldots : x_{n_f} : y_{n_f} : z_{n_f} : d_f : d_h$ are locally weakly observable.*

Now, we investigate if Proposition 4.1 can be extended to any analytic $d_r(t)$.

Proposition 4.2 *The subsystem ζ_o is observable for any analytic $d_r(t)$.*

Proof 4.2 *Since ${}^0\zeta_o$ is observable by Proposition 4.1, it remains to verify if assuming ${}^k\zeta_o$ being observable implies that ${}^{k+1}\zeta_o$ is observable in its turn. From (4.3), we first notice that the codistribution ${}^0\Omega_o$ associated to the observable state ${}^0\zeta_o$ obtained by ${}^0\zeta_o$ has the following form*

$$ {}^0\Omega_o = \begin{bmatrix} * & 0 \\ * & {\Omega_{\zeta_d}}^{(1)} \end{bmatrix}. $$

Therefore, by applying the inductive step from ${}^k\zeta$ to ${}^{k+1}\zeta$, one gets:

$$ {}^k\Omega_o = \begin{bmatrix} * & 0 \\ \vdots & \vdots \\ * & 0 \\ * & {\Omega_{\zeta_d}}^{(1)} \end{bmatrix} \rightarrow^{k+1} \Omega_o = \begin{bmatrix} * & 0 & 0 \\ \vdots & \vdots & \vdots \\ * & {\Omega_{\zeta_d}}^{(1)} & 0 \\ \dots & * & {\Omega_{\zeta_d}}^{(1)} \end{bmatrix} $$

from which follows:

$$ rank\left({}^{k+1}\Omega_o\right) = rank\left({}^k\Omega_o\right) + rank\left({\Omega_{\zeta_d}}^{(1)}\right). $$

If $n_f \geq 2$, we have that $rank\left({\Omega_{\zeta_d}}^{(1)}\right) = \dim\left(\zeta_d\right)$, and consequently:

$$ rank\left({}^{k+1}\Omega_o\right) = rank\left({}^k\Omega_o\right) + \dim\left(\zeta_d\right) = \dim\left({}^{k+1}\zeta_o\right). $$

It follows that the ${}^k\zeta_o$ observability implies the ${}^{k+1}\zeta_o$ observability. As a consequence, for analytic unknown disturbance d_r, the vehicle scaled state ζ_r, the landmark scaled positions ζ_f and the scaled input disturbances ζ_d are locally weakly observable.

Remark 4.1 *The observability analysis here proposed is valid apart from singularities, e.g. the observability problem is singular whenever vehicle arrives at desired position and whenever translational velocities are zero. An observer necessarily have to take these singularities into account. A deeper discussion on the observability singularities of the appearance servoing is deferred to future work.*

4.2.2 Static Appearance Servoing

The problem of determining which subsystem can be distinguished directly from available measurements statically can be investigated on the basis of the jacobian $J = \frac{\partial h\left({}^{0}\zeta\right)}{\partial {}^{0}\zeta}$, which coincides to $J = \Omega^{(0)}$. Given that

$$\text{null}\left(\Omega^{(0)}\right) = [0, 0, 0, I_{4,4}] \ ,$$

one can conclude that the statically observable subsystem is ${\zeta_o}^{(0)} = \left(\bar{\xi}_r, \bar{\xi}_1, \ldots, \bar{\xi}_n\right)$, while the unobservable subsystem is ${\zeta_{\bar{O}}}^{(0)} = \left(\lambda, \bar{d}_r\right)$. Unfortunately, this result is weak, i.e., distinguibility is guaranteed only in a neighborhood of ${\zeta_o}^{(0)}$. For instance, if only two landmarks are being measured, there is an ambiguity on the invertibility problem of $y = h({\zeta_o}^{(0)})$ and two solutions can be found for ${\zeta_o}^{(0)} = h^{-1}(y)$ almost everywhere. This ambiguity is solved if non singular configurations of $n \geq 3$ landmarks are available. In this case, the ratios $x_r : z_r : x_1 : y_1 : z_1 : \ldots : x_n : y_n : z_n$ can be computed statically, i.e., directly from available measurements y, while input disturbances are not observable. For example, [70] proposes a motion estimation technique in order to extract the relative pose from correspondences of $n \geq 3$ landmarks, both in the current and desired images, explicitly considering the planar motion constraint.

4.3 Observable space recostruction

4.3.1 Static Solution

Consider measurements defined directly on the image plane (eq. (1.2.3)), the invertibility problem leads to the following non-homogeneous linear system of equations:

$$A \begin{bmatrix} \sin(\theta_r) \\ \cos(\theta_r) \end{bmatrix} = c, A = \begin{bmatrix} a_{i,j} & b_{i,j} \\ \vdots & \vdots \end{bmatrix}, c = \begin{bmatrix} c_{i,j} \\ \vdots \end{bmatrix}, \forall i \neq j,$$

where:

$$a_{i,j} = (1 + x_{c,i}x_{d,j})\, y_{c,j}y_{d,i} - (1 + x_{c,j}x_{d,i})\, y_{c,i}y_{d,j}$$

$$b_{i,j} = (-x_{c,i} + x_{d,j})\, y_{c,j}y_{d,i} + (x_{c,j} - x_{d,i})\, y_{c,i}y_{d,j}$$

$$c_{i,j} = (-x_{d,i} + x_{d,j})\, y_{c,i}y_{c,j} + (-x_{c,i} + x_{c,j})\, y_{d,i}y_{d,j}.$$

Hence a set of $\frac{n!}{2(n-2)!}$ equations with unknown variables $\sin\theta_r$ and $\cos\theta_r$ is derived. Using standard linear and nonlinear least–square methods, a solution can then be found if at least three nonsingular configurations of the landmarks are available. E.g., one solution can be derived using

$$\begin{bmatrix} \sin(\theta_r) \\ \cos(\theta_r) \end{bmatrix} = A^{+}c.$$

The scaled position of the robot on the plane, i.e., $\bar{x}_r$ and $\bar{z}_r$, is then derived using the following equation:

$$\bar{x}_r = \frac{(y_{c,i} - y_{d,i}(\cos\theta_r + x_{c,i}\sin\theta_r))}{y_{c,i}}$$

$$\bar{z}_r = -\frac{(x_{d,i}y_{c,i} - x_{c,i}y_{d,i}\cos\theta_r + y_{d,i}\sin\theta_r)}{y_{c,i}}.$$

A similar solution is presented in [70].

4.3.2 Dynamic Solution

In this section we propose the design of an asymptotically stable nonlinear observer (or filter) that reconstructs a scaled subspace of the vehicle state, polynomial vehicle input disturbances of order k and landmark positions, i.e., the augmented observable state ${}^{k}\zeta_o$. The presented observer considers that inputs are completely unknown, i.e., treated as a disturbance. It is worthwhile to note that, even though ζ_d is observable, practical limitations impose a limit on the polynomial description of input disturbances, which has to be at most of an

arbitrary order k. Following [76], the observer dynamics is given by the auxiliary system

$$\begin{cases} {}^k\hat{\zeta}_o{}^{(1)} = f_o\left({}^k\hat{\zeta}_o\right) + v \\ y = h\left({}^k\hat{\zeta}_o\right) \end{cases} .$$

Let $e_o = {}^k\zeta_o - {}^k\hat{\zeta}_o$ be the observer error. Using the notation $\tilde{*}(x)$ to represent the symbolic operation $*(x) - \hat{*}(x)$, e.g., $\tilde{f}_o({}^k\zeta_o) = f_o({}^k\zeta_o) - f_o({}^k\hat{\zeta}_o)$, its dynamics is given by

$$\dot{e}_o = \tilde{f}_o\left({}^k\zeta_o\right) - v\,.$$

Let us choose $v = KJ({}^k\hat{\zeta}_o)^\dagger(Y - H({}^k\hat{\zeta}_o))$, where $Y = \left[y^{(0)},\, y^{(1)},\, \ldots,\, y^{(l)}\right]^T$ is named extended output vector (here we follow the convention adopted in [78]), $H({}^k\hat{\zeta}_o) = \left[h({}^k\hat{\zeta}_o)^{(0)},\, h({}^k\hat{\zeta}_o)^{(1)},\, \ldots,\, h({}^k\hat{\zeta}_o)^{(l)}\right]^T$ is the extended output function (l is at least the minimum order of the time derivatives required for the system to be observable), $J({}^k\hat{\zeta}_o)^\dagger$ is the pseudoinverse of the extended output jacobian $J({}^k\zeta_o) = \partial_{{}^k\zeta_o} H({}^k\zeta_o)$ evaluated at ${}^k\hat{\zeta}_o$, and K is a positive definite constant gain matrix. If the system is locally weakly observable, the local approximation $v = -K(e_o + \epsilon({}^k\zeta_o, {}^k\hat{\zeta}_o))$ is derived, where $\epsilon({}^k\zeta_o, {}^k\hat{\zeta}_o)$ (or simply ϵ) is the pseudoinverse approximation error.

Letting $V = \frac{1}{2}\, e_o^T e_o$ be the Lyapunov candidate, we have

$$\dot{V} = e_o^T \left(\tilde{f}_o\left({}^k\zeta_o\right) - K(e_o + \epsilon)\right). \tag{4.4}$$

If $\left\| \frac{e_o + \epsilon}{e_o} \right\|$ and $\left\| \partial_{{}^k\zeta_o} f_o\left({}^k\zeta_o\right) \right\|$ are bounded, matrix K is chosen to let (4.4) satisfy the stability criterion, i.e., $\dot{V}$ n.d.. The convergence for ${}^k\hat{\zeta}_o(0)$ in a local neighborhood of the real scaled state ${}^k\zeta_o(0)$ is guaranteed since the value of ϵ in the worst case is related to the maximum admissible $\|e_o(0)\|$.

Considering a matrix $K = \text{diag}\,(K_1, K_2, \ldots, K_h, \ldots)$, the error dynamics is stable if

$$K_i > \sup\left(\text{norm}\left(\frac{\partial f_{o_i}\left({}^k\zeta_o\right)}{\partial^k\zeta_o}\right)\right)\max\left(\left|\frac{e_{o,i}}{e_{o,i}+\epsilon_i}\right|\right), \tag{4.5}$$

where f_{o_i} corresponds to the element i of the vector f_o. If $\frac{e_o}{e_o+\epsilon}$ is bounded by some arbitrary worst value (corresponding to some maximum acceptable error $\left\|{}^k\zeta_o - {}^k\hat{\zeta}_o\right\|$), K can be chosen in order to guarantee stability.

The particular solution of condition (4.5) for an observer designed in order to reconstruct polynomial disturbances of order $k = 0$ is:

$$\begin{aligned}
K_1 &> \sup\left(\sqrt{\left|\overline{\text{dh}}\cos(\theta) + \overline{\text{df}}\sin(\theta)\right|^2 + 1}\right)\sup\left(\left|\frac{e_i}{e+\epsilon_i}\right|\right)\\
K_2 &> \sup\left(\sqrt{\left|\overline{\text{df}}\cos(\theta) - \overline{\text{dh}}\sin(\theta)\right|^2 + 1}\right)\sup\left(\left|\frac{e_i}{e+\epsilon_i}\right|\right)\\
K_3 &> \sup\left(\left|\frac{e_i}{e+\epsilon_i}\right|\right)\\
K_i &> 0, \forall i \geq 4.
\end{aligned}$$

4.4 Pose Regulation

The (dynamic or static) observers designed in section 4.3 are able to reconstruct the scaled robot state, e.g., $\bar{\xi}_r = (\bar{x}_r, \bar{z}_r, \theta_r)$. Therefore, this section solves the servoing control problem assuming the knowledge of $\bar{\xi}_r$, given that a control law $u(\xi_r)$ is readily available.

4.4.1 Appearance Pose Regulation of an Omnidirectional Vehicle

In this section we discuss the application of the observer proposed in section 4.3.2 to two classical controller schemes that solve the pose regulation of an omnidirectional vehicle problem, from which one is

an IBVS scheme and the other is a PBVS scheme. Both the dynamic and static observers reconstruct the scaled robot state, e.g., $\bar{\xi}_r = (\bar{x}_r, \bar{z}_r, \theta_r)$. Therefore, this section solves the servoing control problem assuming the knowledge of $\bar{\xi}_r$, given that a control law $u(\xi_r)$ is readily available.

PBVS controller

Let us define the pose error variable $e_c = \xi_{r,\text{cur}} - \xi_{r,\text{des}} = \xi_r$ (since, without loss of generality, the desired position is assumed to be the origin of the frame $\langle W \rangle$), with dynamics given by $\dot{e}_c = G(\theta_r)\, u$. Straightforwardly, an input–state feedback linearization would be $u = -K_c G^{-1}(\theta_r)\, e_c$. With the choice of a diagonal positive definite K_c, resulting error dynamics $\dot{e}_c = -K_c e_c$ is asymptotically exponentially stable with exponential rate determined by K_c.

Consider now the scaled pose error variable $\bar{e}_c = \zeta_r = \bar{\xi}_r$. Assuming the knowledge of an estimate $\hat{\zeta}_r$ but not of ξ_r, we can adapt the control law as follows. Let's choose $u = -sign(\lambda) K_c G^{-1}\left(\hat{\theta}_r\right) \hat{\zeta}_r$, which results in error dynamics $\dot{e}_c = -sign(\lambda) K_c G(\theta_r)\, G^{-1}\left(\hat{\theta}_r\right) \hat{\zeta}_r$. If an asymptotically stable observer for ζ_o is adopted, $\lim_{t\to+\infty} \hat{\zeta}_r = \zeta_r$. As a consequence, assuming the observer transient is fast w.r.t. the controlled system dynamics, it can be assumed to be negligible, and error dynamics becomes $\dot{e}_c = -sign(\lambda) K_c G(\theta_r)\, G^{-1}(\theta_r)\, \Lambda e_c = -sign(\lambda) K_c \Lambda e_c$, where

$$\Lambda = \begin{bmatrix} \frac{1}{\lambda} & 0 & 0 \\ 0 & \frac{1}{\lambda} & 0 \\ 0 & 0 & 1 \end{bmatrix}.$$

Therefore, the controlled dynamics of $\dot{e}_c$ is still asymptotically exponentially stable, although the exponential rate is now determined by $K_c\Lambda$. The final control scheme is shown in Fig. 4.2.

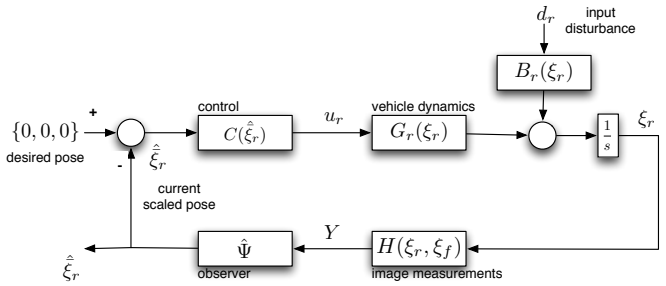

Figure 4.2: PBVS control scheme.

IBVS controller

Let us define the error in the image space, i.e., $e_c = y_{\text{des}} - y_{\text{cur}}$, whose dynamics is given by

$$\dot{e}_c = J_y(\xi_r, \xi_f)u, \;\; \text{with} \;\; J_y(\xi_r, \xi_f) = \frac{\partial y}{\partial \xi_r} G\left(\xi_r\right).$$

In this case, the application of an input-output feedback linearization results in the control law $u = -K_c {J_y}^{\dagger}(\xi_r, \xi_f)\, e_c$. Again, choosing K_c diagonal and positive definite, the error dynamics is asymptotically exponentially stable with exponential rate determined by K_c.

Assuming the knowledge of an estimate $\hat{\zeta}_o$, the control law turns to $u = -\text{sign}(\lambda) K_c {J_y}^{\dagger}(\hat{\zeta}_r, \hat{\zeta}_f) e_c$, with error dynamics

$$\dot{e}_c = -\text{sign}(\lambda) K_c J_y(\xi_r, \xi_f) {J_y}^{\dagger}(\hat{\zeta}_r, \hat{\zeta}_f) e_c.$$

If an asymptotically stable observer of ζ_o is adopted, the same rationale of the PBVS case can be applied and hence $\lim_{t\to+\infty} \hat{\zeta}_r = \zeta_r$ and $\lim_{t\to+\infty} \hat{\zeta}_f = \zeta_f$. Noticing that $J_y(\zeta_r, \zeta_f) = \lambda J_y(\xi_r, \xi_f)$, the error dynamics can be simplified to $\dot{e}_c = -\text{sign}(\lambda)\lambda K_c e_c$, which is asymptotically exponentially stable as the original control law, but with exponential rate determined by λK_c. The overall control scheme is represented in Fig. 4.3.

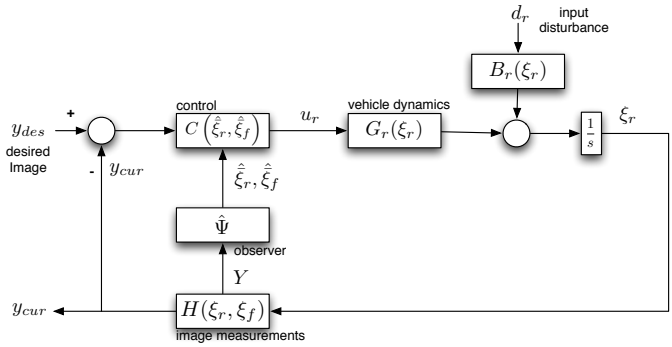

Figure 4.3: IBVS control scheme.

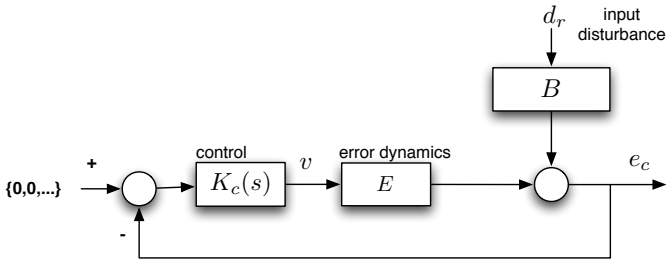

Figure 4.4: IBVS and PBVS control scheme for disturbance rejection.

Disturbance Rejection

Regardless of the approach chosen for the vehicle control, the closed loop control diagram of Fig. 4.4 is applicable, where $E = -sign(\lambda)K_c\Lambda$ in the PBVS case and $E = -\text{sign}(\lambda)\lambda K_c$ in the IBVS case and where an additional design degree of freedom $C(s)$ has been added. Assuming that the observer transient is finished, i.e., observer error e_o become negligible, both PBVS and IBVS MIMO control schemes become equivalent to one decoupled SISO control scheme for each error component e_c. Consequently, the diagonal transfer function matrix that describes the effect of an input disturbance on the error e_c of the system is

$$e_c(s) = [1 + C(s)E]^{-1} B d_r(s)\,.$$

Hence, using the description of the input disturbance given by the observer, standard countermeasures from control theory can be adopted to design a robust $C(s)$ that reduces the effect of the disturbance in the loop.

4.4.2 Appearance Pose Regulation of an Unicycle Vehicle

Let $\xi_{r,cur}$ represent the actual pose of the robot and $\xi_{r,des}$ represents the desired pose of the robot. Without loss of generality we may consider that the reference frame $\langle W \rangle$ is coincident to the desired position of the robot, i.e., $\xi_{r,des} = (0, 0, 0)$. Now, let's consider the pose displacement between $\xi_{r,cur}$ and $\xi_{r,des}$ on polar coordinates $\xi_{rp} = [\rho, \beta, \phi]^T$ described by $\Phi_p : \mathbb{R}^2 \times S \rightarrow \mathbb{R}^+ \times S^2$, as in eq. (1.9). System dynamics is given by

$$\begin{bmatrix} \dot{\rho} \\ \dot{\beta} \\ \dot{\phi} \end{bmatrix} = \begin{bmatrix} -\cos\beta & 0 \\ \frac{\sin\beta}{\rho} & -1 \\ \frac{\sin\beta}{\rho} & 0 \end{bmatrix} \begin{bmatrix} v_f \\ \omega \end{bmatrix}. \tag{4.6}$$

A stabilizing control law $(v_f, \omega) = f_u(\xi_{\mathrm{rp}})$ for the non-linear system dynamics (4.6) that solves the pose regulation problem $\xi_{rp} \rightarrow 0$, originally appeared in [79]:

$$\begin{cases} v_f = k_1 \rho \cos\beta \\ \omega = k_2\beta + k_1 \left(\dfrac{\sin\beta\cos\beta}{\beta} \right) (\beta + k_3\phi) \end{cases}, \tag{4.7}$$

where k_1, k_2, k_3 are arbitrarily chosen positive constants. Eq. 4.7 renders the derivative of the Lyapunov candidate $V = 1/2(\rho^2 + \beta^2 + \phi^2)$ negative definite.

Now let's consider the scaled pose displacement $\zeta_r = \bar{\xi}_r$ on polar coordinates, it is easy to verify that

$$\bar{\xi}_{\mathrm{rp}} = (\bar{\rho}, \beta, \phi) = \left(\frac{\mathrm{sign}(\lambda)}{\lambda}\rho, \beta, \phi \right).$$

Now, assuming the knowledge of an estimate $\hat{\zeta}_{rp} = \hat{\xi}_{rp}$ but not of ξ_{rp} itself, we can apply the control law (4.7) using the estimated scaled state $\hat{\zeta}_{rp}$ as $(v_f, \omega)^{\wedge} = f_u\left(\hat{\zeta}_{\mathrm{rp}}\right)$. Note that the notation $^{\wedge}$ is used here to emphasize the application of the control law to the estimated state $\hat{\zeta}_r$. Assuming the existence of an asymptotically stable observer of ζ_r, we have that for $t \to \infty$ then $\lim_{t\to\infty} \hat{\zeta}_{\mathrm{rp}} \to \bar{\xi}_{\mathrm{rp}}$. Hence, for $t \to \infty$ we have that the control law applied to the scaled polar coordinates of the vehicle differ from the original one from $(v_f, \omega)^{\wedge} = f_u\left(\bar{\xi}_{\mathrm{rp}}\right) = \left(\frac{\mathrm{sign}(\lambda)}{\lambda} v_f, \omega\right)$. The adapted control law is equivalent to the original one (eq. (4.7)), but with the first constant now defined as:

$$\bar{k}_1^{\wedge} = \frac{\mathrm{sign}(\lambda)}{\lambda} k_1,$$

which is still positive definite. Hence, asymptotic stabilization of ξ_{rp} is still guaranteed.

4.5 Simulation Results

4.5.1 Omnidirectional Vehicle

In this section both PBVS and IBVS control schemes, as described in section 4.4 are validated under simulations. In these, even though the vehicle is affected by external forces, the proposed control schemes guarantees stability. Results show that pose regulation is successfully achieved whenever analogous classical controllers fail, notwithstanding that those require the use of a priori information that in practical situations is not available.

The desired configuration of the robot is considered to be coincident to the origin of the world frame $\langle W \rangle$ and the initial vehicle configuration is $\xi_r = (-10\,\mathrm{m},\, -2\,\mathrm{m},\, \pi/2\,\mathrm{rad})$. Maximum vehicle velocities are $\max\left(\mathrm{abs}\left(v_f, v_h, \omega\right)\right) = (10\,\mathrm{m/s}, 10\,\mathrm{m/s}, 10\,\mathrm{rad/s})$. The vehicle is affected by a constant external disturbance

$$d_r = (0.1\,\mathrm{m/s}, 0.1\,\mathrm{m/s}, 0.1\,\mathrm{rad/s}).$$

In simulations are carried out using the minimum set of landmarks required in order to have ζ_o observable, i.e., 2 measured landmarks. Landmarks are positioned in the environment at $\xi_1 = (1\,\text{m},\, 2\,\text{m},\, 1\,\text{m})$ and $\xi_2 = (1\,\text{m},\, 2\,\text{m},\, -1\,\text{m})$. The unknown scale factor is chosen to be $\lambda = y_1$, i.e., the height of the first landmark. The system observer is designed as described in Section 4.3.2 considering only the first derivative of system outputs, i.e., assuming $\dot{d}_r = 0$. Inputs are completely modelled as a disturbance, i.e., no odometry (input) information is used in the observer. Observer state is arbitrarily initialized. As already mentioned, the implementation of an observer must take in consideration observability singularities. Whenever close to singularities, it is well known that the observer Extended Output Jacobian $J(\xi)$ becomes ill-conditioned. Hence, whenever the observer paths are crossing kinematic singularities, a Jacobian transpose gradient estimator is adopted as an alternative to the observer described in section 4.3.2. This procedure is done on the basis of the Jacobian condition number. For both IBVS and PBVS cases, the observer gains are $K_* = 3$, whilst the controller gains are $K_{cc,*} = 1$. We will present results where the controller performs disturbance rejection, and $K_{ci,*} = 10.1$, and also when no disturbance rejection is performed, and $K_{ci,*} = 0$. Quantization effects and measurement noise are not considered.

Results are presented as follows:

- Fig. 4.6-a, b shows time evolution of errors e_o and e_c for the PBVS controller using disturbance rejection.
- Fig. 4.5-a, b shows time evolution of errors e_o and e_c for the PBVS controller without disturbance rejection.
- Fig. 4.8-a, b shows time evolution of errors e_o and e_c for the IBVS controller using disturbance rejection.
- Fig. 4.7-a, b shows time evolution of errors e_o and e_c for the IBVS controller without disturbance rejection.

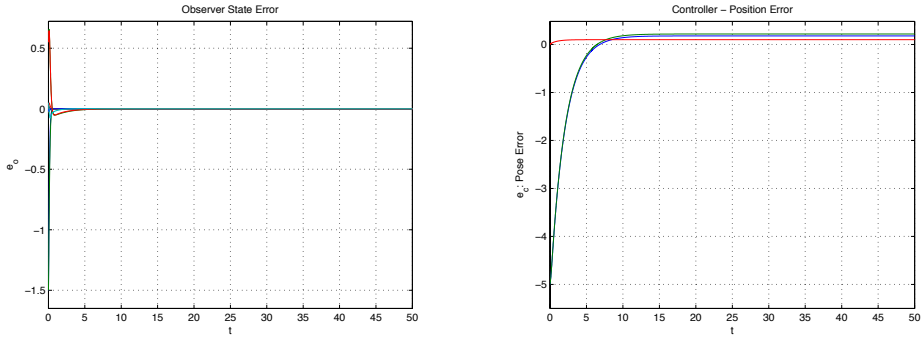

a) b)

Figure 4.5: PBVS without disturbance rejection:: Observer error e_o (a); and Controller error Observer error e_c (b).

It is worthwhile to point out that the observability problem, which is the very basis of this approach, is singular whenever the vehicle arrives in the desired position and when the translational velocities are both zero. In particular, when linear velocity is zero, the observability problem is singular if only two landmarks are available. A complete characterization of the singularities and the possible solutions to overcome such a problem are deferred to future work. Moreover, the choice of proper constants is very important, given that observer asymptotic stability is only guaranteed if condition (4.5) is respected.

4.5.2 Unicycle Vehicle

In this section both the presented observers, i.e., Dynamic Appearance Servoing (DAS) and Static Appearance Servoing (SAS), are simulated. In both cases, a stabilizing controller that solves the pose regulation problem is presented. The vehicle used for these examples is an unicycle–like vehicle, which is equipped with a calibrated *Omnidirectional Sight Camera*, i.e., a camera with unlimited Field–Of–View (FOV). Quantization effects and measurement noise are not consid-

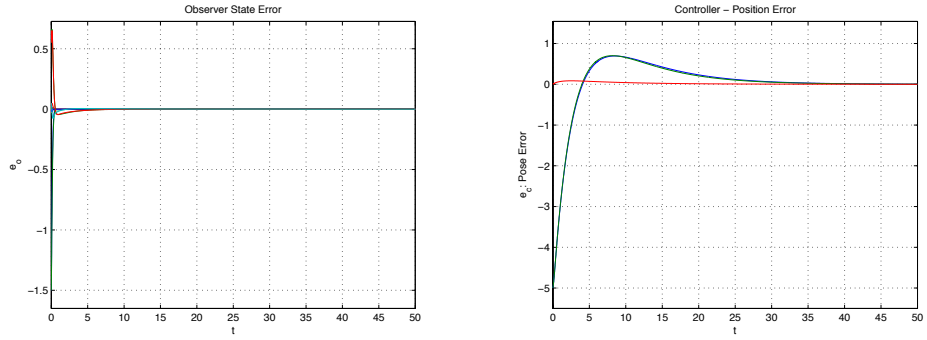

a) b)

Figure 4.6: PBVS with disturbance rejection:: Observer error e_o (a); and Controller error Observer error e_c (b).

ered.

The simulations are carried out with the minimum set of feature needed by the observers, i.e., 2 measured landmarks for the DAS and 3 landmarks for the SAS. The control law implemented in the simulations is based on the one presented in [66], as discussed in Section 4.4, which proves to satisfy practical stability requirements. As a consequence, both simulations terminate when the vehicle is closed to the desired configuration, i.e., when $\|\bar{\xi}_d\| < \mu$ with μ arbitrarily chosen. In both the simulations reported, the desired configuration of the robot is considered coincident to the origin of the world frame $\langle W \rangle$, the initial vehicle configuration is $\xi_r = (-10[\text{m}], -2[\text{m}], 0[\text{rad}])$ and the scale factor is $\lambda = y_1$, i.e., the height of the first feature. To increase the realism of the simulations, the controllers are supposed to work with sampling time of 10 [ms].

Dynamic Appearance Servoing

The DAS problem has been solved using an observer–based regulator. The system observer is designed as described in Section 4.3.2 consider-

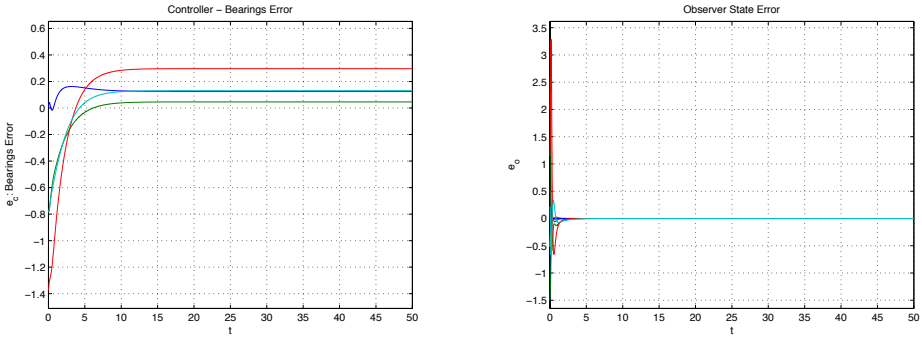

a) b)

Figure 4.7: IBVS without disturbance rejection:: Observer error e_o (a); and Controller error Observer error e_c (b).

ing only the first derivative of system outputs, i.e., assuming $\dot{d}_r = 0$. Inputs are completely modelled as a disturbance, i.e., no odometry (input) information is used in the observer. Observer state is arbitrarily initialized, and then, the estimated state is refined during a 5 [s] of a linear motion, after which the controller is activated.

As mentioned in 4.3.2, the implementation of an observer must take in consideration observability singularities. Whenever close to singularities, it is well known that the observer Extended Output Jacobian $J(\xi)$ becomes ill-conditioned. Hence, whenever the observer paths are crossing kinematic singularities, a Jacobian transpose gradient estimator is adopted as an alternative to the observer described in section 4.3.2. This procedure is done on the basis of the Jacobian condition number. The observer gains are $K_* = 1.1$, whilst the controller gains are $K_* = 1$.

The features are positioned in the environment at

$$\xi_1 = (1[\text{m}],\, 2[\text{m}],\, 1[\text{m}]),$$

and $\xi_2 = (1[\text{m}],\, 2[\text{m}],\, -1[\text{m}])$. The stop condition threshold is set to $\mu = 0.07$. Fig. 4.9-a, b and c shows the time evolution of the vehicle

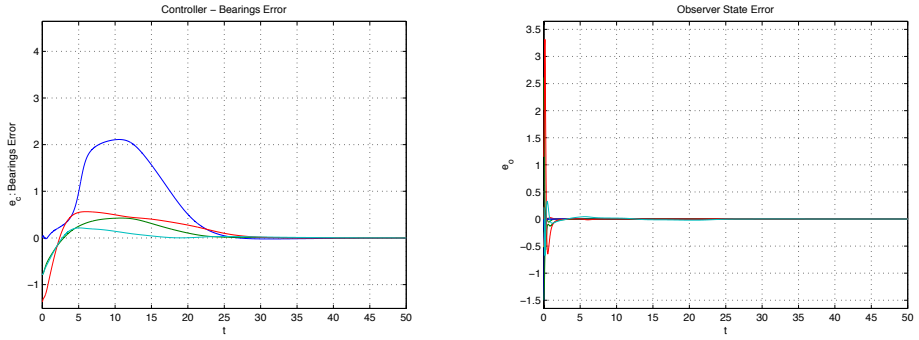

a) b)

Figure 4.8: IBVS with disturbance rejection:: Observer error e_o (a); and Controller error Observer error e_c (b).

configuration: x_r, z_r and θ_r respectively, while Fig. 4.9-d shows the vehicle trajectory on the plane of motion. The observer scaled state errors, i.e., $\zeta_o - \hat{\zeta}_o$, are instead reported in Fig. 4.10.

Static Appearance Servoing

In the simulations for the SAS problem, the scaled state $\bar{\xi}_r$ is obtained by the algebraic solution of $\bar{\xi}_r = h^{-1}(y)$, as described in section 4.2.2. The features are positioned in the environment at $\xi_1 =$ (1[m], 2[m], 1[m]), $\xi_2 =$ (1[m], 2[m], -1[m]) and

$$\xi_3 = (2[\text{m}],\ 3[\text{m}],\ -1[\text{m}]).$$

The controller gains are $K_* = 1$, while the stop condition threshold is $\mu = 0.01$.

Again, the time evolution of the vehicle configurations ξ_r are reported in figure Fig. 4.11-a, b and c, respectively, while Fig. 4.11-d shows the vehicle trajectory on the plane of motion.

4.5.3 Discussion

It is worthwhile to point out that the observability problem, which is the very basis of this approach, is singular whenever the vehicle arrives in the desired position and when the translational velocities are both zero. In particular, when linear velocity is zero, the observability problem is singular if only two landmarks are available. A complete characterization of the singularities and the possible solutions to overcome such a problem are deferred to future work. Moreover, the choice of proper constants is very important, given that observer asymptotic stability is only guaranteed if condition (4.5) is respected.

Besides such drawbacks, the simulations clearly show that the pose regulation is successfully achieved when disturbance rejection is applied, and stability is only marginal if disturbance rejection is not applied. It is important to note that analogous classical controllers would obtain results similar to those from the schemes where disturbance rejection is not applied due to the fact that external forces (disturbances) are not foreseen or modelled in these.

4.6 Conclusion

A new definition of visual servoing, named the Appearance Servoing, is proposed in this chapter. Considering an unicycle and an omnidirectional vehicle equipped with a omnidirectional monocular camera, a complete analysis and characterization of the problem is shown. Both a PBVS and an IBVS observer-based pose regulation control schemes are proposed for solving the problem. Moreover, both a dynamic and a static solution is proposed. Finally, results are validated under simulation.

Future developments concern the investigation of observability singularities and the application of optimal control as a potential solution to singularity cases. Moreover, a deeper investigation of robust controllers and an online disturbance rejection based on disturbance information coming from the observer are compelling topics for future

research. Finally, the implementation of the appearance servoing control algorithms presented on different real platforms, e.g., a vehicle and/or a serial manipulator, is strongly envisaged.

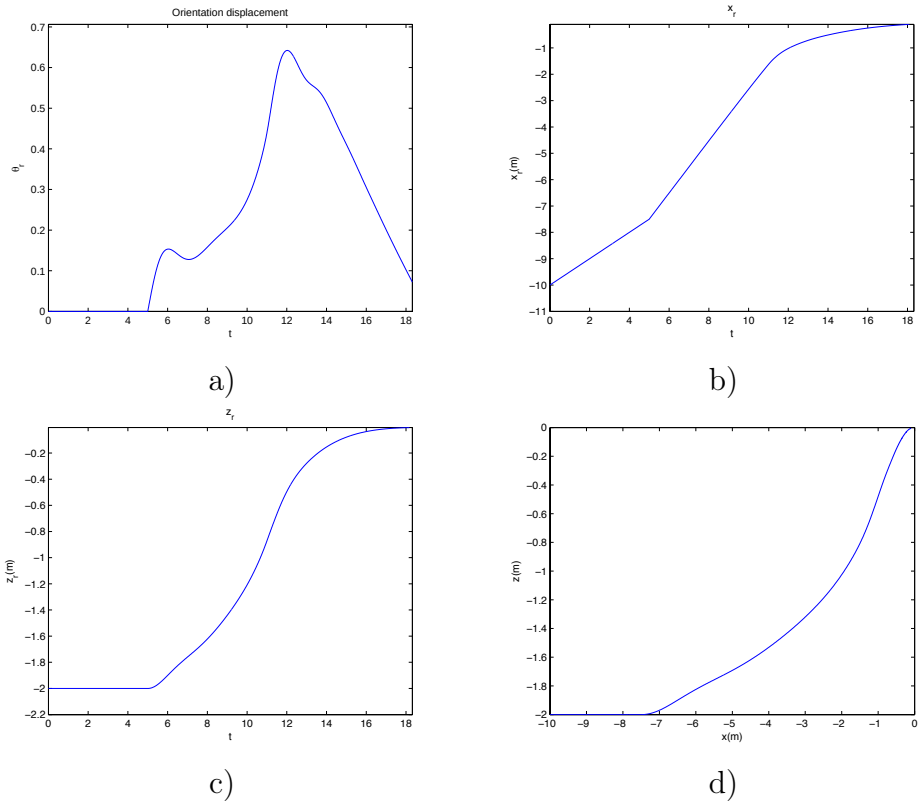

Figure 4.9: Dynamic Appearance Servoing:: θ_r (a); x_r (b); and, z_r (c); and, vehicle trajectory (d).

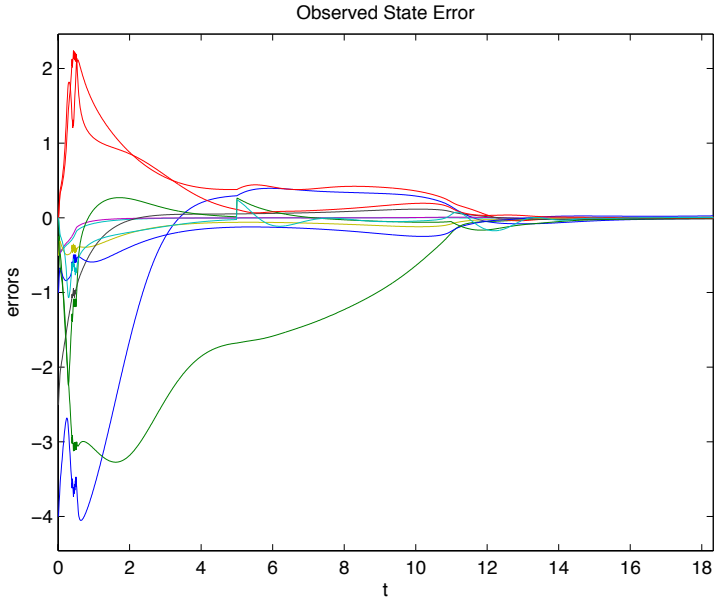

Figure 4.10: Observer state error: $\zeta_o - \hat{\zeta}_o$.

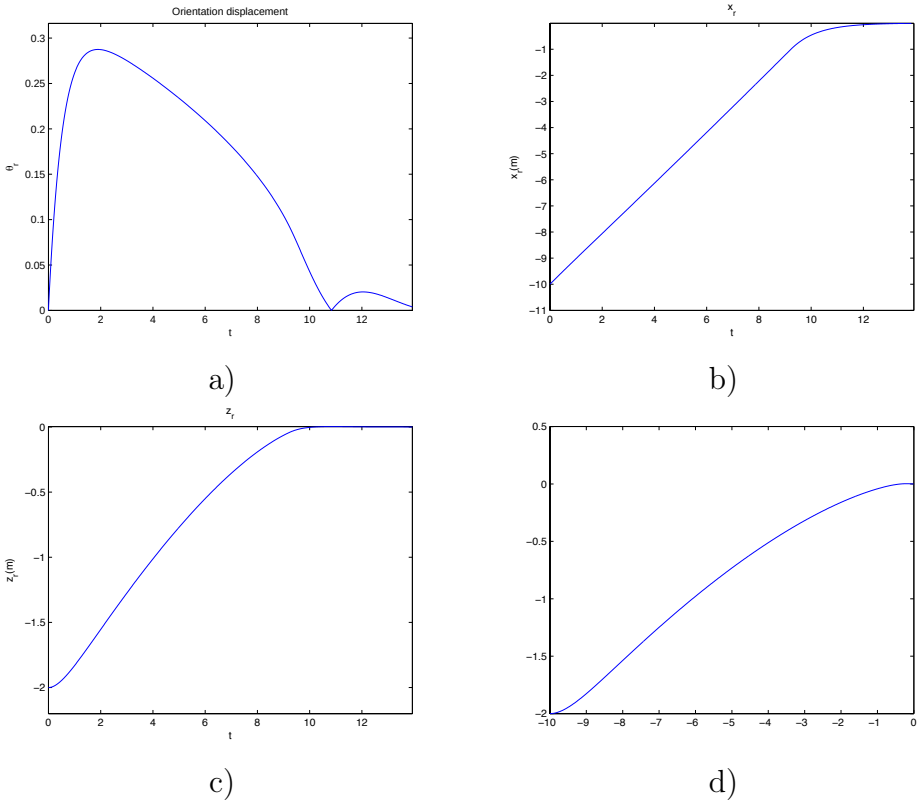

Figure 4.11: Static Appearance Servoing: θ_r (a); x_r (b); and, z_r (c); and, vehicle trajectory (d).

Chapter 5

On the use of Appearance Topological Maps

In this chapter we present an experimental study case of appearance topological mapping and navigation (also presented in [18,33,80,81]). In this, the map is composed of acquired images only, mapping the path as a set of keyframes and organizing the acquired images in an appearance topological map.

In the presented approach, no metric information is related to the collected images, and consequently, connections between images are obtained by visual appearance. The mapping phase is thus very flexible and completely relies on scene feature richness. However, simplicity in the appearance–based map results in a more difficult navigation phase, since localization, planning and control algorithms must be only image related. Whichever visual servoing scheme is adopted, the desired image with desired feature positions must be correctly associated with the current image and features. In the proposed solution, point features detection and association are implemented using *Scale Invariant Feature Transform* descriptors (SIFT, [9]), and are given for granted in the rest of the chapter.

5.1 Proposed Mapping

Although the appearance based topological map is not a novel concept in literature, our approach proposes a generalization to low-cost monocular cameras. Briefly, the map is represented as a weighted graph $G = (F, S)$, where F_i is the node i (or the image I_i), and each link $S_{i,j}$ represents a similarity metric between nodes F_i and F_j. Since $S_{i,j}$ is related to the feature descriptor used, it is chosen as

$$S_{i,j} = \frac{\#(F_i \cap F_j)}{\min(n_i, n_j)}, \tag{5.1}$$

that is the number of SIFT features matched between nodes F_i and F_j normalized by the minimum of $n_i > 0$ (total number of features in image I_i, $\#F_i$) and $n_j > 0$ (total number of features in image I_j, $\#F_j$). The links $S_{i,j}$ may denote how similar are the images I_i and I_j, therefore is a measure of the probability of successful navigation between the two nodes. Notice that $S_{i,j} \in [0, 1]$, where $S_{i,j} = 0$ if there is no feature in common between images I_i and I_j and $S_{i,j} = 1$ if all the features of I_i (I_j) belong to the image I_j (I_i).

5.1.1 Map Building

The map building process is divided into two different steps. In the exploration phase, the robot randomly explores the environment and collects a sequence of images to describe the travelled robot trajectory. To relate the map size to the quantity of new information acquired, we adopt a similarity–based solution. Then, the map manager processes the acquired images and builds a connected image graph by enforcing new image links between similar nodes (and detecting possible closed loops) and, in case, deleting the images that are too similar to each other. The overall process is divided in the *intra-map* merging on–board the robot, where the number of new mapped images are reduced before they are transmitted to the map manager, and the *inter-map* merging, where the new entities are (off–line) added to the global map by the map manager.

The described map building process starts when the current image in view is not related to any prerecorded image or when the localization process does not complete successfully: in both cases, the problem is known in literature as *kidnapped robot problem.*

5.1.2 Localization and Navigation

As shown in the previous section, the similarity measure (5.1) plays a fundamental role in the architecture. Furthermore, it allows the computation of a heuristic estimate of the distance between nodes in the appearance space as

$$D_{i,j} = \frac{1 - S_{i,j}}{S_{i,j}}, \tag{5.2}$$

that is crucial for the navigation, i.e. sequence of way–point images in the topological map. More precisely, as the robot enters in a mapped environment, it asks to the map manager the topological path to follow from its current view to the desired image. The optimal topological path through actual and desired nodes is computed using the A* algorithm based on the admissible heuristic estimate of the distance (5.2). The sequence of selected images thus obtained corresponds to the most robust path, i.e. the sequence of images with the highest number of features in common. It is worthwhile to note that the heuristic estimate of the distance (5.2) is not a physical distance measure, since the triangle inequality is not verified.

5.2 Experimental Results

In this chapter, experimental results of the overall architecture are presented. Even though the adoption of heterogeneous robots is feasible for the presented solution, the experimental results are related to the same platform, a unicycle–like robot, equipped with a fixed monocular camera. The visual-servoing scheme adopted is based on the work developed in [80].

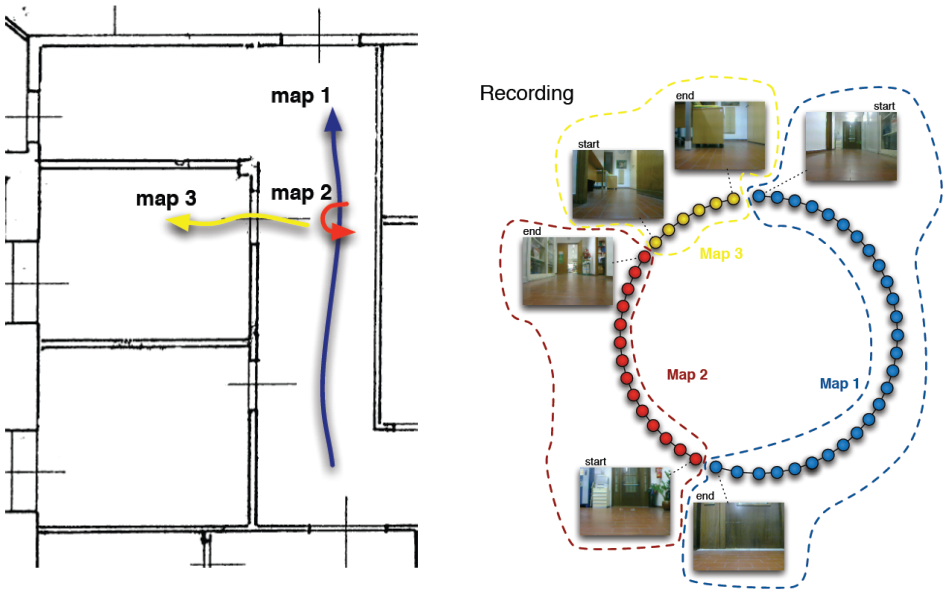

a) b)

Figure 5.1: Exploration trajectories travelled by the exploring vehicle for the map building process of the Interdepartmental Research Center "E. Piaggio" (a) and raw sensed data, organized as sequences of the same exploration phase (b).

The experimental setup comprises of a Quickcam Ultravision camera, whose resolution is 320x240 pixels, mounted over the front-part of a K-team Koala vehicle. The controller bandwidth is almost 7Hz.

In the experiments, the same robot equipped with a single camera is used to collect data. The robot has followed three different random trajectories starting from three different unknown locations in the unknown indoor environment of the Interdepartmental Research Center "E. Piaggio" (see fig. 5.1-a). The maps, named *Map I, II* and *III*, are represented as raw collected data in fig. 5.1-b as three different collection of images, grabbed at different time instants. The *intra-map* and

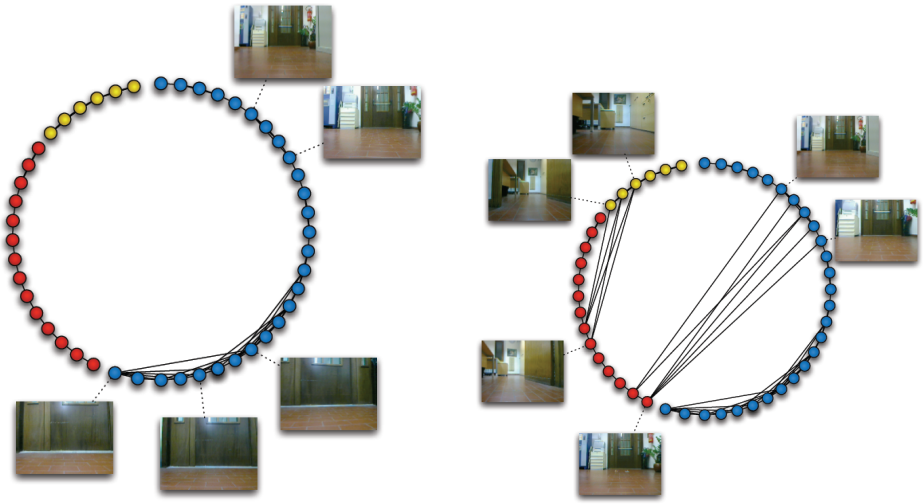

a) b)

Figure 5.2: The *intra-map* merging (a) and the *inter-map* merging (b).

inter-map merging processes are then executed to reduce and organize the collected raw data (see fig. 5.2).

5.2.1 Localization and Navigation

The robot is firstly *kidnapped*and a desired image is given (fig. 5.3-a). The localization in the map is simply obtained by a rotation on the spot, grabbing the current image from the camera and passing it to the map–manager. As the robot is localized in the map, the navigation planner plans an image trajectory, based on similarity quality among images (fig. 5.4).

The image sequence is a set of ordered way–point images. The visual guided robot motion between two successive images in the image sequence is governed by the optimal feature trajectory planner proposed in [80]. The final experimental results, depicted in fig. 5.5, report the image sequence used by the robot as well as the map they

a) b)

Figure 5.3: Desired image to reach at the end of the navigation task (a) and image reached at the end of the navigation phase (b).

belong.

Finally, the image reached at the end of the overall navigation task is reported in fig. 5.3-b, to be compared with the desired one reported in fig. 5.3-a.

5.3 Conclusions

In this section, pure appearance based visual maps are constructed without considering any three–dimensional spatial data. This way, control and navigation of multiple, heterogeneous robots are feasible. Although the lack of metric information may lead to robot control challenging, an image based path planner is presented. Optimal trajectories in the robot working space are obtained building words on an alphabet of basic manoeuvres. The proposed architecture relies on the idea of a middleware between the map–manager, that can be fixed in the environment or placed on a moving agent, and the robots. The proposed architecture has been practically tested in an indoor, static environment, thus showing the effectiveness of the proposed approach.

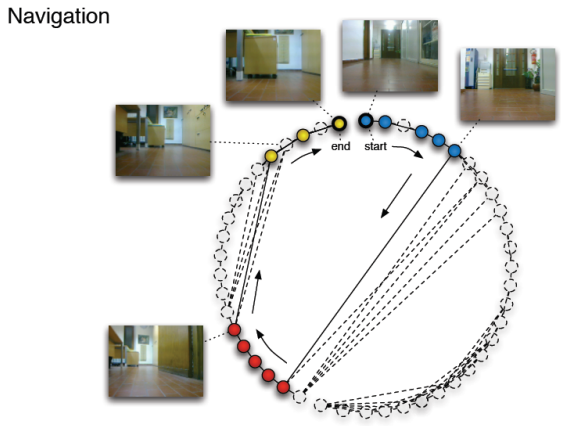

Figure 5.4: Planned image trajectory in the map.

Figure 5.5: Sequence of images travelled by the robot during the navigation phase.

Bibliography

[1] M Cummins and P Newman. Accelerated appearance-only slam. In *Proc. IEEE International Conference on Robotics and Automation (ICRA'08)*, pages 1828–1833, 2008.

[2] Rohan Paul and Paul Newman. Fab-map 3d: Topological mapping with spatial and visual appearance. In *Proc. IEEE International Conference on Robotics and Automation (ICRA'10).*, pages 1–8, Mar 2010.

[3] M Cummins and P Newman. Fab-map: Probabilistic localization and mapping in the space of appearance. *The International Journal of Robotics Research*, Jan 2008.

[4] Mark Cummins and Paul Newman. Probabilistic appearance based navigation and loop closing. In *Proc. IEEE International Conference on Robotics and Automation(ICRA'07)*, April 2007.

[5] Iwan Ulrich and Illah Nourbakhsh. Appearance-based place recognition for topological localization. In *Proc. IEEE International Conference on Robotics and Automation (ICRA'00)*, Jan 2000.

[6] P. Lamon, I. Nourbakhsh, B. Jensen, and R. Siegwart. Deriving and matching image fingerprint sequences for mobile robot localization. In *Proc. IEEE International Conference on Robotics and Automation (ICRA'01)*, 2001.

[7] Vivek A. Sujan, Marco A. Meggiolaro, and Felipe A. Belo. Information based indoor environment robotic exploration and modeling using 2-d images and graphs. *Auton. Robots*, 21:15–28, August 2006.

[8] A. Torralba, K. P. Murphy, , W. T. Freeman, and M. A. Rubin. Context-based vision system for place and object recognition. In *Proc. of the Ninth IEEE International Conference on Computer Vision - Volume 2*, ICCV '03, pages 273–. IEEE Computer Society, 2003.

[9] D. Lowe. Distinctive image features from scale-invariant keypoints. In *International Journal of Computer Vision*, volume 20, pages 91–110, 2003.

[10] Stephen Se, David Lowe, and Jim Little. Mobile robot localization and mapping with uncertainty using scale-invariant visual landmarks. *International Journal of Robotics Research*, 21:735–758, 2002.

[11] A Bicchi, D Prattichizzo, A Marigo, and A Balestrino. On the observability of mobile vehicle localization. In *Proc. IEEE Mediterranean Conf. On Control And Systems*, 1998.

[12] R Hermann and A Krener. Nonlinear controllability and observability. *IEEE Trans. on Automatic Control*, 22(5):728 – 740, Jan 1977.

[13] F. Chaumette and S. Hutchinson. Visual servo control, Part I: Basic approaches. *IEEE Robotics and Automation Magazine*, 13(4):82–90, December 2006.

[14] F. Chaumette and S. Hutchinson. Visual servo control, Part II: Advanced approaches. *IEEE Robotics and Automation Magazine*, 14(1):109–118, March 2007.

[15] A. C. Sanderson and L. E. Weiss. Image–based visual servo control using relational graph error signals. In *Proc. IEEE International Conference on Robotics and Automation (ICRA'80)*, pages 1074–1077, 1980.

[16] A. Remazeilles, F. Chaumette, and P. Gros. Robot motion control from a visual memory. In *Proc. IEEE International Conference on Robotics and Automation (ICRA'04)*, volume 5, pages 4695–4700 Vol.5, 2004.

[17] F Chaumette. Image-based robot navigation from an image memory. *Robotics and Autonomous Systems*, Jan 2007.

[18] Daniele Fontanelli, Paolo Salaris, Felipe Augusto Weilemann Belo, and Antonio Bicchi. Visual appearance mapping for optimal vision based servoing. In *Experimental Robotics*, volume 54 of *Springer Tracts in Advanced Robotics (STAR)*, pages 353–362. Springer Berlin / Heidelberg, March 2009.

[19] John J. Leonard and Hugh F. Durrant-Whyte. Mobile robot localization by tracking geometric beacons. In *Proc. IEEE International Conference on Robotics and Automation (ICRA'91)*, volume 7, pages 376–382, June 1991.

[20] J. J. Leonard and H. F. Durrant-Whyte. Simultaneous map building and localization for an autonomous mobile robot. In *Proc. IEEE International Conference on Intelligent Robots and Systems (IROS'91)*, pages 1442–1447 vol.3, 1991.

[21] R Smith and P Cheeseman. On the representation and estimation of spatial uncertainty. *The International Journal of Robotics Research*, Jan 1986.

[22] A Davison. Real-time simultaneous localisation and mapping with a single camera. In *Proc. of the Ninth IEEE International Conference on Computer Vision - Volume 2*, Jan 2003.

[23] Sebastian Thrun, Wolfram Burgard, and Dieter Fox. *Probabilistic Robotics*. MIT Press, 2005.

[24] Thomas Lemaire and Simon Lacroix. Monocular-vision based slam using line segments. In *Proc. IEEE International Conference on Robotics and Automation (ICRA'07*, pages 2791–2796, 2007.

[25] T. Ohno, A. Ohya, and S. Yuta. Autonomous navigation for mobile robots referring pre-recorded image sequence. In *Proc. IEEE International Conference on Intelligent Robots and Systems IROS('96)*, volume 2, pages 672–679 vol.2, 1996.

[26] E. Mouragnon, M. Lhuillier, M. Dhome, F. Dekeyser, and P. Sayd. Monocular vision based slam for mobile robots. In *Proc. of the 18th International Conference on Pattern Recognition (ICPR '06)*, pages 1027–1031. IEEE Computer Society, 2006.

[27] E. Royer, J. Bom, M. Dhome, B. Thuilot, M. Lhuillier, and F. Marmoiton. Outdoor autonomous navigation using monocular vision. In *Proc. IEEE International Conference on Intelligent Robots and Systems (IROS'05)*, pages 1253–1258, 2005.

[28] Eric Royer, Maxime Lhuillier, Michel Dhome, and Thierry Chateau. Localization in urban environments: Monocular vision compared to a differential gps sensor. In *Proc. of the 2005 IEEE Computer Society Conference on Computer Vision and Pattern Recognition (CVPR'05) - Volume 2*, pages 114–121. IEEE Computer Society, 2005.

[29] T. D. Barfoot. Online visual motion estimation using fastslam with sift features. In *Proc. IEEE International Conference on Intelligent Robots and Systems (IROS'05)*, pages 579–585, 2005.

[30] P. Jensfelt, D. Kragic, J. Folkesson, and M. Bjorkman. A framework for vision based bearing only 3d slam. In *Proc. IEEE International Conference on Robotics and Automation (ICRA'06)*, pages 1944–1950, 2006.

[31] N. Karlsson, E. di Bernardo, J. Ostrowski, L. Goncalves, P. Pirjanian, and M. E. Munich. The vslam algorithm for robust localization and mapping. In *Proc. IEEE International Conference on Robotics and Automation (ICRA'05)*, pages 24–29, 2005.

[32] P. Elinas, R. Sim, and J. J. Little. σSLAM: Stereo vision SLAM using the Rao-Blackwellised particle filter and a novel mixture proposal distribution. In *Proc. IEEE International Conference on Robotics and Automation (ICRA'06)*, pages 1564–1570. IEEE, IEEE Press, May 2006.

[33] D. Fontanelli, A. Danesi, F.A.W. Belo, P. Salaris, and A. Bicchi. Visual servoing in the large. *The International Journal of Robotics Research*, 28(6):802–814, 2009.

[34] Henrik Andreasson, Tom Duckett, and Achim Lilienthal. Mini-slam: Minimalistic visual slam in large-scale environments based on a new interpretation of image similarity. In *Proc. IEEE International Conference on Robotics and Automation (ICRA'07)*, pages 4096–4101, 2007.

[35] O. Booij, B. Terwijn, Z. Zivkovic, and B. Krose. Navigation using an appearance based topological map. In *Proc. IEEE International Conference on Robotics and Automation (ICRA'07)*, pages 3927–3932, 2007.

[36] Y. Matsumoto, K. Ikeda, M. Inaba, and H. Inoue. Visual navigation using omnidirectional view sequence. In *Proc. IEEE International Conference on Intelligent Robots and Systems (IROS'99)*, volume 1, pages 317–322 vol.1, 1999.

[37] K. Kidono, J. Miura, and Y. Shirai. Autonomous visual navigation of a mobile robot using a human-guided experience. In *In Proc. of 6th Int. Conf. on Intelligent Autonomous System*, pages 620–627, 2000.

[38] A Davison, I Reid, N Molton, and O Stasse. Monoslam: Real-time single camera slam. *IEEE Trans. on Pattern Analysis and Machine Intelligence*, Jan 2007.

[39] Kwang Wee Lee, W Wijesoma, and I Javier. On the observability and observability analysis of slam. In *Proc. IEEE International Conference on Intelligent Robots and Systems (IROS'06)*, pages 3569 – 3574, Oct.

[40] L Perera, A Melkumyan, and E Nettleton. On the linear and nonlinear observability analysis of the slam problem. In *IEEE International Conference on Mechatronics (ICM'09)*, pages 1 – 6, Apr 2009.

[41] S Sukkarieh, A Sanfeliu, and J Andrade-Cetto. On the observability of bearing-only slam. In *Proc. IEEE International Conference on Robotics and Automation (ICRA'07)*, Jan 2007.

[42] D Woffinden and D Geller. Observability criteria for angles-only navigation. *IEEE Trans. on Aerospace and Electronic Systems*, 45(3):1194 – 1208, Jul 2009.

[43] Guan Xin, Yi Xiao, and He You;. Research on unobservability problem for two-dimensional bearings-only target motion analysis. In *Proc. of 2005 International Conference on Intelligent Sensing and Information Processing*, pages 56 – 60, Jan 2005.

[44] A. Martinelli, F. Pont, and R. Siegwart. Multi-robot localization using relative observations. In *Proc. IEEE International Conference on Robotics and Automation (ICRA'05)*, pages 2797 – 2802, april 2005.

[45] A Martinelli and R Siegwart. Observability properties and optimal trajectories for on-line odometry self-calibration. In *2006 45th IEEE Conference on Decision and Control*, pages 3065 – 3070, Dec 2006.

[46] G. Basile and G. Marro. On the observability of linear, time-invariant systems with unknown inputs. *Journal of Optimization Theory and Applications*, 3:410–415, 1969.

[47] R. Guidorzi and G. Marro. On wonham stabilizability condition in the synthesis of observers for unknown-input systems. *IEEE Trans. on Automatic Control*, 16(5):499 – 500, oct 1971.

[48] K. Watanabe and D. M. Himmelblau. Instrument fault detection in systems with uncertainties. *International Journal of Systems Science*, 13(2):137 – 158, 1982.

[49] Ron J. Patton and Jie Chen. Optimal unknown input distribution matrix selection in robust fault diagnosis. *Automatica*, 29(4):837 – 841, 1993.

[50] Andrew W. Fitzgibbon and Andrew Zisserman. Automatic camera recovery for closed or open image sequences. In *Proc. of the 5th European Conference on Computer Vision-Volume I (ECCV '98)*, pages 311–326. Springer-Verlag, 1998.

[51] Maxime Lhuillier. A quasi-dense approach to surface reconstruction from uncalibrated images. *IEEE Trans. Pattern Anal. Mach. Intell.*, 27(3):418–433, 2005.

[52] R. Hartley and A. Zisserman. *Multiple View Geometry in Computer Vision*. Cambridge University Press, 2003.

[53] Marc Pollefeys, Reinhard Koch, and Luc J. Van Gool. Self-calibration and metric reconstruction in spite of varying and unknown internal camera parameters. In *ICCV*, pages 90–95, 1998.

[54] Olivier Faugeras, Quang-Tuan Luong, and T. Papadopoulou. *The Geometry of Multiple Images: the Laws That Govern the Formation of Images of a Scene and Some of Their Applications*. MIT Press, 2001.

[55] J. Campbell, R. Sukthankar, and I. Nourbakhsh. Techniques for evaluating optical flow for visual odometry in extreme terrain. In *Proc. IEEE International Conference on Intelligent Robots and Systems (IROS'04)*, volume 4, pages 3704–3711 vol.4, 2004.

[56] D Nister, O Naroditsky, and J Bergen. Visual odometry. In *Proc. of the 2004 IEEE Computer Society Conference on Computer Vision and Pattern Recognition (CVPR'04)*, volume 1, pages I–652 – I–659 Vol.1, Jan 2004.

[57] A. Levin and R. Szeliski. Visual odometry and map correlation. In *Proc. of the 2004 IEEE Computer Society Conference on Computer Vision and Pattern Recognition (CVPR'04)*, volume 1, pages I–611–I–618 Vol.1, 2004.

[58] Bogdan Kwolek. Visual odometry based on gabor filters and sparse bundle adjustment. In *Proc. IEEE International Conference on Robotics and Automation (ICRA'07)*, pages 3573–3578, 2007.

[59] O. Naroditsky D. Nister and J. Bergen. Visual odometry for ground vehicle applications. *Journal of Field Robotics*, 23, 2006.

[60] Jason Campbell, Rahul Sukthankar, and Illah Nourbakhsh. Visual odometry using commodity optical flow. In *Proc. of the American Association of Artificial Intelligence (AAAI*, 2004.

[61] Stefano Soatto. 3-d structure from visual motion: Modeling, representation and observability. *Automatica*, 33:1287–1312, 1997.

[62] Giuseppe Basile and Giovanni Marro. On the observability of linear, time–invariant systems with unknown inputs. *Journal of Optimization Theory And Applications*, 3(6):410–415, 1969.

[63] Bruno Siciliano, Lorenzo Sciavicco, and Luigi Villani. *Robotics: Modelling, Planning and Control*. Jan 2009.

[64] Seth Hutchinson, Greg Hager, and Peter Corke. A tutorial on visual servo control. *IEEE Trans. on Robotics and Automation*, 12:651–670, 1996.

[65] R.W. Brockett. Asymptotic stability and feedback stabilization. In Millmann Brockett and Sussmann, editors, *Differential Geometric Control Theory*, pages 181–191. Birkhauser, 1983.

[66] P. Murrieri, D. Fontanelli, and A. Bicchi. A hybrid-control approach to the parking problem of a wheeled vehicle using limited view-angle visual feedback. *Int. Jour. of Robotics Research*, 23(4–5):437–448, April–May 2004.

[67] E. Malis and F. Chaumette. 2-1/2-d visual servoing with respect to unknown objects through a new estimation scheme of camera displacement. *Int. Journal of Computer Vision*, 37(1):79–97, 2000.

[68] Y. Mezouar and F. Chaumette. Path planning for robust image–based control. *IEEE Trans. on Robotics and Automation*, 18(4):534–549, August 2002.

[69] G. L. Mariottini, G. Oriolo, and D. Prattichizzo. Image–based visual servoing for nonholonomic mobile robots using epipolar geometry. *IEEE Trans. on Robotics*, 23(1):87–100, February 2007.

[70] X. Zhang, Y. Fang, and X. Liu. Visual servoing of nonholonomic mobile robots based on a new motion estimation technique. In *48th IEEE Conference on Decision and Control*, Dec 2009.

[71] R. Tatsambon Fomena, O. Tahri, and F. Chaumette. Distance-based and orientation-based visual servoing from three points. *IEEE Trans. on Robotics*, 2011.

[72] C. Collewet and F. Chaumette. Positioning a camera with respect to planar objects of unknown shape by coupling 2-d visual servoing and 3-d estimations. *IEEE Trans. on Robotics and Automation*, 18(3), June 2002.

[73] C. Collewet and F. Chaumette. Visual servoing based on structure from controlled motion or on robust statistics. *IEEE Trans. on Robotics*, 24(2):318–330, April 2008.

[74] L. Weiss, A. Sanderson, and C. Neuman. Dynamic sensor-based control of robots with visual feedback. *IEEE Journal of Robotics and Automation*, 3(5):404–417, 1987.

[75] Giuseppe Basile and Giovanni Marro. *Controlled and Conditioned Invariants in Linear System Theory*. Jan 1992.

[76] G. Besançon (Ed.). *Nonlinear observers and applications, Lecture Notes in Control and Information Science 363*. Springer Verlag, 2007.

[77] Felipe A. W. Belo, Paolo Salaris, and Antonio Bicchi. 3 known landmarks are enough for solving planar bearing slam and fully reconstruct unknown inputs. In *Proc. IEEE International Conference on Intelligent Robots and Systems (IROS'10)*, 2010.

[78] Fabio Conticelli and Antonio Bicchi. Observer design for locally observable analytic systems: Convergence and separation property. In Alberto Isidori, FranÃ§oise Lamnabhi-Lagarrigue, and Witold Respondek, editors, *Nonlinear control in the Year 2000*, volume 258 of *Lecture Notes in Control and Information Sciences*, pages 315–330. Springer Berlin / Heidelberg, 2000.

[79] M Aicardi, G Casalino, A Balestrino, and A Bicchi. Closed loop smooth steering of unicycle-like vehicles. In *Proc. of the 33rd IEEE Conference on Decision and Control*, volume 3, pages 2455 – 2458 vol.3, 1994.

[80] Paolo Salaris, Felipe Augusto Weilemann Belo, Daniele Fontanelli, Luca Greco, and Antonio Bicchi. Optimal paths in a constrained image plane for purely image-based parking. pages 1673–1680, 2008.

[81] Daniele Fontanelli, Paolo Salaris, Felipe Augusto Weilemann Belo, and Antonio Bicchi. Unicycle–like robots with eye-in-hand monocular cameras: From pbvs towards ibvs. In *Visual Servoing via Advanced Numerical Methods*. Springer Berlin / Heidelbergp, 2009.